WIND RESOURCE CHARACTERIZATION AND UTILIZATION VIA WIND TURBINES AT METU NCC

A THESIS SUBMITTED TO
THE BOARD OF CAMPUS GRADUATE PROGRAMS
OF MIDDLE EAST TECHNICAL UNIVERSITY
NORTHERN CYPRUS CAMPUS

BY

FAHAD HANEEF

IN PARTIAL FULFILLMENT OF THE REQUIREMENTS
FOR
THE DEGREE OF MASTER OF SCIENCE
IN

SUSTAINABLE ENVIRONMENT AND ENERGY SYSTEMS

JUNE 2017

Approval of the Board of Graduate Programs

_____
Prof. Dr. Oya Yerin Güneri
Chairperson

I certify that this thesis satisfies all the requirements as a thesis for the degree of Master of Science

_____
Assist. Prof. Dr. Carter Mandrik
Program Coordinator

This is to certify that we have read the thesis and that in our opinion it is fully adequate, in scope and quality, as a thesis for the degree of Master of Science.

_____
Assist. Prof. Dr. Onur Taylan
Supervisor

Examining Committee Members:

Assist. Prof. Dr. Onur Taylan	Mechanical Engineering METU NCC	_____
Prof. Dr. Ali Cevat Taşıran	Economics METU NCC	_____
Assoc. Prof. Dr. Murat Fahrioğlu	Electrical and Electronics Engineering METU NCC	_____
Prof. Dr. Derek K. Baker	Mechanical Engineering METU Ankara	_____
Prof. Dr. Serkan Abbasoğlu	Energy Systems Engineering Cyprus International University	_____

I hereby declare that all information in this document has been obtained and presented in accordance with academic rules and ethical conduct. I also declare that, as required by these rules and conduct, I have fully cited and referenced all material and results that are not original to this wok.

Name, Last name: Fahad, Haneef

Signature : _____

ABSTRACT

WIND RESOURCE CHARACTERIZATION AND UTILIZATION VIA WIND TURBINES AT METU NCC

Haneef, Fahad

MSc., Sustainable Environment and Energy Systems Program

Supervisor: Assist. Prof. Dr. Onur Taylan

June 2017, 127 pages

The objective of this thesis is to investigate the wind energy potential at Middle East Technical University Northern Cyprus Campus (METU NCC) by statistically analyzing the measured data between 2013-2016 at METU NCC wind mast. Fact that Cyprus is an island, not enriched with fossil fuels, electricity generation is dependent upon heavy consumption of imported fuel oil. Numerous studies have proven the island's solar potential but little has been done for wind power feasibility. Investigating the feasibility of wind power generation at METU NCC will not only promote wind power generation in the region and help minimize the dependency on fuel oil, but also encourage investors to invest in wind energy in Cyprus. This wind resource assessment study mainly focuses on statistical evaluation of the wind energy potential of a site and this methodology is applicable to any site for conducting preliminary wind resource assessment. The feasibility analysis in this research is performed with the help of different statistical software's such as MS Excel, Matlab, WRPlot, R software and WAsP. The site evaluation includes characterization of wind speeds, examining wind shear exponent effect in a complex terrain, statistical distributions of wind speed and wind shear exponent, annual energy production (AEP) estimation and economic analysis of a number of wind turbines. Based on the results, it is suggested that METU NCC wind mast site has fair potential for wind power generation and with an average wind speed of 5-5.5 m/s, it can be categorized as IEC Class I site. Synthetic dataset such as TMY wind data (by meteonorm) for METU NCC is found to be inefficient as

it entirely fails to represent the actual site resources. The study recommends, first a value of 0.176 as a representative wind shear exponent for METU NCC site and secondly, Beta distribution parameters, which are predicted using maximum goodness of fit method, are the most suitable for wind shear exponent distribution. From the test results, it is evidently revealed that wind speed distribution is better presented by Gamma distribution than any other distribution. Furthermore, polynomial regression technique is found to be an accurate method to describe a turbine power curve. As per this preliminary analysis, AEP for 500 kW turbine is about 543, 622 and 662 MWh at 50 m, 65 m and 75 m hub heights, respectively. The AEP for 750 kW wind turbine is 957, 1085 and 1151 MWh at hub heights of 50 m, 65 m and 75 m, respectively. Similarly, AEP calculated for 1 MW wind turbine was 1113, 1279 and 1363 MWh at the same three heights, respectively. Economic feasibility analysis showed that electricity generation from 500 kW wind turbine would have capacity factors (CF) of 12%, 14% and 15% with a levelized cost of energy (LCOE) 0.157, 0.139 and 0.132 USD/kW for 50 m, 65 m and 75 m hub heights. A 750 kW wind turbine would have CF of 15%, 17% and 18% with an LCOE 0.136, 0.122 and 0.116 USD/kW respectively. In case of 1 MW turbine CF was 13%, 15% and 16% with LCOE to be 0.153, 0.136 and 0.129 USD/kW respectively. The feasibility study indicates that, a 750kW wind turbine at 75m hub height would be the most lucrative, technically and economically feasible system for METU NCC.

Keywords: Wind Resource Assessment, Wind Speed, Wind Energy, Wind Shear Exponent, Wind Speed Distribution, Goodness of fit

ÖZ

ODTÜ KUZEY KIBRIS KAMPUSU'NDAKI RÜZGAR ENERJİSİ NİTELENDİRMESİ VE RÜZGAR TÜRBİNLERİ ARACILIĞIYLA KULLANIMI

Haneef, Fahad
Yüksek Lisans, Sürdürülebilir Çevre ve Enerji Sistemleri
Tez Yöneticisi: Yrd. Doç. Dr. Onur Taylan
Haziran 2017, 127 sayfa

Bu tezin amacı, Orta Doğu Teknik Üniversitesi Kuzey Kıbrıs Kampusu (ODTÜ KKK)'ndaki rüzgâr enerjisi potansiyelini, 2013-2016 yılları arasında ODTÜ KKK rüzgâr direğinde ölçülen verileri kullanarak istatistiksel olarak analiz etmektir. Kıbrıs'ın fosil yakıtlar bakımından zengin bir ada olmamasından dolayı, adadaki enerji üretimi büyük çoğunlukla ithal edilen yakıtlardan sağlanmaktadır. Adanın güneş potansiyeli birçok çalışma ile ispatlanmasına rağmen, rüzgâr enerjisi fizibilitesi ile ilgili çok az çalışma yapılmıştır. ODTÜ KKK'de rüzgâr enerjisi üretiminin fizibilitesinin araştırılması, bölgedeki rüzgâr enerjisi üretimini teşvik edecek ve dışa bağımlılığını en aza indirmeye yardımcı olmakla birlikte aynı zamanda yatırımcıları Kıbrıs'ta rüzgâr enerjisine yatırım yapmaya teşvik edecektir. Bu rüzgâr enerjisi değerlendirme çalışması, bir konumun rüzgâr enerjisi potansiyelinin istatistiksel olarak değerlendirilmesine odaklanmaktadır ve bu çalışmada bahsedilen yöntem herhangi başka bir konuma da uygulanabilir. Bu araştırmadaki fizibilite analizi; MS Excel, Matlab, WRPlot, R yazılımı ve WAsP gibi farklı istatistiksel yazılımlar yardımıyla gerçekleştirilmiştir. Konum değerlendirme; rüzgâr hızlarının karakter analizi, karmaşık bir arazide rüzgâr değişim üssü etkisini, rüzgar hızının ve rüzgâr değişim üssünün istatistiksel dağılımlarını, yıllık enerji üretim (AEP) tahminini ve bir dizi rüzgâr türbininin ekonomik analizini incelemektedir. Elde edilen sonuçlara göre, ODTÜ KKK rüzgâr direğinin olduğu bölgenin rüzgâr enerjisi üretimi için makul bir potansiyele sahip olduğu ve ortalama rüzgâr hızı 5-5,5 m/s olan IEC Sınıf I sitesi olarak nitelendirilebilir. Yapılan ölçümler ile tipik meteorolojik yıl rüzgâr verisi

istatistiksel olarak karşılaştırıldığında, bu verilerin ODTÜ KKK kaynaklarını tamamen temsil etmediği görülmüştür. Çalışma, ODTÜ KKK ölçüm bölgesi için rüzgâr değişim üssü olarak 0.176 değerini önermektedir. Ayrıca, maksimum uyum iyiliği yöntemi kullanılarak tahmin edilen beta dağılım parametreleri, rüzgâr değişim üssü dağılımı için en uygun yöntemleri önermektedir. Test sonuçlarına göre, rüzgâr hızı dağılımı için gamma dağılımının diğer dağılımlardan daha iyi sonuç verdiği açıkça görülmektedir. Ayrıca, polinom regresyon tekniğinin türbin güç eğrisini tanımlamak için doğru bir yöntem olduğu saptanmıştır. Bu ön analize göre, 500 kW türbin için AEP, sırasıyla 50 m, 65 m ve 75 m yüksekliklerde yaklaşık 543, 622 ve 662 MWh olurken, 750 kW'lık rüzgâr türbini için AEP, sırasıyla 50 m, 65 m ve 75 m'lik göbek yüksekliklerinde 957, 1085 ve 1151 MWh'dir. Benzer şekilde, 1 MW rüzgâr türbini için hesaplanan AEP, aynı üç yükseklikte sırasıyla 1113, 1279 ve 1363 MWh'dir. Ekonomik fizibilite analiz sonuçlarına göre; 50, 65 ve 75 m türbin göbek yüksekliği olan 500 kW'lık bir rüzgâr türbininin kapasite faktörü (CF) sırasıyla %12, %14 and %15 olurken ve seviyelendirilmiş enerji maliyeti (LCOE) yine aynı sırayla 0.157, 0.139 and 0.132 USD/kW olarak tahmin edilmiştir. Aynı yüksekliklerde 750 kW'lık bir rüzgâr türbininin CF oranları %15, %17 ve %18 iken LCOE değerleri 0.136, 0.122 ve 0.116 USD/kW olarak hesaplanmıştır. Yine benzer şekilde 1 MW türbin için CF'si sırasıyla %13, %15 ve %16 iken, LCOE değeri sırasıyla 0.153, 0.136 ve 0.129 USD/kW olarak bulunmuştur. Fizibilite çalışması, 75 m türbin göbek yüksekliğinde 750 kW'lık bir rüzgâr türbininin ODTÜ KKK için en kazançlı, teknik ve ekonomik olarak uygulanabilir bir sistem olduğunu göstermektedir.

Anahtar Kelimeler: Rüzgâr Kaynağı Değerlendirmesi, Rüzgâr Hızı, Rüzgâr Enerjisi, Rüzgâr Değişim Üssü, Rüzgâr Hızı Dağılımı, Uygunluk İyiliği

DEDICATION

To My Beloved Family

For their unconditional support, trust and encouragement

ACKNOWLEDGMENT

After an intensive period, today is the day: writing this note of thanks is the finishing touch on my thesis. It has been a period of intense learning for me, not only in the scientific arena, but also on a personal level. Writing this thesis has had a big impact on me. I would like to reflect on the people who have supported and helped me so much throughout this period.

First and foremost, I offer my heartiest gratitude to my thesis advisor Assist. Prof. Dr. Onur Taylan of the Mechanical Engineering Department at Middle East Technical University Northern Cyprus Campus, who has supported and guided me throughout the completion of my thesis with his patience, skill and knowledge. The door to Dr. Taylan office was always open whenever I ran into a difficult spot or had a question about my research or writing. He consistently allowed this research to be my own work, but steered me in the right direction whenever he felt I needed it.

Besides my advisor, I would like to thank the rest of my thesis committee: Prof. Dr. Ali Cevat Taşıran, Prof. Dr. Derek K. Baker, Prof. Dr. Serkan Abbasoğlu and Assoc. Prof. Dr. Murat Fahrioğlu for their insightful comments and encouragement, which incented me to widen my research from various perspectives. I am grateful to Hüseyin Öner and Dr. Murat Fahrioğlu from REDAR group for providing me with the necessary wind speed data to successfully conduct this research.

I want to especially pay my genuine gratitude to Prof. Dr. Ali Cevat Taşıran for his remarkable advising and the time devoted to constructive “hair-pulling “during my time at METU NCC. Without his deep knowledge and incredible commitment, my experience and accomplishments would have been greatly diminished. I am deeply indebted to him and it was a privilege to be his student.

My sincere thanks also goes to Assist. Prof. Dr. Mustafa Murat Özer who provided me an opportunity to join their Physics group as a teaching assistant, without such financial support it would not have been possible to conduct this research with peace of mind.

With a special mention to Humayun Ahmed, Loiy Al-Ghussain, Syed Muhammad Hasan Ali and Arsalan Tariq for reading my work along the way and for their scientific inputs and valuable advices, which helped me to carry on towards relevant results. Besides the technical assistance, I would also like to acknowledge and thank other graduate students and friends Pradeep Jayaweera, Hana Kasht, Shahab Miri, Ipek Ertel, Linda Bahar Can, Fassahat Ullah Qureshi, Obaidullah Mohiuddin, Madina Obaidullah, Bushra Fatima, Muhammad Saleh Rashid, Ali Hamza and many others who made my stay and experience at METU NCC more joyful than a graduate student ever expects to be.

Last but not the least, I must express my very profound gratitude to my parents and siblings for providing me with unfailing support and continuous encouragement throughout my years of study and through the process of researching and writing this thesis. This accomplishment would not have been possible without them.

TABLE OF CONTENTS

LIST OF TABLES

LIST OF FIGURES

Chapter 1

INTRODUCTION

1.1 Motivation

Middle East Technical University Northern Cyprus Campus (METU NCC) is situated in Northern part of the Mediterranean island of Cyprus. Surrounded by Mediterranean Sea, electricity generation on the island solely relies on the importation of oil and gas to fuel power plants. In recent years, increasing energy demands, dwindling oil and gas prices, depleting resources and environmental impact of conventional fuels urged the university authorities to drop of their dependence on foreign sources of electricity generation. To be independent of these fossil fuels, METU NCC started transiting to their full potential of implementing sustainable power as a viable source of generating clean energy. In 2016, the university's own 1 MW PV power plant started working, reducing huge dependency on fossil fuels and help curtailing their adverse environmental impacts. University also plans to install a commercial wind power plant on campus, not only to reduce electricity cost but also to promote research and campus environment sustainability. The primary motivation for this thesis is to characterize the measured wind speed data and assess the wind energy potential for a defined geographical location, which is an important first step in the feasibility assessment of a wind power plant. Characterization of wind speed data involves analyzing in detail the measured data for quality and uncertainties to obtain an accurate estimation of the wind resources across the installation site. The wind resources directly affect the estimated energy output of the wind turbine. This research focuses on developing superior approaches as well as novel strategies that contradicts to the traditional process. Two major contributions are presented; (i) method to incorporate uncertainties/errors in the actual data, and (ii) new analysis approach for wind shear exponent assessment for a complex terrain, as well as its dependency on factors like wind speed, terrain, air density, etc. Statistical distributions like Weibull, Rayleigh and Lognormal will be used to identify wind speed variation with height and season, to

yield the annual energy production for any combination of wind speeds and turbine power curve.

1.2 Global Energy Scenario

Energy accessibility in any country has a straight connection with the solidity of its economy. Energy consumption per capita is an index tool, which reflects the success of any society. According to World Bank data, in 2014, world energy consumption per capita was about 3144 kWh/capita [1] The stability of global energy structure is dwindling, as the world's demand for energy is going to increase significantly in the next few decades, especially emission free electrical power.

The World Energy Outlook 2015 [2] from the OECD's International Energy Agency (IEA) sets out the present situation of electricity demand increasing twice as fast as overall energy use and electricity demand almost doubled from 1990 to 2011. Which is likely to rise by more than two-thirds from 2011 to 2040. In 2012, 42% of primary energy used was converted into electricity. In 2016, there was an increase of 7.5 TWh in the total electricity production of OECD, which has reached to 929.7 TWh. Increased demand is most dramatic in Asia, which is projected to increase on average 4.0% or 3.6% per year respectively to 2035 [3]. Th5 huge segment of energy is carried by China, who is still dominating the largest producer and consumer of coal in the world. It is predicted that by the end of 2030, China will pass over America, by being the largest consumer in oil and gas market. Launching the ETP (Energy Technology Perspectives) 2014 report, the IEA executive director said: "Electricity is going to play a defining role in the first half of this century as the energy carrier that increasingly powers economic growth and development. While this offers opportunities, it does not solve our problems; indeed, it creates many new challenges." [2].

Growing economy and industrialization has made it inevitably hard today, to sidestep the relentless reliability of our energy demands on fossil fuels consumption. However, over the past 15 years, energy industry has been through significant changes. Looking at the world energy resources in 2015[4] in Figure 1.1, it becomes evident that these

changes have been drastic in the past few years. For instance, there was just 1.1% increase in global energy demand in 2014, as compared to 2.5% increase in 2013. In 2015, it remained almost same and stable. With a share of 32.9%, oil remained the foremost choice. Surprisingly, the predominant fuel coal saw a decline of 0.6% in 2014 and further 2.8% drop in 2015, accounting for 32% of primary energy consumption. Natural gas is the only fossil fuel projected to grow more, contributed 23% share to the energy needs in 2015. Among the renewable energy sources, hydropower had the largest share in global electricity generation, almost 71% of total electricity by renewable's. Hydro shared 6.8% of the global energy consumption, while nuclear accounted for 4.4%, solar and wind were 1.4% and 0.45%, respectively in 2015.

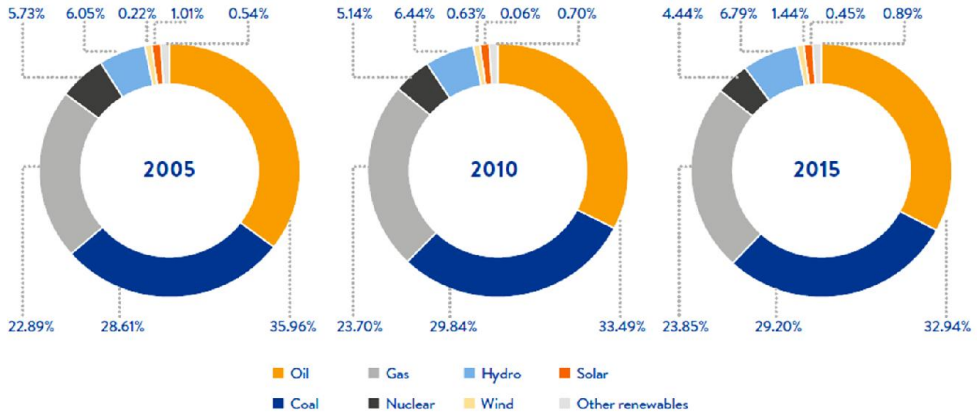

Figure 1.1 Comparative Global Energy Consumption [4]

Depleting oil, gas and coal resources and their adverse socio-economic impacts are the driving factor behind the tremendously increasing popularity of renewable energy resources because they provide pertinent solution to the consequences of problems. With rapidly growing power demand and concerns over energy security and local pollution, deployment of renewables has been accelerating and is expected to continue to do so. Renewables account for nearly half of the increase in global power generation to 2035, with variable sources – wind and solar photovoltaic – making up 45% of the expansion in renewables [5]. Renewable energy sources contribution in power

generation in 2014 was about 30% of the total installed capacity globally, 23% of which is used for electricity generation. Although transition from conventional fuels to renewable is not pacing at the speed everyone wants, it is taking momentum day by day. Solar and wind only have seen a dramatic increase in annual growth in past few years. By the end of 2015, solar powered electricity with 51% average annual growth, contributed 227 GWe to global installed capacity, with tremendous 80% drop in PV module price since 2007. Similarly, wind power reached an installed capacity of 432 GWh with an annual average growth of 23% in 2015 and it is hoped to be more than double by the end of 2030. In countries like Denmark and Germany, wind alone contributed 42% and 13%, respectively, to country's power production. Table 1.1 illustrates the growth comparison of installed capacities and shares of renewable energy sources from 2004 to 2014 [6].

Table 1.1 Renewable Energy Resources Share in Global Energy System [6]

Source	**Installed Capacity**				**Average Annual Growth (%)**	**2014 Production (TWh)**	**Share** (%)
	2004		**2014**				
	(GW)	Share (%)	(GW)	Share (%)			
Hydro	715	18.8	1,055	17.1	4	3,898	16.6
Wind	48	1.3	370	6.0	23	728	3.1
Biomass	39	1.0	93	1.5	9	423	1.8
Solar	3	0.1	181	2.9	51	211	0.9
Geothermal	9	0.2	13	0.2	4	94	0.4
Total Renewables	814	21.4	1,712	27.7	8	5,353	22.8
(Oil,Gas,Coal) **and Nuclear**	2,986	78.6	4,468	72.3	4	18,127	77.2
TOTAL	3,800	100	6,180	100	5	23,480	100

1.3 Energy Situation in Northern Cyprus

Northern Cyprus is a part of Cyprus, which is the third largest island in the Mediterranean Sea, situated at 35° north of the Equator. Total area of Northern Cyprus is 3354 km^2 [7]. Due to the reason that Northern Cyprus has no oil or gas reserves, Island's electricity production is mainly dependent upon burning of fossil fuels. Electricity generation, transmission and distribution is handled by a local utility company KIB-TEK (The Cyprus Turkish Electricity Authority) [8]. 350 MW electric power is generated by burning fuel oil no.6 containing around 3.5% of sulfur content, without realizing the fact that this not only poses health issues but also has severe damaging effect to the environment in form of greenhouse gas (GHG) emission. Financial constraints, lack of interest and dedication about environmental impacts and solar and wind energy potentials being not accurately known, are the possible reasons behind usage of conventional method of electricity generation.

Cyprus is an island suffering adversely from the scarcity of water, which makes hydropower not feasible on the island. In addition, solar thermal power plants are not economically feasible for small scale. The only feasible options are PV and wind power. Meteorological data and several case studies have proven the fact that Mediterranean islands tend to have large solar resources [9]. Similarly, many researches have done calculating the solar potential of the Northern Cyprus, finding that north Cyprus receives an average daily global solar radiation of 5 kWh/m^2. According to a study done by Erdil et al. [10], Northern Cyprus has long sunshine hours of approximately 12-13 hours in summer with a solar radiation value ranging from 7-8 kWh/m^2. Even though it is evident that island has a huge potential for solar power, still there is not enough progress done to harness solar resources, currently there is only one 1.3 MW photovoltaic power plant installed in Serhatkoy [11]. Recently, universities in the island have step up to raise awareness for island solar potential by installing PV plants in their campuses. In 2016, Middle East Technical University Northern Cyprus Campus and Cyprus International University have installed 1 MW and 1.3 MW photovoltaic power plants respectively [12] [13] [14]

On the other hand, very few research has been done so far to estimate the island wind energy potential. According to Partasides [15], even though Cyprus has limited wind resources but there are certain regions which receive 5-6 m/s wind on average. To meet the renewable energy goal, set by European Union 2020, Southern Cyprus especially has taken keen interest into exploiting the wind resources of the island. Under the Clean Development Mechanism (CDM) protocol, various wind farms received private funding's to be established in different parts of Southern Cyprus. According to United Nations Framework Convention on Climate Change(UNFCCC) CDM projects document Mari, Orites, Kambi, Stivo, Klavdia, Alexigros and Agia anna wind farms are to be established in Southern Cyprus [16] [17] [18] [19] [20] [21] [22]. Orites and Ketonis wind farms of 144 MW installed capacity, in Paphos and Larnaca respectively, have started contributing into the national grid [23]. Unfortunately, nothing substantial has been done by the Northern Cyprus authorities so far, regarding wind energy exploitation. A feasibility case study carried out by Altunc et al [24] analyzed the wind energy potential at various sites such as Kalecik, Sınırüstü, Yenierenköy, Sadrazamköy and Taşkent. According to the analysis these sites, at 30m height, have average wind speed of 3.6, 3.1, 4.3, 5.6 and 3.8 m/s. Study claimed that Sadrazamköy indicated significant potential of wind power generation and author claimed that a capacity factor of 35% or above can be achieved at this location. A technical assessment of wind power potential for Selvilitepe site in Northern Cyprus was done by Solyali et al. [25]. The wind speed data was collected for 10 min intervals between years 2007 and 2014 at this site. From the collected data and analysis, it was calculated that at 30m power density is at 207 W/m^2 and mean wind speed is 5.11m/s, at 50m power density is at 221 W/m^2 and at 90m power density is 329 W/m^2 with mean speed of 5.96 m/s. The study also reported an overlayered picture of the measurement sites in Northern Cyprus and the locations and sizes of the CDM registered wind farms in Southern Cyprus as shown in Figure 1.2.

Figure 1.2 Map of the measurement sites in Cyprus [25]

In another study [26], a 10 kW rated wind energy system was considered for profitability analysis method (i.e. Internal Rate of Return (IRR) method) to find the feasibility of a residential system installed in Northern Cyprus. Results showed that IRR for this wind energy system was 14.1%, which was higher than the PV system, and they concluded that there are some locations in Cyprus where wind energy systems are economically viable. In year 2001, Southern Cyprus funded a feasibility study project [27] to statistically analyze the windiest five locations along the coastline of the island, the cumulative frequency using Weibull distribution indicated that at least 40% of the time average wind speeds were in range of 5-7 m/s especially at southeast coast, which is feasible to encourage wind energy extraction via medium or small wind turbines.

Wind energy can be a significant part of the energy problems, if sufficient support and increased political will are applied to its development in the region. Hence, current study aims to contribute to ongoing efforts of raising awareness about wind energy utilization in the area.

1.4 Envionrmental Sustainability at METU NCC & Case Studies

Middle East Technical University, Northern Cyprus Campus (METU NCC) has taken substantial steps for sustainability practice from the beginning. Green Campus Initiative and offering a graduate program in sustainable environment and energy systems are some examples of the prominent contributions by the university to promote sustainability and create awareness for globally warming and climate change. In addition to that, installation of solar and wind resources measuring station in campus to provide researchers a platform to conduct research and contribute to recent advancement in renewable energy technologies [28].

To reduce its dependency on national grid and to minimize the usage of fossil fuel, numerous studies have been conducted to determine the feasibility of installing a PV power plant in campus and penetration of this large-scale PV plant into the main grid. Due to the findings of those feasibility studies, university has recently installed 1 MW PV plant for campus own power generation [9] [29] [30]. However, only one feasibility study undertaken by [31], estimating the wind energy potential at METU NCC using one year observed data at METU NCC wind measuring station and author concluded that there is not enough wind potential for exploiting wind resources at METU NCC. However, this study was just for a generalized overview of the site feasibility and it was based on only one-year hourly wind speed with fixed values of wind shear coefficient that led to ambiguities in the results. Because the location of the tower in campus is not ideal to take one fixed value of wind shear exponent, it is located in a complex terrain on a hilly area having a valley in East, grassland and small trees in North, flat land on West side and residential building on it south side approximately, as shown in Figure 1.3.

According to NASA report [32] for environmental guidelines criteria for the development of wind energy conversion system, if the terrain within 10 km radius surrounding of turbine has elevation difference of more than 60 m, it should be considered as a complex terrain. Therefore, the wind resource assessment at the site

should be carefully taken into account considering this site as a complex terrain, and a more detailed study is needed for this assessment.

Figure 1.3 Satellite view of Wind Tower at METU NCC

Chapter 2

LITERATURE REVIEW AND PROBLEM STATEMENT

The ability to characterize the available wind resources of any site is a pivotal factor in the wind energy development, site assessment and wind plant operation. A detailed wind resource assessment shows the necessary information needed to decide if the desired location has abundant resources available or not. Resource assessment is not a new concept. As discussed earlier, the motivation for selecting a study on campus sustainability is a result of the energy conditions of Northern Cyprus. The reason to select wind to contribute to this concept has also been explained in terms of analyzing the potential of wind energy on the campus wind mast site as well as the benefits of not only promoting wind power generation in the region and help minimizing the dependency on fuel oil, but also encourage investors to invest in wind energy in Cyprus.

Several wind resource assessment studies reported in the literature are being reviewed and discussed here. As a preliminary step in assessing a site wind potential, wind speed diurnal, seasonal and annual characteristics are analyzed, which provides an overview of the site's wind conditions. Baseer et al. [33] in their study emphasized on significance of analyzing seasonal and diurnal variations of wind speed data. Five-year hourly average wind speeds at 10, 50 and 90 m height were used to characterize the data for assessment of wind potential at a largest industrial site for Jubail, Saudi Arabia. Since the weather station located in an industrial area, wind shear exponent was calculated rather than using the typical 1/7 rule. Two parameter Weibull distribution was chosen for the analysis with a bin size of 1 m/s. Weibull parameters were calculated using maximum likelihood method. The results showed that wind shear exponent varies based on seasonal and diurnal analysis for different combinations like 10m to 50m and 10m to 90m showed small variations for seasonal calculation, but on the other hand diurnal variations showed the opposite results. An average 0.217 value of wind shear exponent was used to calculate energy output.

To investigate the effect of different sampling rates and averaging period on turbulence and turbulence power under typical atmospheric condition, Tabrizi et al. [34] discussed the case of installing small wind turbine on rooftop. A comparison was made between the characteristics calculated and the values already defined by International Electrotechnical Commission small wind turbine design standard (IEC61400-2). The study also discusses the two fundamental key parameters for wind measurements are 1) rate of sampling and 2) averaging period of sampled data. 10 min average wind speed data were taken at different sampling rates: 1 Hz, 4Hz and 10 Hz from a wind station on top of a large warehouse in Port Kennedy, Perth, Western Australia. Sampling rate and frequencies chosen for this case study were entirely based on previous literature. First analysis performed on 10 Hz data, by dividing 10 min data into 5 min and 1 min periods, showed that in neutral conditions maximum relative % difference between vertical component of turbulence intensity for 10 min and 1 min averaging periods is 11% and for unstable condition it was found to be 9.4%, as indicated in Figure 2.1 [34].

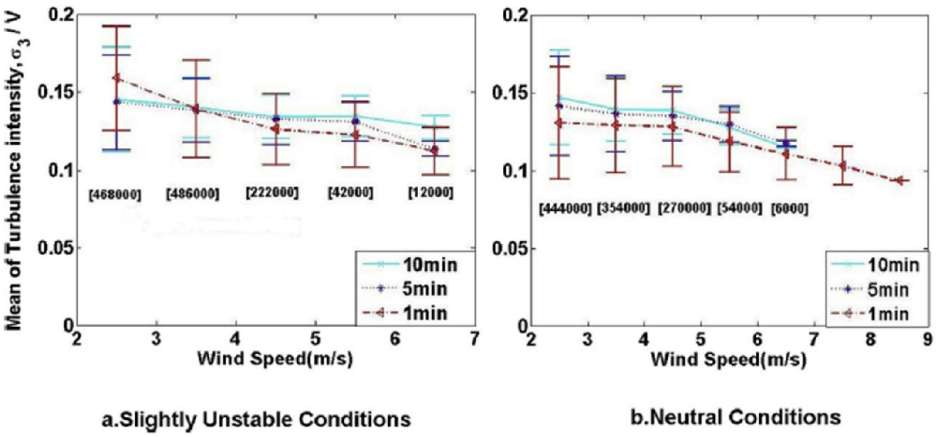

Figure 2.1 Effect of different averaging time on mean of turbulence intensity (vertical)

Contrary to vertical component, longitudinal and lateral components showed more sensitivity to averaging period. As an example, in Figure 2.2 maximum difference between longitudinal component of turbulence decreases from 29% to 22% by changing the average period from 10 min to 1min. Which implies that for neutral and

unstable atmospheric conditions, a decrease in averaging period decreases the turbulence intensity. Author concluded that the longer the averaging period, the more likely the variations will be, because longer periods allows capturing the wide range of wind conditions and larger standard deviations in wind speeds will be observed. As a result it is suggested to use 10 min values instead of 1 min or 5 min because the accuracy of the results will not be sufficient enough to conduct any research using these. [35]

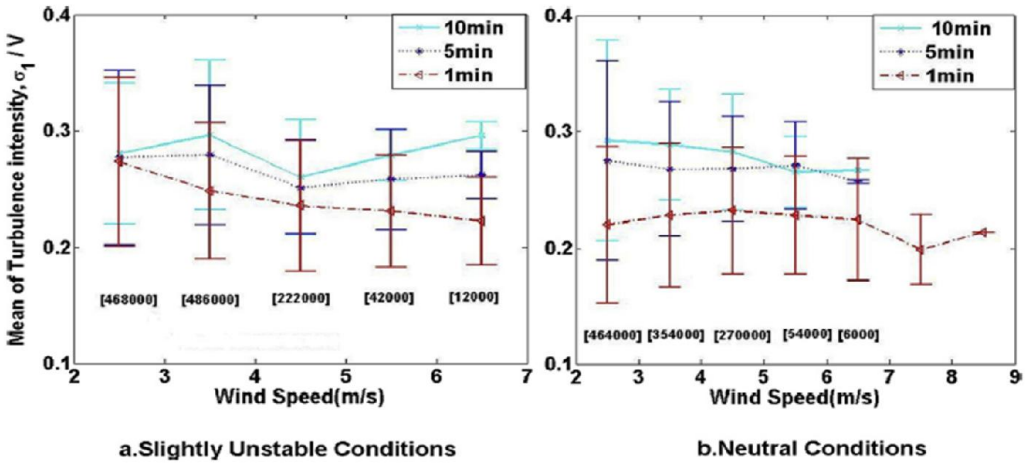

Figure 2.2 Effect of different averaging time on mean of turbulence intensity (longitudinal)

Kubik et al. [36] presented sensitivity analysis, using the hourly means of 10 min meteorological data from an airfield in West Freugh, Scotland, for power estimation at hub height. Wind speeds were extrapolated to 60m hub height using different values of wind shear exponent and surface roughness for power law and log law respectively. Results of the study indicated that wind shear exponent is comparatively more sensitive parameter than surface roughness from logarithmic law, a slight change in wind shear exponent value can lead to significant difference in turbine's hypothetical power output. More care must be taken while identifying a site's exponent value because it is a dynamic value that can vary with respect to day, season and topography. On the other hand, log law showed less variation as you moved above the ground due to decrease in surface roughness value. In the end if only one value of exponent must

be used than theoretical output must be validated by comparing with a nearby real wind power plant output. Honrubia et al. [37] explored the ways in which turbulence and vertical component of wind profile can significantly influence the power curve of wind turbine in a complex terrain of south of Spain. Study discussed that as the power curve is related to topography of the installing location, so it will be naturally affected by any change in turbulence. Similarly, turbulence intensity and wind shear exponent values are location-based parameters, which must be calculated using measured wind data on that specific site. Data for this study were collected using a Lidar system over a period of 3 months. Methodology presented in this study was based on "bin method" as described in international standard for turbine power curve characterization IEC 61400-12-1. The results exhibited that for stable condition wind shear exponent values were very high and low turbulence intensity. whereas unstable conditions lead to increase in turbulence intensity and variation in wind shear exponent. Diurnal analysis showed during daytime, when surface temperature of ground is higher than above ground, wind speeds do not vary much within difference heights. The opposite was observed during nighttime. One of the conclusion made from analysis were that using the higher value of shear leads to higher uncertainty in the calculated power.

Typical wind resource assessment methods as defined by IEC are still widely used but they still have some deficiencies. Wagner et al. [38] conducted the similar study for heights 10m, 40m, 60m, 80m, 100m, 116m and 165 meter for a flat terrain situated in northwest of Denmark. This study made a major contribution to the research by demonstrating the deficiencies in the typical wind resource assessment methods. The study argued that normally turbine power is calculated using extrapolated wind speed to hub heights, which suffers from inheriting uncertainties like assuming that wind speed at hub height is true representative of speed throughout the rotor surface area is adequate for small wind turbine only but it is not truly valid for large diameter and high hub heights turbines. Because rotor swept area of large turbine is exposed to immediate wind speed variation comprises of turbulence, wind shear exponent and wind direction. As a result, significant deviations are found between the hypothetically calculated power and actual produced power. The study proposes a new methodology

to calculate wind speed by slicing rotor swept area into 4-5 parts and measure wind speed corresponding to each part. The speed is named "equivalent wind speed" and was calculated by averaging the 10 min wind speeds at the corresponding area ratio A_i/A using below formula.

$$U_{eqM1} = \frac{1}{A}\sum_i \overline{U}.A_i \tag{1}$$

where A_i is corresponding area of the specific data point on rotor and A is the total swept area of rotor. The simulated results proved that using equivalent wind speed enhances the correlation between wind speed and electrical power output and it also considers the wind shear exponent and turbulence intensity variation across the swept area of turbine.

Another case study done by Honrubia et al. [39], it was emphasized that large wind turbine power curve calculations should consider more parameters than using just only hub height wind speeds. To support the suitability of the idea, wind speeds at 9 different elevation points were analyzed by extrapolating measured data using log law and power law. 10 min average values were chosen for the study, reason being that energy contained in smaller period is quite small. The results showed high variation across swept area of large-scale multi-MW turbines. Mahbub et al. [40] presented wind speed characteristics for a site in east of Saudi Arabia, using data from 1-07-2006 to 1-4-2009 using wind speeds at 10m,20m,30m and 40m heights. The wind shear exponent found using half-hourly mean wind speed varied between 0.24-0.27. Author stated that wind shear exponent values significantly depends upon climatological variations within 24 hours a day and there is no noticeable trend for seasonal variation of wind shear exponent. It was also concluded that wind shear exponent variation decreases with height, because an increase in height results in decrease in variation range of wind speeds. For example, at 40m height, half-hourly mean wind speed fluctuated from 4.7-7 m/s while at 20m it varied from 3-7 m/s. Schwartz and Elliott [41] characterized the wind shear exponent values calculated using wind speed data of 13 tall tower from 50m level to up to 113m at central plains. Power law was used to

calculate wind shear exponent values from hourly mean data for emphasizing the importance of site specific wind shear exponent over using typical 0.143(1/7) wind shear exponent value. Annual, diurnal and seasonal wind shear exponent calculated values were averaged by making a restriction of ignoring the wind shear exponent values calculated using wind speeds less than 3m/s because turbine cut-in speed is 3 m/s so rest of the values are of no importance. Annual wind shear exponent values reported ranged from 0.138 to 0.254 which is still greater than using 1/7 rule for extrapolation except one small value. Monthly mean capacity factor was found to vary between 25% to 57% for 60m and 30% to 60% for 100m hub heights. Schwartz and Elliott [42] in another study analyzed the wind speed data of tall towers for Kansas, Indiana and Minnesota up to 100m height for following reasons 1) to help understand wind variations due to regional climate 2) Numerical models prediction validation 3) Characterize wind shear exponent over the turbine rotor area. 10 min raw time series of wind speed and direction were converted into average annual, seasonal and diurnal graphs by NREL. Any anomaly present in data due to icing or equipment failure were deleted after inspection. The efficient way found in the study for detection of abnormality in data was to compare the monthly % of calm wind speeds from all measurement level with each other. If one month had more calms than the others or if calm wind percentage was showing an increasing trend with height, that data was tagged as interrupted or false data.

In a feasibility study by Saeidi et al. [43] for wind potential in two provinces of Iran, 10-minute wind speed data for year 2007 measured at 10, 30 and 40m were statistically analyzed. Wind shear exponent values for four different sites were calculate using curve fitting technique instead of using typical methods of power law or log law. Annual average wind shear exponent values found were 0.078, 0.184, 0.121 and 0.185. The results of 10 min wind speed data from a RASS sodar in Northern Spain from Aug 2002 to Jan 2004 used in a study by Perez et al. [44] for parameterization of wind profile suggested that amongst Power and Logarithmic law, former proved better approach for wind shear exponent calculation. Hourly medians of wind shear exponent values were calculated for each month which yielded a strong opposition between day

and night values. The exponent reported were less than 0.2 at daytime and more than 0.5 during the night. Linear regressions using hourly wind speed median showed wind shear exponent value to be from 0.2 to 0.4 throughout the day.

Archer and Jacobson [45] compared the different ways in which the wind speed can be extrapolated to hub height. The study used measured data from 1327 surface stations for year 2000, across the United States to investigate the spatial and temporal distributions of wind speeds in the U.S. After analyzing the extrapolated results from 10m to 80m using several methods, least square error fit method was found to be the most accurate among all while other methods underestimated the resources 60% of the tested cases. Results showed that average wind speeds at 80m were 1.3-1.7 m/s greater than those obtained using log law and power law with constant coefficients. An wind shear exponent value of 1/7 for power law underestimated the predicted values at hub height by an annual mean of 1.3 m/s 60% of the time. while, surface roughness= 0.01 lead to an annual mean underestimation of 1.7 m/s on average. for temporal and spatial evolution, daily average and hourly averages were used respectively. The study gives an account to the fact that wind speeds are Rayleigh in nature by showing that hourly wind speed frequency distributions for year 2000 at all selected stations was found very close to measured wind speeds. which further implies that wind speed for a given hour, averaged over either a month or a year, is still a fairly steady parameter. Results showed that monthly mean for a certain hour was found to be within 45-60% of annual mean speed for the similar hour. In addition, wind speed at 80m in most of the cases followed the similar trend of 10m wind speed. Another prominent finding of the study was that for sites having higher annual mean wind speed, annual wind speed is steady factor, for example in worst cases annual mean standard deviations were ±68%, in contrast to annual speeds the monthly standard deviations were ±94%. This clearly implies that longer average time results in more consistent winds and lower standard deviations. Even if the standard deviation for a given hour are high, total power produced for an averaging time still follows the mean speed.

Sisterson et al. [46] discussed the difficulties faced in using power law for wind resource assessment. Study was carried out at Argonne National Laboratory (ANL) in Illinois by using data measured at heights of 6m and 23m for a 4-year period. Power law results indicated that even with daily averages, use of power law with 1/7 wind shear exponent value to extrapolate 6m wind data to 45 m underestimated the values by 40%. Hourly values averaged over 10-mins were used to calculate site specific wind shear exponent values. Finding of the analysis seasonal variation of daily medians of wind shear exponent values were ranging from 0.14 for winter and higher than 0.20 in summer. The total difference between both seasons was found about 30% with an annual median to be 0.17. These high variations were found not only for season but diurnal variations were also significantly large. It was reported that for extreme cases an wind shear exponent value of 1 and above was also observed in some cases. The data yielded by Weisser and Foxon [47] study provide convincing evidence for implications of diurnal variations of wind speeds for wind resource assessment, by analyzing the hourly average wind speeds for the case study of Grenada. Two-parameter Weibull density function was used to identify probability of future wind regimes. Data was divided into two seasons, period of December to May was named Dry Seasons and from June to November named as Rainy season. Dry seasons represent stronger winds whereas rainy seasons are subjected to lower wind speeds. Based on results author concluded that for the studied site there is larger fluctuating output throughout the entire seasons, that is why serious care must be taken for underpinning of power calculations especially when timed output is essential for meeting the electricity demand. It was observed that for both seasons power output during the night is approximately twice the output during the daytime.

Lun and Lam [48] studied the effect of different topography on shape and scale parameters of two parameter Weibull distribution. Long-term hourly mean wind speed measurements of almost 30 years were used from three different locations in Hong Kong, a metropolitan area, a well-crowded city center and an open sea land area. Data analysis of all three stations showed enormous variation for both parameters; shape parameter from 1.63 to 2.03 and scale parameter ranging between 2.76 to 8.92. The

study emphasized on the use of longer period wind series for wind resource assessment because few year data can be misleading because of long-term averages. while, longer data period certainly results in better representative of the site assessment analysis. Pashardes and Christofides [49] produced the wind atlas for Cyprus island by using hourly mean values of wind speed and direction from 1981-1992 measured at 20 meteorological station across the island. Wind shear exponent variations across the whole island were measured and predicted results were compared with Wind Atlas Analysis and Application Program (WAsP) model results. Wind shear exponent assessment showed that annual mean wind shear exponent for coastal areas is about 0.15, whereas for location inside the island it is higher ranging between 0.3-0.4.

Dorvlo [50] estimated Weibull distribution parameters using long term average wind data (1986-1998) measured at 10m height at four different sites in Oman. The study used various techniques to calculate scale and shape parameters, instead of using typical method, method of moments, linear regression and chi square method were used. Huge variations were found in both parameters of Weibull distribution by all three methods. Based on the results from Kolmogorov-Smirnov test statistics it was concluded that chi-squared method gives best fit to wind speed distribution. Farrugia [51] assessed the significance of site-specific wind shear exponent especially for a Mediterranean Island. Mean wind speed data from 10m and 25m heights for a period of Aug 1995 to July 2001 were examined using power law. Based on the findings of the study it was concluded that wind shear exponent variations are not only terrain specific but also one must consider the suitable sampling interval of the measured data also. Overall, annual mean of wind shear exponent was found 0.36 for the Malta Island Garcia et al. [52] estimated the Weibull and lognormal distributions parameters using data from 1992-1995 at 20 different stations in Navarre. 10 min wind speeds were recorded but since preferred resolution is hourly so the average of six data per hour were taken for the analysis. Data were inspected for any abnormalities and missing values were deleted from the analyzed data. R-squared values were calculated to check the suitability of Weibull and lognormal distributions. The results indicated that for

high wind speeds Weibull best fits the data but for wind speeds less than 2 m/s, lognormal better predicts the distribution.

Kirchhoff and Kaminsky [53] developed the claim that wind shear exponent actually follows normal distribution. Data for this study were collected using a cup anemometer installed at 18.29 m above ground at the hilltop during October 1980 in Windsor, Massachusetts. Since then 15-minute interval average wind speeds and wind direction were measured for a period 02/21/1982 to 09/18/1982. In addition to that, two kite anemometers were also used at an elevation of 55m and 120m above ground. Using 10-minute wind speed data with a sample rate of 30 second, 173 measurements of wind shear exponent were calculated to determine the random nature of wind shear exponent from linear relationship as shown in Figure 2.3.

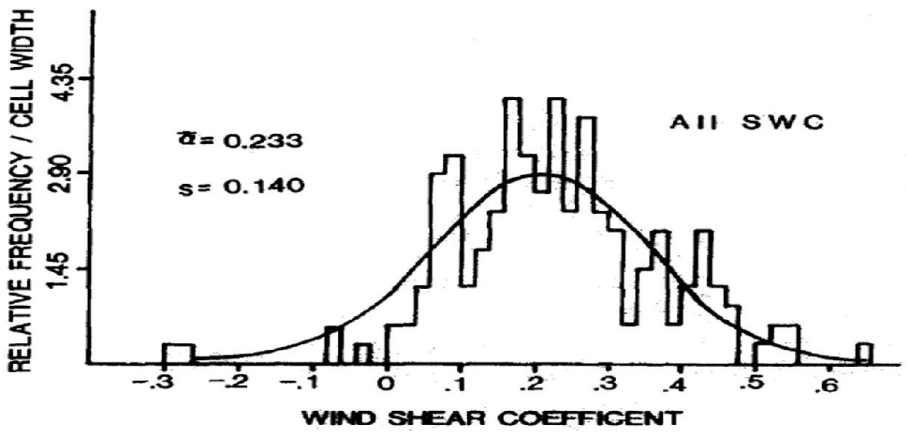

Figure 2.3 Frequency distribution of wind shear exponent [53]

The assumption was justified by conducting a chi-squared test at 5% confidence level. Negative and zero values of wind shear exponent were also observed for winds in the direction centered about 90°. Similarly negative and zero wind shear exponent values were also reported by Doran[54] for a complex terrain.

Rehman and Al-Abbadi [55] have encouraged debate on estimating wind shear exponent values by analyzing variation in wind shear coefficient and their effect on

wind energy output. This study used averaged half hourly measured wind data at 20m, 30m and 40m from 17/07/1995 to 30/12/1998 for a site in Saudi Arabia.

Two different approaches were proposed for calculation:

1) Use long term average wind speeds for calculating wind shear exponent at different heights (only consider positive wind shear exponent values and remove all zero's and negative values)

2) Use averaged half hour wind speed which corresponds to only wind shear exponent values ranging between ≥0 and ≤0.51 and ignore the rest

Table 2.1 shows the influence of diurnal and seasonal variations on wind shear exponent values is quite significant. Hence, for accurate energy output predictions hourly or monthly averages of wind shear exponent must be used to incorporate seasonal and diurnal variations.

Table 2.1 Half hourly mean values of wind shear exponent at different heights [55]

Wind Shear Exponent Between	**Based on all positive values of wind shear exponent**				**Based on all positive values of wind shear exponent ≤ 0.51**				**On overall mean wind speed**
	No	Max	Mean	SD	No	Max	Mean	SD	
α_1----30 and 20 m (WS3 and WS1)	43481	4.51	0.27	0.29	37068	0.51	0.18	0.15	0.19
α_2----40 and 30 m (WS5 and WS3)	21765	3.02	0.22	0.19	20242	0.51	0.19	0.14	0.07
α_3----40 and 20 m (WS5 and WS1)	27926	2.80	0.25	0.23	25141	0.51	0.20	0.15	0.14
α_4----30 and 20 m (WS4 and WS2)	49451	4.44	0.32	0.34	39961	0.51	0.20	0.14	0.29
α_5----40 and 30 m (WS6 and WS4)	36945	5.28	0.24	0.28	32931	0.51	0.17	0.14	0.06
α_6----40 and 20 m (WS6 and WS2)	46608	2.96	0.26	0.26	41023	0.51	0.18	0.14	0.19

The smallest values reported, corresponds to α_2 and α_5, are because the surface effects getting less as we move towards higher altitudes. Study recommended that wind shear exponent values shall be determined using long term average wind speed rather than

hourly averages. Annual average wind shear exponent of 0.194 was selected as best representative of the studied site. Their analysis results also showed an underestimation of the wind energy by 6% compared to the shear coefficient obtained from the power law. In addition to wind shear exponent values, air density values were also calculated using the measured ambient air temperature and surface pressure, instead of taking one value for analysis. Air density found was 1.18 kg/m^3 and it tends vary not only with temperature and pressure but seasonal and hourly variations as well.

The strong dependency of wind shear exponent on numerous factors was analyzed briefly by Ray et al.[56]. They discussed that wind shear exponent is dependent on numerous factors, including the wind speed, elevation from ground, the ground's surface roughness and its roughness variation, the atmospheric stability, and the land topography. It is mandatory to examine the variation of wind shear coefficient with height and other factors instead of taking one constant value using 1/7 power law. Lubitz [57] reported the uncertainty that might rise if wind speed data from an anemometer shorter than 40m is used for wind speed measurements. Hourly wind speed values from anemometer below 40m were used from 5 tall towers in central United States to extrapolate wind speeds to hub height of above 70m. Data were sorted out for a quality check and if any value at lowest level was ≥ 3.5 m/s it was tagged as inconsistent and then removed. In addition, if the difference between two wind speed directions was greater than 60°, that reading was also removed from data. 1/7 power law, 2 level power law fit and a hybrid model of both power law techniques were used to calculate wind shear exponent variations. Predicted wind speeds using wind shear exponent values from these models were compared with measured data by calculating mean absolute error (MAE) and mean error (ME). Results of the study showed that MAE increases with increase in height of prediction level from the anemometer height. Study also reported that tower with low wind speeds showed higher variation while increase in wind speeds leads to wind shear exponent value closer and closer to 1/7. It was concluded that predicting an error in extrapolation techniques used is much more difficult and huge errors can be expected sometimes. Therefore, extrapolation techniques should only be applied when there is no other option available.

Bientz et al. [58] evaluated a site at Autonomous University of Yucatan, Mexico for wind shear exponent variation due to the complex topography of the Yucatan Peninsula. 10-minute wind speed values were obtained by averaging the 2 second measured speeds for 18 months. Power law results showed that for investigated site, wind shear exponent values vary from 0.17 to 0.26 with an average of 0.21. Frequency distribution of calculated wind shear exponent values was also obtained by using a bin size of 0.05. Distribution showed that wind shear exponent values are ranging from -0.2 to 0.6 with a maximum of 0.2 which agrees with the average wind shear exponent calculated. Based on the findings, it was determined that using average wind speeds is an inadequate approach, hence frequency distribution provides more trust worthy and clear picture of the vertical wind profile. Fırtın et al. [59] evaluated the wind shear exponent effect on energy production of a wind turbine. 10-minute wind speeds were collected at 50m, 30m and 10m from Oct 2008 to Sep 2009 in Balikesir. During quality test, any missing interval or null data was removed for the inconsistencies. Power law was used to calculate wind shear exponent values for different combinations of height. The analysis result showed a difference of 50% approximately between predicted wind energy using extrapolated wind speeds and energy output using actual measured wind speed data. Power law results for wind shear exponent calculation between 30m and 50m reported 36% of the total wind shear exponent values were negative, 46% between 0-0.14 and rest were more than 0.14. The data appear to suggest that negative values are probably due to the atmospheric instability, turbulence and topographical variations. In a study presented by Minnesota Department of Commerce for Wind Resource Analysis Program [60], Wind shear coefficient for 39 different regions in USA were calculated and it was found that 92% of the time wind shear exponent values were above 0.14 and 2% of the wind shear exponent calculated were negative numbers.

Rehman and Al-Abbadi [61] in their study compared the annual energy yield between wind shear exponent as 0.143 and locally calculated wind shear exponent 0.255 for the city Dhulom in Saudi Arabia. Half hour mean wind speeds were obtained from 20m, 30m and 40m heights measured between 01/12/1998 to 12/10/2002. Air density variations were also reported by using data from 2m above ground level measuring

station. Based on the results, wind shear exponent of 0.255 and air density 1.06 kg/m^3 were recommended. Energy difference of 10-20% higher than 1/7 value was found by using 0.255 wind shear exponent. Fyrippis et al. [62] assessed the wind energy potential of Naxos Island, Greece by characterizing wind speed data using Weibull and Rayleigh distributions. 10 min wind speed data were averaged to hourly values for one-year data. Reason for preferring hourly values to 10-minute data was to reduce the time and cost of processing the long-term data. Mean wind speeds were characterized by plotting data and standard deviations with 95% confidence level. To evaluate the best fit distribution mean root-square error (RMSE), chi-square test and modelling efficiency were conducted. Analysis indicated weibull distribution would be the best choice for the investigated site. Tiang and Ishak [63] technically reviewed the feasibility of using Rayleigh distribution for small scale wind turbine in Penang Island, Malaysia. Hourly data were obtained from a mast of 12.5 m height for a period of one year. The result indicated that for the island grid connected wind power may not be the feasible option but at a small-scale wind energy can be a sustainable option for the Penang city. Islamet al. [64] did the similar study for the cities of Kudat and Labuan in Malaysia by using data of 2006-2008. 10-second wind speeds were averaged over 5 minutes and then further to hourly data. Analysis showed that Weibull distribution is a suitable distribution function for both sites.

Another crucial factor in analyzing the strength of a site wind potential is the wind speed distribution. 50 years ago, for the very first time, wind speed statistical study was carried out by treating it as a discreet random variable for the Gamma distribution [65] [66]. Over the time, numerous statistical distributions have been tested for best representation of wind speed data, few of those were Pearson, Chi-square, Gamma, 2-parameter Weibull, 3-parameter Weibull, Rayleigh and Johnson functions [67] [68] [69] [70]. Based on analysis results, few non-normal distributions are chosen for appropriation in well describing the wind speed distribution, for instance inverse Gaussian [71], Log-normal [72], 2-3 parameter Weibull distribution [73] [74] [75] and square-normal distributions [76] are few of those appropriate models.

Weibull distribution is one of the most popular and reliable distribution function used in wind power analysis. It is very common practice to use Weibull distribution approach due to its versatile, flexible and useful nature for analyzing wind speed variations for modelling wind energy resources [77] [78] [79] [80].

However, Li [81] and Mostafaeipour et al. [82] suggested that this distribution is not a good choice for low speed location because it has a main limitation that it does not precisely represent the probabilities of observing zero or very low wind speeds. Olaofe and Folly [83] in their study used three distribution function for assessment of 1 year wind resources at 10,50 and 70m height respectively for identification of best distribution of wind speed variation. They found out that Rayleigh distribution modelled the best fit for wind resources with complete accuracy. They suggested that a distribution function must not be chosen based on the general rule of thumb always. Aidan and Ododo [84] reported that for sites having very low/calm wind speed, the Weibull function does not model well the wind speed. Ulgen et al. [85] wind speed characteristics were analyzed using the hourly measured values over a period of 1997-2002 for Aksehir Konya, Turkey. Weibull and Rayleigh distribution functions were evaluated to find the best for the site data. Based on root mean square error Rayleigh distribution was found in best agreement with the actual data probability for statistical distribution. It was concluded that for site having an annual average wind speeds up to 5m/s, Rayleigh distribution is the preferable choice. Brower [86] said that not only low wind speeds but if there are two peeks in wind speed data, Weibull distribution will not accurately fit the data.

Since Weibull distribution does not accurately fits for location with low wind speed, three statistical distribution functions Exponential Weibull, Rayleigh and Lognormal will be used in this study to identify a function which gives the best presentation of wind speed variation with height and season.

2.1 Study Objective

The overall objective of this study is to conduct comprehensive wind resources assessment and analysis for METU NCC site. In addition, this case study explores the feasibility of installing a wind energy system as a complement to the green energy strategy of the university. Following are the specific objectives of this study:

- To analyze the measured wind speed data for any anomalies and uncertainties
- To analyze the drawbacks and make a comparison of synthetically generated Typical Meteorological Year data (TMY) as compared to measured site data
- To model the wind shear exponent (α) with different statistical methods
- To Analyze the diurnal and seasonal variation of calculated wind shear exponent values and its statistical distribution
- To extrapolate the measured wind speeds to a desired hub height using optimum wind shear exponent value
- To find the best distribution fit to measured data amongst various statistical distributions
- To model the power curve of selected wind turbines by various approaches
- To compute annual energy from a 500,750 and 1000 kW wind turbine at studied site
- To perform preliminary economic analysis of selected turbines

Chapter 3

METHODOLOGY

3.1 Roadmap for Wind Resources Assessment

The ability to characterize the available wind resources of any site is a pivotal factor in the wind energy development, site assessment and wind plant operation. A detailed wind resource assessment shows the necessary information needed to decide if the desired location has abundant resources available or not. Wind resource assessment is a crucial activity evolving with implementing complex analytical methods to evaluate the technical feasibility and economic viability of the target site.

A comprehensive description of conventional wind site assessment techniques and steps is provided by the NREL in the "Wind Resource Assessment Handbook" [87]. The preliminary step in the assessment starts with identifying the area where wind is viable. Once the location is determined, wind resources measurement is carried out until sufficient amount of data is collected. Next step involves long-term data validation, extrapolating the resources to hub height, obtaining representative distributions and their parameters. Finally, the annual energy production is estimated which combines computing selected turbine output via power curve and the relevant economic evaluation parameters. A stepwise progress stages are illustrated by the Figure 3.1 below, where yellow fields involve calculation processes while blue indicates data sources.

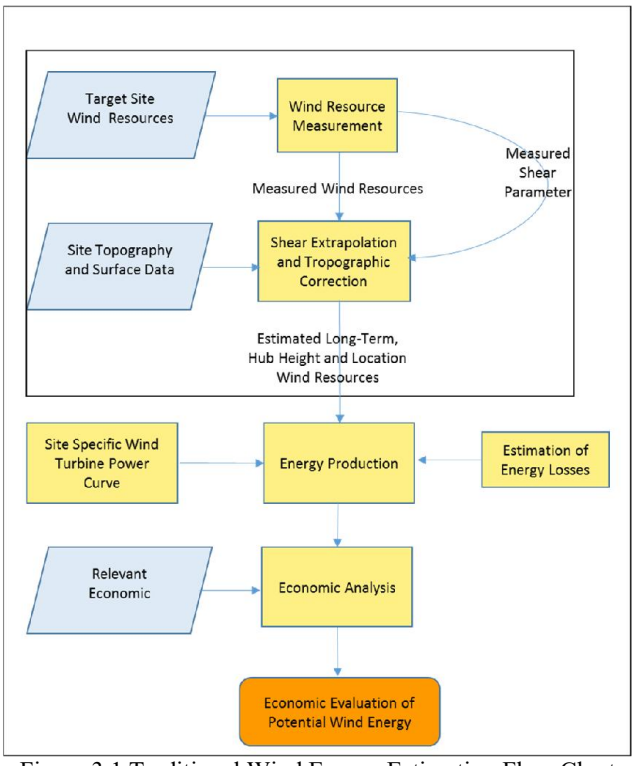

Figure 3.1 Traditional Wind Energy Estimation Flow Chart

3.2 Study Site Description

The wind tower is located at Middle East Technical University Northern Cyprus Campus, which is nearby Guzelyurt city.

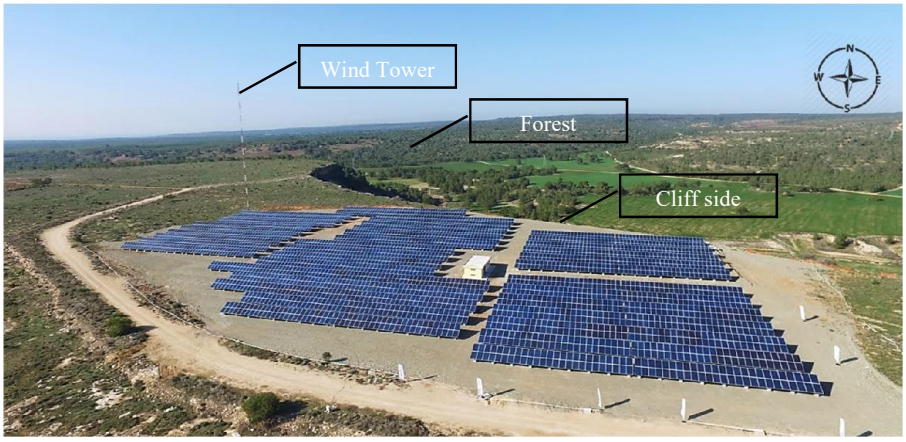

Figure 3.2 Topographical properties of wind tower surrounding [88]

More specifically, it is located about 200-meter Northwest of the Engineering Laboratories building of the campus. The geographical coordinates of the wind tower are latitude of 35°15'11.42" North, 33° 0'53.46" East longitude and an elevation of 127-meter above sea level. The topography around the tower can be clearly seen in Figure 3.2, a cliff side with grassland and small forest area from North to South East Direction, flat barren land from West to North-West and PV plant and campus buildings from South to South-West Direction. A clear satellite view of the site is also shown in Figure 1.3.

A 60-meter wind tower installed on site in the year 2013 is facilitating collection of data required since February 2013. As it is crucial to study the effect of terrain i.e. wind shear exponent effect on the wind velocity profile. Wind speed is measured at heights of 30, 40, 50 and 60 m above ground level as shown in Figure 3.3.

Figure 3.3 60-meter tall wind tower at METU [88]

Figure 3.4 presents the schematic diagram of the wind tower. Following devices are installed on the tower to measure, wind speed, wind direction, temperature, humidity etc.

1. Anemometer:

   An anemometer is a device used to measure the wind speed. Rotating cup anemometers of Thies Clima company are installed on wind tower at 30, 40, 50 and 60 meters height to measure the speed. Anemometer does not measure the wind speed directly, instead the number of revolution it makes are recorded by opto-electronic and converted into a square wave signal. The signal frequency and rotational speed of anemometer are directly proportional. Later on, these are transmitted to a data acquisition device called datalogger, which further records the values and provides ten-minute average (resolution can be adjusted according to needs) values of maximum wind speed, minimum wind speed and standard deviation of wind speed. Further details and specification of the cup anemometer can be found here [89].

2. Wind vane

   Wind vanes are used to measure the direction of wind speed. NRG WINDVANE MODEL 200P [90] is installed at 48 m and 58-meter height on tower to measure the direction. Datalogger records the data and provides a 10-minute average (adjustable) of wind directions.

3. Shield, Humidity Sensor

4. Thermometer (for measuring Temperature)

   Barometer (for measuring Pressure)

   Datalogger

   Solar charge controller and battery (to store solar panel energy)

5. GPS-GPRS antenna

6. Solar panel (for powering the sensors and other devices)

7. Lightning rod (to divert lightning harmlessly into the ground)

8. Warning lamp (for aviation)

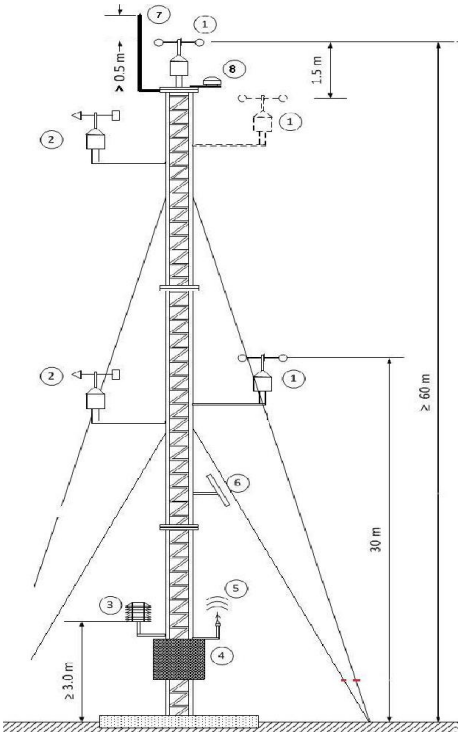

Figure 3.4 Schematic Diagram of Wind Mast at METU NCC [31]

3.3 Resource Site Data Analysis

3.3.1 Data Importing and Validation

Measured data from the anemometer, wind vanes and other sensors are recorded into the on-site datalogger and then further it is transmitted wirelessly to a local PC regularly via GSM system. System provides the industry standard 10-min average values of the minimum, maximum, standard deviation, wind speed, wind directions, temperature, pressure and humidity. Once these data are downloaded, it needs to be carefully assessed to screen anomalies and flag the missing or invalid data along with

its timestamp. Several missing days and hours in the dataset were found due to hardware errors. Wind mast started operating functionally on 18.2.13, due to hard storm the data between 18.2.13-19.2.13 was completely lost and anemometer 3 (at 40 meter) got damaged in the same storm. It was fixed by the end of September 2013, so the analysis for 2013 does not include data of 40 m height. Similarly, by the end of 2015, 15/12/2015 anemometer 1 at 60 m height was damaged and it was repaired by the end of May 2016. Even though it was properly functioning for the rest of the time-period, upon analyzing the data it was found that 60 m measurements have large deviations. Approximately 20% of the measured wind speeds at 60 m were lower than the wind speeds recorded at 50 m height which makes the data suspicious as physically it is not possible, because wind velocity increases with increase in height. Further analysis and discussion about this issue will be shown in upcoming sections. Overall, 30 m and 50 m height datasets are the only reliable and error-free datasets, so mostly analysis made in the study are based on these two datasets.

3.3.2 Wind Data Uncertainty Analysis

Since wind is variable in nature and it is a weather phenomenon caused by local and global winds. As the wind speeds fluctuate all the time, so does the energy content. As a result, there is always an uncertainty inherited in the recorded wind data. So, no matter how much care has been taken all the analysis made based on these measurements are prone to errors. Error of 1% in measuring the wind resources can result in 2-4% energy output error. Measured values are subjected to two types of uncertainties:

1. Standard Error:

It is the combination of Systematic Error and Standard Deviation. Systematic errors are those errors which are usually due to calibration problem or manufacturing error and they are already incorporated into the measuring device. Sometimes they are also referred as tolerance limit. Such type of error cannot be revealed by averaging the measured data.

$$x \pm \Delta x \tag{2}$$

Here x is the measured value, and Δx is the absolute system error/uncertainty in it. For the anemometer used, it is 1% of the measured value [89].

Standard deviation (σ) is assumed to be the measurement uncertainty due to the random error. It expresses the variability or deviation of measured quantity.

Standard error (S.E.) is calculated by taking the square root of squares of systematic error and standard deviation.

$$S.E. = \sqrt{\Delta x^2 + \sigma^2} \tag{3}$$

2. Temporal Resolution:

Temporal resolution is a crucial factor in wind resource analysis, averaging the data over a specific time span may result in losing the critical information. For example, majority of the studies carried out in literature relied on hourly or daily wind speed data by averaging the 10-minute values mostly to save time and cost, which might have resulted in either underestimating or overestimation of the site potential. Because of the randomly changing nature of wind, systems lack the ability to duplicate the conditions from one hour to another or one day to the next. Decision makers need to comprehend the stochastic wind nature effect in the wind resources assessment analysis. Therefore, there is a dire need of high-frequency wind data to simulate the realistic nature of resources available on the site. It has been argued and verified in various case studies that a decrease in averaging period decreases the turbulence intensity; and the more data information available, the more certain analysis results will be [34] [58] [91]. The international Electrotechnical Commission (IEC) has specifically recommended, using the 10-min average data regarding wind turbines and power generation analysis, in IEC 61400-12-1 standards [92]. Figure 12 depicts the wind speed variation on a typical day (19 Jan 2016), as it is evident that temporal resolution can be misleading sometime. For example, at 12:50h to 13:10h where wind speed increased drastically by 6 m/s and then again it increased by 4-5 m/s in next time

interval and similarly within next hour it plunged by 5 m/s suddenly. In such conditions if hourly average is to be used, it will either over-predict or underestimate the system output. Likewise happens when daily wind speeds are used for assessment methods. As shown in Figure 3.5 daily average does not take into account high wind speeds occurred during 3-4-hour time period. So, it is strongly advised to use a minimum of 10-min average at least in site feasibility analysis.

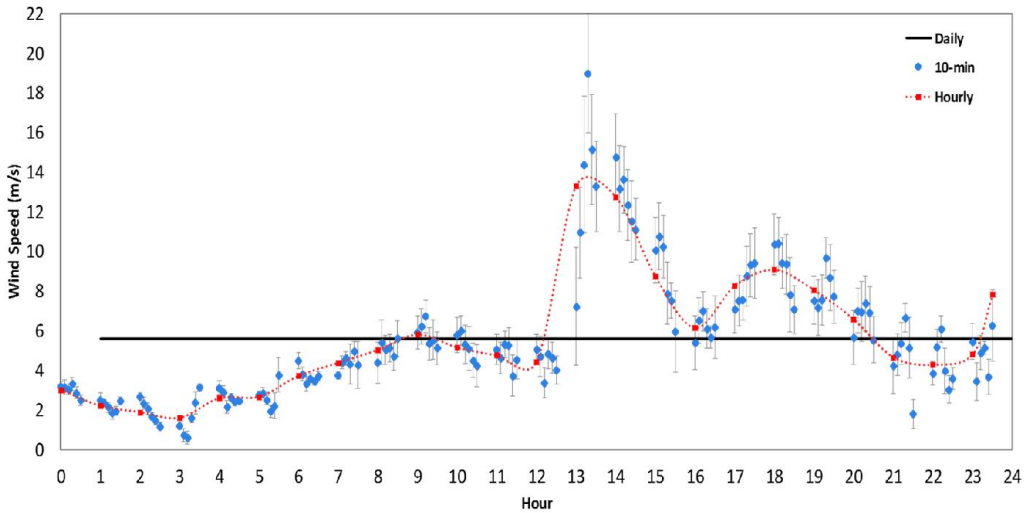

Figure 3.5 Diurnal variation of 30m wind speed on a typical day (19 Jan 2016)

Even though there is not optimal choice defined in literature, which defines a perfect bin width for the data analysis, but some methods have been determined which more or less serve the purpose very well. Therefore, finding an appropriate bin width requires experimentation with these suggested methods. As a rule of thumb, it should be made sure that whichever method is used, bin width is neither too small nor too large.

a. **Method of Sturges**: This method is used by default in R software, it generally approximates the data shaped to be normally distributed, so it may perform poorly if data is not normally distributed [93].

$$k = [log_2 n + 1] \tag{4}$$

where k is bin size and n is the number of data.

b. **IEC Method:** The International Electrotechnical Commission (IEC) has recommended using a contagious bin size of 0.5 m/s in IEC standards for wind turbines power generation [94].

c. **Freedman Diaconi's Rule (FD):** This is a very robust approach widely used in practice [95].

$$k = 2\frac{\mathrm{IQR}(x)}{n^{1/3}} \tag{5}$$

where IQR represents interquartile range of data x and n is the number of data.

d. **Square-Root method:** This method is used by default by MS-Excel and some other software's for plotting histogram automatically.[96]

$$k = \sqrt{n} \tag{6}$$

Figure 3.6 shows a comparison between different bin size methods for bin width of 30-meter wind speed data (2013-2016) histogram. As shown in comparison choosing a small bin size results in less fluctuations at each bin, which in case of wind speed is efficient method. Similarly, a larger bin can result in very bad resolution of the data. Therefore, FD rule portrays the underlying distribution of the wind speeds quite effectively. Further comparison using wind power output will be made in the following sections.

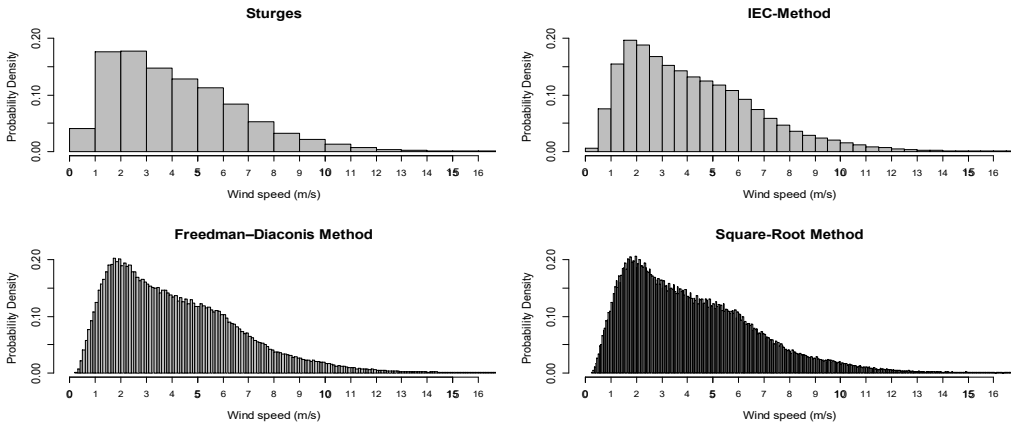

Figure 3.6 Histogram of 30-meter wind speed data of all years (2013-2016)

Another comparison illustrated by Figure 13 highlights the importance of choosing a right time resolution for the analysis. Figure 13 shows density histograms of 10-min, hourly and daily wind speed data of all years (2013-2016), it is quite prominent that hourly and daily values are not the quite representative of real scenario, as they both are overpredicting the wind speed probabilities. Because hourly and daily values are averages of an hour and day, respectively, they fail to incorporate the variation of wind speed within that specific time period. Hence, for reliable and precise analysis of the data, time resolution must be kept as low as possible.

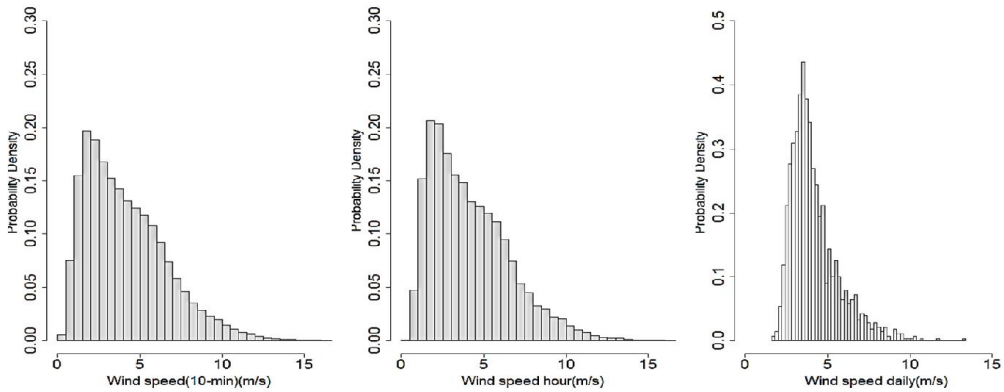

Figure 3.7 Histogram of 30-meter wind speed with different resolutions (2013-2016)

3.3.3 Comparison with Typical Meteorological Year Data

When a short span data is used for long-term wind resources assessment, by averaging it further we are losing a major chunk of information. Uncertainty still arises in the analysis results because a finite number of year wind data is not the representative of upcoming year or 20-year long time span or longer.

One of the most convenient and common sequence of data generation is Typical Meteorological Year (TMY) data. Hourly wind speed values are generated by calculating the long-term cumulative distribution function (CDF) of long-term weather data and each selected month is the most typical month of these long-term weather data as being the best representative of that specific month [97] [98]. METEONORM is a software that generates synthetic TMY data by interpolating existing TMY data from nearby stations [99]. The problem arises when there are no available weather stations nearby and the data is generated by interpolation of far by stations. In this case, it is not clear that either it brings into consideration the effect of different variables like distance, elevation, humidity, temperature, seawater effect, topography of the area, etc. Kubik et al. [100] investigated the accuracy of the simulated output data of a wind farm using synthetically generated data by interpolating nearby meteorological station in West Freugh. Simulation results were compared with actual output of a wind farm in North Rhins, Scotland and comparison showed that although in long-term energy generation there was no big variation but there was significant difference between simulation and reality on an hourly power generation basis. In another study, Kubik et al. [101] mentioned that it has become a well-established approach to use typical meteorological data to simulate future wind power generation, in order to check regional wind variability due to climate effect. Authors argued that this type of approach is inadequate because such data can be affected while interpolating, by a site's own unique topography. Further, since the data are based on historical data records so they may not incorporate in-situ changes like buildings construction and tree growth in the area, etc. Additionally, Kotroni et al. [102] explicitly suggested that existing typical meteorological year datasets are totally inappropriate for any type of

wind power potential study. They stated that TMY datasets are mainly purposeful for solar related applications simulations, thus appropriate wind resource data must be used to predict energy output because performance of the wind turbine system not only depends on long term climatic conditions but also on short term effects of it.

Figure 3.8 shows an explicit comparison between probability densities and cumulative distribution functions of hourly measured wind speed data at METU NCC and two versions of TMY data generated using software METEONORM v6 and v7. It is evident that synthetically generated data do not represent a site's characteristics. Although there are locations for which it does predict accurately but for METU NCC that is not the case. Both versions of the TMY data fails to follow the distribution of actual measured data.

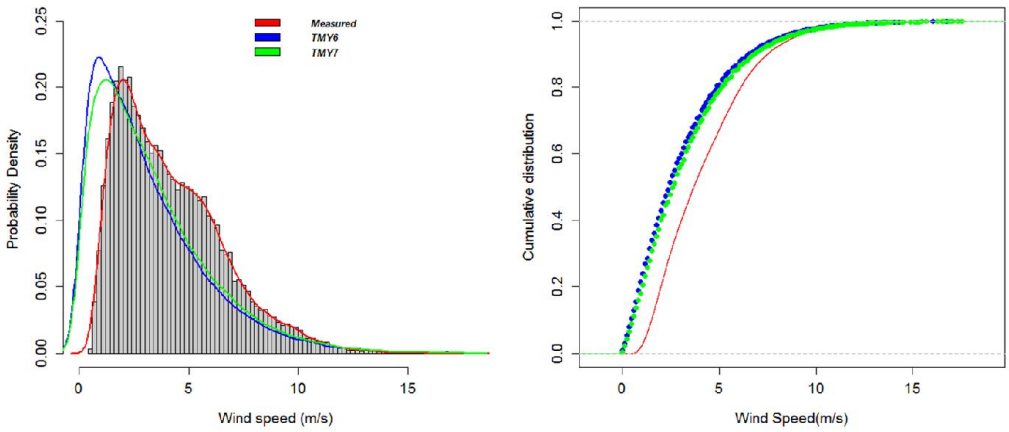

Figure 3.8 PDF & CDF comparison of measured wind speeds 30m (2013-2016) & TMY generated wind speeds

Another comparison shown in Figure 3.9 between monthly averages of measured wind speed data and TMY data substantiates the point that using a finite number of year data to estimate long-term wind power leads to uncertainties in the results. Use of any version of TMY data for METU NCC location is not feasible, as it clearly underestimates the site wind potential. Further comparative analysis is shown in upcoming section in terms of goodness of fit.

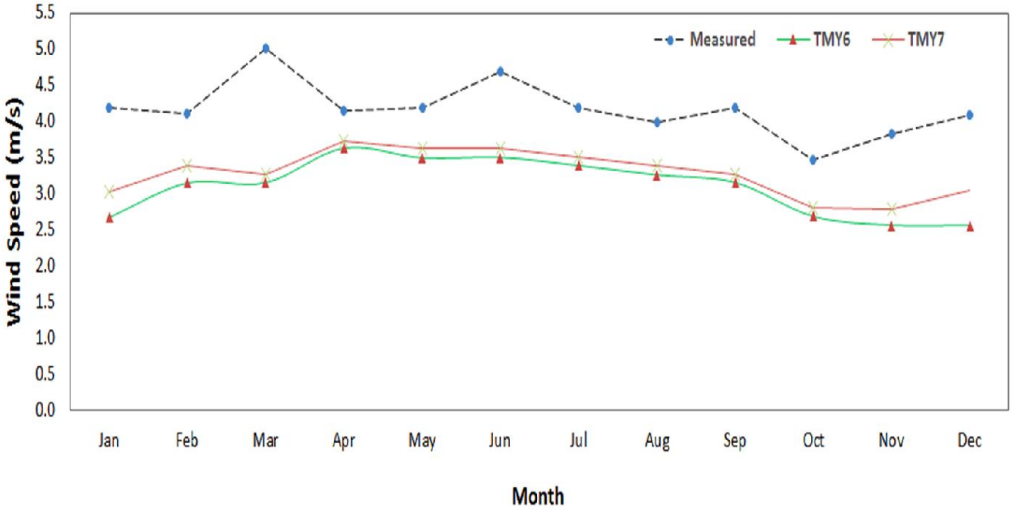

Figure 3.9 Average monthly wind speeds

3.4 Wind Speed Characteristics at METU NCC

As a preliminary step in assessing a site wind potential, wind speed diurnal, seasonal and annual characteristics are analyzed, which provides an overview of the site's wind conditions. Figure 3.10 plots the monthly wind speeds of all years.

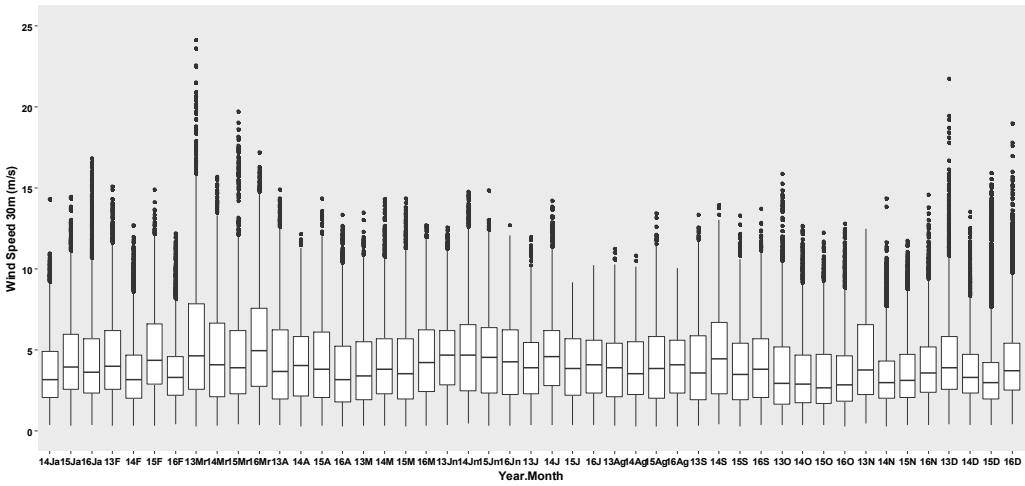

Figure 3.10 Box plot of 10 min wind speed (30 meter) data of all years (2013-2016)

Such a typical box and whisker plot is quite informative as it highlights the summary of data in terms of seasonal and monthly variations. It generally consists of median, maximum, minimum and the lower (25%) and upper (75%) quantile recorded in each month. This is the most efficient way to examine the underlying theory of distributed data series, as it shows either wind speeds are skewed or widely spread in each month or how far the maximum wind speeds were recorded from the data majority. It can be inferred from the plot that winter months (November-March) have wide spread data with majority of maximum wind speeds, while summer season has a plateau as there are very few values recorded as maximum and mostly data is skewed around an average wind speed of 5 m/s, which makes METU NCC site to fall under IEC wind class I [103].

Figure 3.11 represents the plots of probability density function (pdf) and cumulative distribution function (cdf) of wind speed at both 30 m and 50 m. It can be interpreted from the plots that probability of low wind speeds is higher at lower heights as compared to the upper heights, where distribution is more widely spread than skewed or taller.

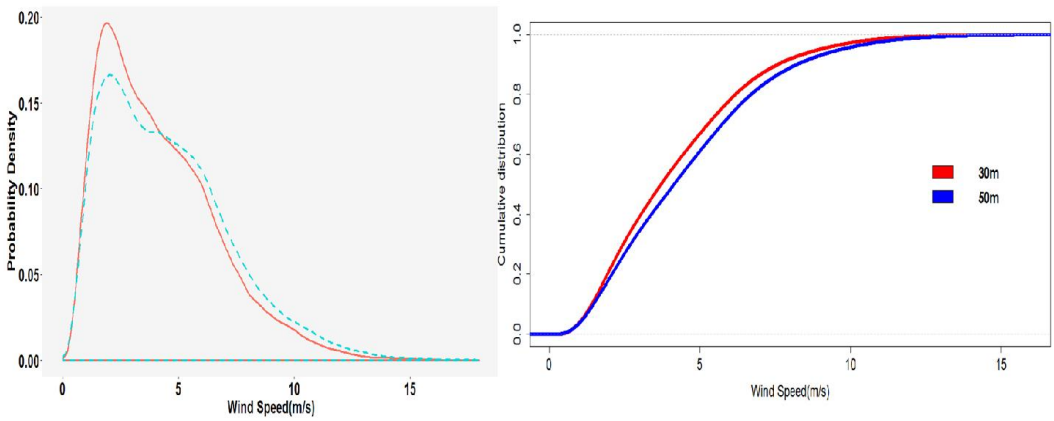

Figure 3.11 Probability Density and Cumulative Distribution Function of 30m & 50m wind speeds of all years (2013-2016)

Diurnal variations of 10-min average wind speed at different heights are shown below in Figure 3.12. Over a 24-hour period, wind fluctuates in a similar pattern at both heights.

Such variations are very typical of wind because of thermal stability phenomenon, as during daytime sun heats up the land, which causes low-pressure air to rise and forces the flow of cool sea air. While, it is the opposite at nighttime, since nights are usually cold, which means less temperature difference between land and sea air, thus less turbulent calm wind speeds at night.

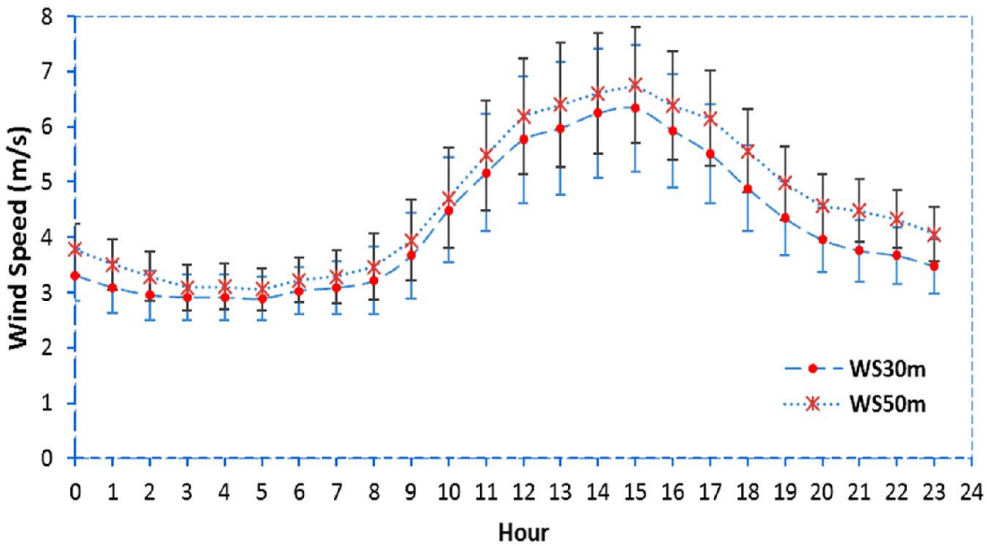

Figure 3.12 Averaged diurnal variation of wind speed at 30m & 50m height (2016)

Wind roses of wind direction at 48-meter height were created using WRplot software. Wind rose is quite helpful in significantly characterizing the wind speed variations due to the topographical effects as it shows the frequency and distribution of wind direction. From Figure 3.13 it is noticeable that winds from the west are the most dominant ones throughout the year, which is the flat land area. Then, about 14% of the time wind blows from the south-west direction, which consists of campus buildings and flat area as well. The more noticeable side is the east direction, which is the cliff side with major elevation difference between tower location and land area. Wind from this side is not easy to assess as part of the wind coming from this side gets affected by the cliff, resulting in reducing the wind speed. So, most of the winds coming from the east are around 2-3 m/s only.

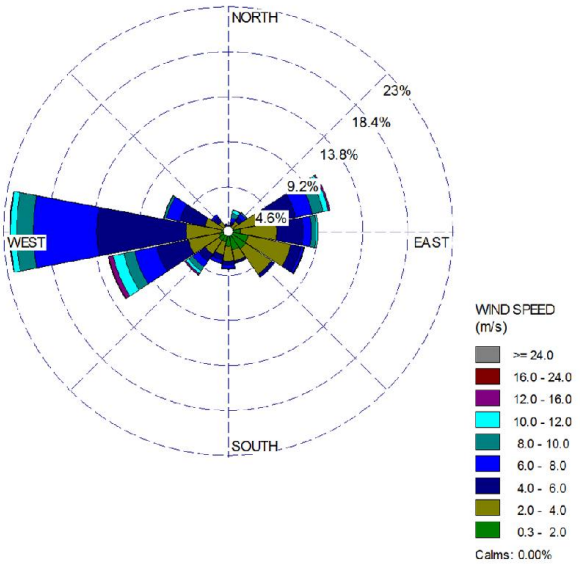

Figure 3.13 Wind Rose of wind speed direction at 48meter height for year 2016

3.5 Wind Power Density

The total kinetic power in the wind is indicated by the wind power density (WPD), which is a measure of amount of energy extractable from wind at a specific location. Elliot et al. [104] suggested characterizing the site based on WPD instead of wind speed available, as power output has cubic relation with wind speeds. WPD is calculated by:

$$WPD = \frac{1}{2}\sum \rho\, v^3 \tag{7}$$

where v is the average monthly wind speed, and ρ is the air density at sea level. It is important to discuss that since air density is a function of temperature and pressure so as any variation into these variables result in air density variation. Although practically air density value is used as 1.225 kg/m^3, care must be taken while using a suitable air density values because it is a crucial parameter in WPD calculations, which can be calculated using the ideal gas law as:

$$\rho = \frac{P}{RT} \tag{8}$$

Figure 3.14 highlights some important aspect of average monthly temperature and pressure variations throughout the year 2016. There are not significant variations in the pressure values but temperature varies quite exponentially entire year.

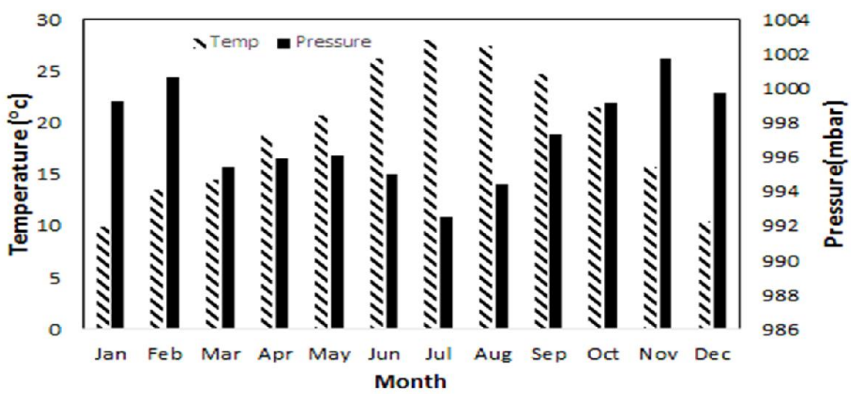

Figure 3.14 Monthly average temperature and pressure (2016)

3.6 Turbulence Intensity

Turbulence intensity (TI) is another important factor used in wind analysis to predict the effects of structural loading, dynamic load on turbine blades and fatigue on wind turbine lifetime. High turbulence is undesirable for the stable power production and long life of wind turbine. Turbulence varies with atmospheric stability, surface roughness and topography. Basically, TI is the ratio between wind speed standard deviation (σ_u) and average wind speed ($\overline{v}$) and calculated as:

$$TI = \frac{\sigma_u}{\overline{v}} \tag{9}$$

3.7 Wind Speed Extrapolation

Theoretically in boundry layer theory, the phenomenon of increase in wind speed with height is referred as wind shear exponent. An extremely important step in wind power assessment is to precisely predict the power produced at turbine hub height. For sites having low wind speeds at lower heights, there is a need of opting higher heights from ground level, which makes it difficult task to measure resources at high levels due to extra cost and other maintenance difficulties. Although such problems are addressed by using remote sensing devices like Lidar and Sodar, they are very much expensive and not possible to afford at each site. As a result, alternative approaches have been developed lately to extrapolate the resources from measuring tower height to desired hub heights [86][105].

3.7.1 Wind Shear Exponent (α) Modelling

Several techniques have been reported in literature for wind shear exponent calculation, as it varies from site to site based on terrain, air density, season and annual wind speed [33][42][61][86][105]. Davenport defined general values of wind shear exponent based on the terrain nature [106], but they are limited to very specific terrains only.

Three approaches have been used in literature so far to determine wind shear exponent values based on site's topography:

1) Power law with an assumption wind shear exponent α = 1/7 or it can be calculated using formula [86],

$$\frac{v_z}{v_r} = \left[\frac{z}{z_r}\right]^{\alpha} \tag{10}$$

where v_z is the wind speed at height z, v_r is the reference height wind speed, z is the height to which wind speed is to be extrapolated and z_r is the reference height.

2) Logarithmic law, originated from boundary layer flow in fluid mechanics, with z_o surface roughness = 0.01 or it can be assumed as [86][105],

$$\frac{v_z}{v_r} = \frac{ln\left(\frac{z}{z_r}\right)}{ln\left(\frac{z_r}{z_o}\right)} \tag{11}$$

3) Using linear regression with an assumption of average wind speed v_o at height h_o, wind shear exponent (α) can be calculated as,

$$\alpha = a + b \ln v \tag{12}$$

where a = 0.37 and b = -0.0881 are empirically found by [107].

Due to mathematical simplification and successful approach, power law has been widely used and preferred over logarithmic law. Power law takes into account the dynamic characteristics of wind shear exponent and its variation with time, season and topography [108] [109], while log law is only reasonably efficient in neutral atmospheric stability and performs well under specific conditions. Ray et al. [56] discussed the potential drawbacks of log law and found that in conditions where wind speeds at two heights are the same or lower wind speed at upper height, log law provides unrealistic values of surface roughness.

Therefore, for this study power law is mainly used to determine the wind shear exponent values.

3.7.2 Power Law

Mathematical models, such as power law, are widely used in wind energy assessment projects. In 1960, Davenport [106] first established this law to analyze gradient wind speed in boundary layer theory, since then it is known as the power law or 1/7 power law. It is written in mathematical form as:

$$\frac{v_z}{v_r} = \left[\frac{z}{z_r}\right]^{\alpha} \tag{13}$$

where α is called the wind shear exponent, which varies with time, season, topography and region etc. If the wind speeds at two heights are known, wind shear exponent for that specific location can be determined easily then. Based on measured data, Davenport suggested below wind shear exponent values for specific type of terrain.

Table 3.1 Wind Shear exponent (α) values based on terrain [105] [106]

Wind shear exponent (α)	Description of terrain
0.950	Coastal waters of inland sea
0.121	Flat shore of ocean small islands
0.130-0.135	Open grasslands without trees
0.143	Open slightly rolling farm land
0.128-0.170	Open level agricultural land with isolated trees
0.170	Open fields divided by los stone walls
0.200	Rough coast
0.220	Gently rolling country with bushes and small trees
0.230	Relatively level meadow land with hedges and trees
0.250-0.303	Level country uniformly covered with scrub oak
0.357	Wooded and treed farm land

Conveniently, it is assumed and well proven that power law can provide reliable estimation of wind shear exponent up to 200-meter heights [110].

3.7.3 Wind Shear Exponent Selection

A representative wind shear exponent (α) for METU NCC site is calculated using three evaluation techniques.

a) **Mean and Median:** Although power law predicts a whole distribution of α values, wind speed varies with time and height; thus, the α value varies with time. Mean and median of the α values were calculated to find an optimum α value.

b) **Least Square Fit Method:** Least square method is the most efficient and common way of finding the best fit for a set of data. A parametric model was created which requires α values as an input to power law to select one α value that minimizes sum of square of the residuals (SSR). The residuals are calculated by taking the difference between observed and predicted wind speed as follows:

$$r_i = v_i - v_p \tag{14}$$

Where v_i and v_p are the observed and predicted wind speeds of ith value respectively

Summed Square of Residuals (SSR) is given by:

$$SSR = \sum_{i=1}^{n} r_i^2 \tag{15}$$

c) **Prediction of Linear Relationship**: Regression is the most commonly used predictive analysis method, which helps users model the relation between two variables. In linear regression, a best line is fit through the wind speeds of two heights. This technique is quite similar to Justus regression equation [107] and described as:

$$lnv_z = m\, lnv_r + \alpha \tag{16}$$

where v_z is the speed at higher elevation and v_r is the reference speed at lower elevation, m is the regression line slope, and K is constant from power law formula.

3.8 Wind Speed Distributions

Wind resource characterization at any site requires in detail understanding of accurate wind availability due to its variable nature. Therefore, other than monthly or annual average wind speed, another crucial factor in analyzing the wind potential of a site is the wind speed distribution. For instance, if two sites have same annual average wind speed, it is not certain if they will produce same annual energy. To understand the wind speed variation at a site, a probability function $f(V)$ is required, which can accurately predict the wind speed distribution of any site. Wind speeds are to be categorized in groups using a certain bin size, to present its probability density function and cumulative distribution function. It is very crucial in design optimization of a wind power system to describe wind variation using a density function or any other statistical function. Numerous case studies presented in literature have shortlisted Weibull, Rayleigh, gamma and lognormal empirical distributions which describe wind speed variations at any site quite precisely [111].

3.8.1 Weibull Distribution

Weibull distribution is one of the most popular and reliable distribution function used in wind power analysis. It was first proposed by W. Weibull for studying tension and fatigue in material strength. [112], since then it has been widely used in wind energy application for more than half a century now because it accurately describes the distribution of wind at any location.

The Weibull probability density function (PDF) is described as:

$$f(v) = \frac{k}{c}\left(\frac{v}{c}\right)^{k\pm 1} e^{\pm\left(\frac{v}{c}\right)^{k}} \text{ (where k >0,v >0,c >1)} \quad (17)$$

where k (dimensionless) and c (m/s) are the shape and scale parameters, respectively.

Similarly, Weibull cumulative density function (CDF) can be defined as:

$$F(v) = 1 - e^{-\left(\frac{v}{c}\right)^k} \tag{18}$$

Weibull shape and scale parameters are the most critical to calculate, as one influences the average probabilistic average wind and the other defines how skewed the distribution curve is. Larger value of c indicates a wide spread distribution and large k means right skewed distribution, indicating high probability of higher wind speeds.

Only main drawback of Weibull distribution is that it provides poor representation of wind speed distribution at site with very low wind speeds [113].

A special case of Weibull distribution, known as Rayleigh distribution with a shape parameter k of 2, is often recommended and used by wind turbine manufacturers for standard performance figures [114]. However, for this study it is not applicable as the shape and scale parameters reported in previous feasibility study was found to be 1.74 [31].

3.8.2 Gamma Distribution

Gamma distribution is another strong candidate distribution which is widely used for wind speed analysis especially for low wind speeds distribution. Probability density function (PDF) of gamma distribution is expressed as follows [115]:

$$f(v) = \frac{1}{\Gamma(\alpha)\beta^{\alpha}} v^{\alpha-1} e^{\left(-\frac{v}{\beta}\right)} \tag{19}$$

Cumulative density function is expressed as [116]:

$$F(v) = \frac{\gamma\left(\alpha, \frac{v}{\beta}\right)}{\Gamma(\alpha)} \tag{20}$$

where α is the shape parameter, β is the scale parameter [117], and Γ is the Euler gamma function [118]. There are some other parameterizations which are commonly used for gamma distribution [117].

1. Shape parameter k and a scale parameter β
2. Shape parameter $\alpha = k$ and rate parameter θ, which is inverse of scale parameter β
3. Shape parameter k and mean $\mu = \frac{k}{\beta}$

Special cases of Gamma distribution are known as exponential and chi-squared distribution.

3.8.3 Lognormal Distribution

Lognormal distribution, sometimes also referred as Galton's distribution, is continuous probability distribution in which log of the variable has normal distribution [119]. The probability density function of this distribution is expressed as:

$$f(v) = \frac{1}{v\sigma\sqrt{2\pi}} e^{-\frac{(\ln v - \mu)^2}{2\sigma^2}} \tag{21}$$

Similarly, CDF of lognormal distribution is calculated as:

$$F(v) = \frac{1}{2} + \frac{1}{2} erf\left[\frac{\ln v - \mu}{\sqrt{2\sigma}}\right] \tag{22}$$

where the two parameters μ and σ are the mean and standard deviation of variable's natural log, respectively, and erf is the complementary error function [120].

3.8.4 Beta Distribution

Beta distribution is a very general type of continuous probability distribution which is defined in the interval between 0 and 1. As the α values always range from 0 to 1 and in literature it has been treated as a constant variable. However, the random nature of wind shear exponent constant does not really agree with this, as it varies under the

effects of terrain, season, height, etc. Beta distribution is tested in this study to find out if it represents wind shear exponent (α) variation quite satisfactory or not. Probability density function (PDF) of beta distribution can be written as [121]:

$$f(x) = \frac{\Gamma(\alpha+\beta)}{\Gamma(\alpha)\Gamma(\beta)}(1-x)^{\beta-1}x^{\alpha-1} \tag{23}$$

The cumulative density function is expressed as:

$$F(x) = I_x(\alpha, \beta) \tag{24}$$

where α and β are shape parameters [122].

3.8.5 Distributions Parameters Estimation

Once the distribution functions are known, next objective is to choose various estimating techniques, in order to fit the distributions to wind speed data by estimating the distribution parameters. Two widely used method [123], in literature, are adopted in this study for parameter estimation.

a. Maximum Likelihood Method/Estimation (MLE)

b. Maximum Goodness of Fit Method/Estimation (MGE)

3.8.5.1 Maximum Likelihood Method/Estimation

MLE method in statistical interpretation is asymptotically optimizing technique for parameters estimation of continuous distributions. If the probability density function $f(x, \theta)$ of wind speed distribution is known, then using the mathematical likelihood function, unknown parameters θ of the wind distribution can be calculated easily. Likelihood function estimates those parameters which will as a result maximize the probability of those specific wind speeds likelihood. Iteration technique in R-software is used to calculate the parameters with minimum log-likelihood value. Likelihood function of MLE is expressed as:

$$L(v,\theta) = \prod_{i=1}^{n} f(v_i,\theta) \tag{25}$$

where v is the observed wind speeds, and $f(v,\theta)$ is the density function.

3.8.5.2 Maximum Goodness of Fit Method/Estimation

One of the alternative estimation method is goodness of fit (GOF) method, which was first derived as minimum distance estimation by Wolfowitz [124] [125] and Kac et al. [126]. Maximum Goodness of Fit Method/Estimation (MGE) also provides quite accurate parameter estimates for continuous distributions. This approach works on finding those parameters which minimizes the distance between measured data hypothetical distribution $F(x)$ and empirical distribution $S(x)$ of distribution in question.

Following three GOF tests are used to assess the suitability of a given distribution[127].

a. Cramer-von Mises criterion

b. Anderson Darling test

c. Kolmogorov-Smirnov test

a) Cramer-von Mises Test

Cramer-von Mises test is the most powerful test, of comparing the cumulative distribution function of hypothetical CDF and empirical CDF, for the goodness of fit. It was first developed by Cramer [128] and von Mises [129]. Cramer-von Mises test is considered much superior than chi-squared and Kolmogorov Smirnov tests, as it measures the difference of hypothetical and empirical CDF by taking the square of mean difference between both. Its function is defined as:

$$W_n^2 = n \int_{-\infty}^{\infty} \{F(x) - S_n(x)\}^2 dF(x) \tag{26}$$

b) Anderson Darling Test

Anderson Darling test is the modified form of Cramer-von Mises test. The only difference is that Anderson Darling test gives higher weights to the tails of distribution. It compares the observed CDF to and expected CDF for the goodness of fit. Anderson Darling test is considered the most powerful test amongst all empirical distribution function test and is mostly favored in any kind of analysis because of its suitability to any continuous distribution. Anderson Darling and Cramer-von Mises tests both belong to the quadratic class of empirical distribution function statistics. Anderson and Darling [130] defined the test statistics as:

$$A_n^2 = n \int_{-\infty}^{\infty} \frac{\{F(x)-S_n(x)\}^2}{F(x)\{1-F(x)\}} dF(x) \tag{27}$$

c) Kolmogorov-Smirnov Test

The Kolmogorov-Smirnov test is the most suitable and commonly used non-parametric test to compare two datasets for difference. The test statistics quantifies the distance between empirical cumulative distributive functions of two datasets (sample and reference) without making any assumption about the distribution of data. Kolmogorov-Smirnov test belongs to the supremum class of the empirical distribution function statistics which quantifies the hypothetical and empirical distributions for any significant vertical differences between them. Andrey Kolmogorov [131] and Nikolai Smirnov [132] defined the test statistics as:

$$D_n = \sup|F(x) - S_n(x)| \tag{28}$$

3.8.6 Goodness of Fit of Fitted Distribution

3.8.6.1 Graphical Analysis

Generally, after the parameters for predefined distributions have been calculated, the next step is to reject the unlikely candidates. The preliminary approach used in this step is to graphically analyze the set of distributions. This step involves plotting the

skewness and kurtosis graph, PDF, CDF, Q-Q plot and P-P plot of the wind speed data against the fitted distributions.

Firstly, descriptive statistics of the wind data corresponding to the fitted distribution are analyzed in terms of skewness and Kurtosis plot linked to third and fourth moments. Cullen and Frey graph [123] is the best amongst these, which displays the skewness and Kurtosis values of different distributions in terms of a value or area on a graph and then plots where given input data lies in that graph. A non-zero skewness suggests non-symmetric data, while the Kurtosis quantifies the tails of data distribution. Since, the non-robustic nature of skewness and Kurtosis due to their very high variance is well-known, so to incorporate for any uncertainty in the plot, non-parametric bootstrapping is used to show the variation of data. Bootstrapping procedure is carried out by randomly sampling the values form the original data. This first step provides a clear indication of which distribution data actually follows most.

The next step in graphical analysis is to compare the empirical distribution and density plot along with the histogram of fitted distributions and measured wind speed data. Following plots are generated for comparing the distributions with dataset.

a. Probability Density Function (PDF) plot to compare the density along with histogram shape

b. Cumulative distribution function (CDF) plot

c. Q-Q plot for comparing theoretical quantile against the empirical quantile to emphasize the lack of fit at the tails of distribution

d. P-P plot comparing the probabilities of theoretical data with empirical dataset to emphasize the lack of fit at the center of distribution

3.8.6.2 Goodness of Fit of Fitted Distribution

Once the suitable distributions are shortlisted, they are further tested for the goodness of fit. This step involves accepting or rejecting of following two hypotheses:

$H_o = F(x) = S_n(x)$ (Data follow a specific Distribution)

$H_a = F(x) \neq S_n(x)$ (Data do not follow the specific Distribution)

Following goodness of fit tests are used in this study, further details of these can be found in previous section.

i) Kolmogorov Smirnov Test (KS) quantifies the distance between hypothetical CDF and empirical CDF

ii) Cramer-von Mises Test (CVM) measures the squared mean difference between CDF's

iii) Anderson Darling Test (AD) same as CVM but more weight is given to the tails

iv) Akaike Information Criterion (AIC) to test the quality of the mode, it does not check for null hypothesis.

3.9 Annual Energy Production (AEP)

One of the most crucial and important steps in wind resource assessment, which is the deciding factor in wind project installation, is to estimate how much energy can be produced annually at the study site. A specific method is required to predict the power performance characteristics of a selected wind turbine. Most common and widely used method is to predict by the power curve of a wind turbine, which is a type of pictorial representation of how much electric power a turbine will generate as a function of wind speed. Power curve helps in analyzing and monitoring the turbine performance, power assessment, energy forecasting etc. without any prior knowledge of how a wind

turbine operates. AEP of a number of horizontal axis wind turbines (HAWT) is analyzed in this study for the feasibility at METU NCC wind mast site.

3.9.1 Power Curve Modelling

Typically, a horizontal axis wind turbine (HAWT) turbine power curve consists of three main parts, each corresponding to specified wind speeds range, as shown in Figure 3.15 [133].

a. Cut-in Speed (v_i)

   Cut-in speed defines the point at which the wind turbine starts generating the power, any value below than that speed will not have any effect on wind turbine power and turbine continues to increase in power as the wind speed increase until it reaches the rated speed. Although it varies from turbine to turbine and it is defined by the manufacturer, but a typical cut-in speed range is between 2.5-4 m/s.

b. Rated Speed (v_r)

   Rated speed is the wind speed at which the turbine produced power is equal to turbine's rated power. For any wind speed, more than rated wind speed will result in turbine's rated power generation until the speed reaches the cut-out or furling speed. Rated speed ranges between 10-13 m/s for most wind turbines.

c. Cut-out Speed (v_c)

   Cut-out speed, also known as furling speed, is the point on curve after that turbine automatically shuts off for safety purposes. It is the maximum allowable wind speed limit to prevent any breakdown or damage to turbine. Generally, cut-out speed is about 25-30 m/s for the wind turbines.

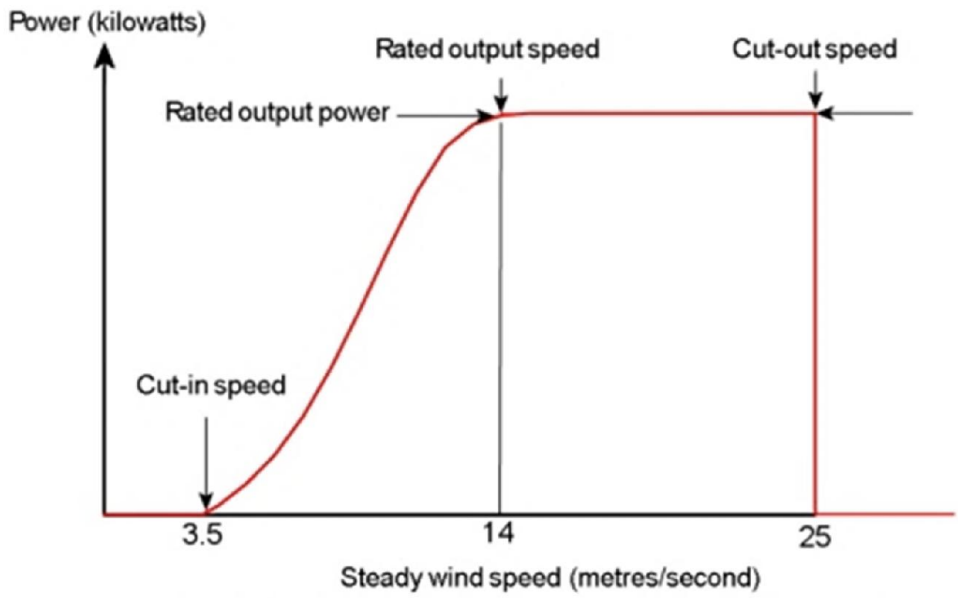

Figure 3.15 Typical wind turbine power curve [134]

Numerous methods have been developed and proposed in literature for wind turbine power curve modelling, some methods use manufacturer provided power curve data while other use the measured wind speed to determine real time power curve [135] [136]. Although all these models quite successfully predict the power curve of turbine, but still none of the model is reported to be the most dominant because of wind speed variations from region to region. So, it is possible that one method may perform very well at one site but it may fail to do so on another site [137]. Therefore, it is recommended to investigate all the possible potential methods to choose the most appropriate method for the site.

3.9.1.1 Manufacturer Power Curve

The most straightforward and traditional approach in turbine power prediction is to directly use the power curve provided by the manufacturer. Turbine manufacturers under real time conditions using aeroelasitc simulators predict wind turbine performance to generate a power curve and coefficient of performance (C_p). These power curves are generated under strict standards for wind industry, as defined by IEC 61400-12-1 [94]. AEP is directly calculated by multiplying the power curve values to

corresponding wind speed and its frequency. Three wind turbines of 500 kW, 750 kW and 1 MW capacity are selected for this study, to select the most suitable turbine in terms of AEP and cost of electricity. Technical specifications of these turbines are provided in Appendix A.

Although manufacturer provided curves are tested under standard conditions, they still lack some accuracy in representing the realistic conditions. As they are being installed in different climates and different terrain like flat land or especially a complex terrain, they do not really represent the actual shape of power curve at that specific location. Therefore, derivation of a generic equation is required which uses the measured wind speed data of that specific site to determine the actual shape of the power curve.

3.9.1.2 IEC Method of Bin

Binning method is commonly practiced industry preferred method for turbine power curve measurements. It is the simplest and straightforward discrete modelling approach for quantifying the relation between wind speed and turbine power. IEC standard 61400-12 recommends binning the 10-minute average wind speeds into a contagious 0.5 m/s wind speed bins. Average power for each bin is then calculated using the mean bin wind speed and plotted against each other to get a power curve of the turbine. Power of the bins is calculated as suggested by [138]:

$$P_{vbin} = \begin{cases} P_r \times \left(\frac{{v_{bin}}^2 - v_i^2}{v_r^2 - v_i^2}\right) & \text{if} \quad v_i \leq v_{bin} < v_r \\ 0 & \text{if} \quad v_{bin} < v_i \\ P_r & \text{if} \quad v_r \leq v_{bin} \leq v_c \\ 0 & \text{if} \quad v_{bin} > v_c \end{cases} \tag{29}$$

where P_r is the rated power of the wind turbine.

3.9.1.3 Curve Fitting

Most generic approach amongst all the techniques mentioned in the literature is wind turbine power curve modelling by means of fitting a curve to manufacturer provided power curve data. These equations are further used on measured wind speed data set to generate the site-specific power curve. Results of various studied present in

literature proved that 2nd or 3rd order polynomial fits give the highest R-square values [139] [140].

3.10 Power Coefficient (C_p)

Coefficient of performance or power coefficient is a common measure of wind turbine efficiency. Generally, it is a good representation of overall system efficiency including turbine blades, generator, gear train, etc. Turbine manufacturers sometimes provide the C_p value or a C_p curve. If C_p value is known already, electrical power produced by the wind turbine at a specific wind speed can be estimated easily using the relation:

$$P = 0.5\ \rho\ A\ v^3 C_p \tag{30}$$

Power coefficient is the ratio of total electric power output of a turbine by the total wind power available to the turbine.

$$C_p = \frac{P_{out}}{P_{in}} \tag{31}$$

where P_{in} is the kinetic power of the wind as:

$$P_{in} = 0.5\ \rho\ A\ v^3 \tag{32}$$

The maximum theoretical value of C_p that can be achieved by a turbine is 0.593, known as the Betz Limit [141]. In practice, no turbine can ever reach this limit due to aerodynamics and mechanical losses.

3.11 Economic Analysis

Levelized Cost of Energy (LCOE) and Net Present Value (NPV) models are considered as the common indicators in current study of economic analysis for estimating the economic feasibility of proposed project. LCOE and NPV calculations are the reliable indicators which give straightforward indication of economic feasibility of any project, to help the decision makers and investors decide. LCOE is a measure of estimating the energy generation cost from any source, while capital cost, operation and maintenance cost are taken to be point estimation for the analysis. It is a measure of an average price to repay the investors with a rate of return equal to the

discount rate. Here, a positive NPV value means that the project is feasible to be invested in and a negative value indicates the losses that may occur, if the project is developed now. It also gives us a clear idea about payback period of the project. As a first approximation, soft costs such as cabling, racking and mounting costs for system installation are not included for the economic calculations. For the NPV and LCOE calculations, the following equations are used, respectively:

$$NPV = \sum_{t=0}^{y} EB_t \times \frac{1}{(1+i)^t} - PP_{cost} \times P_r \tag{33}$$

$$LCOE = \frac{PP_{cost} \times P_r + \sum_{t=1}^{y} (M_C) \times \frac{1}{(1+i)^t}}{\sum_{t=1}^{y} E_{TP} \times \frac{1}{(1+i)^t}} \tag{34}$$

where EB is the economic benefits (USD), PP_{cost} is the power plant cost (USD/kW), M_C is the maintenance cost (USD/kW), E_{TP} is the total energy produced (kWh) in a year, P_r is the turbine rated power (kW), i is the interest rate, t is the year number, and y is the lifetime of the system (year).

Chapter 4

ANALYSIS RESULTS AND DISCUSSIONS

4.1 Estimated Wind Shear Exponent Characteristics

The derivation of wind shear exponent using the measured wind speeds showed negative values of wind shear exponent for about 10% of the data for 30-40m wind shear exponent values, 12% for 30-50m and 20% of the total data for 30-60m height. Negative wind shear exponent values are not usual in wind speed extrapolations and it happens only when the upper height anemometer records low wind speeds than the lower height anemometer. However, various studies as reported in chapter 2 have discussed that for complex terrain, negative values are probably due to the atmospheric instability, turbulence and topographical variations and also if the site has low wind speeds [59] [54] [61] [142]. General hypothesis in such situation is that either anemometers at the site have sensitivity difference and require precise calibration or it might be happening due to high turbulence effect on the tower. Since wind speeds are averaged over 10 mins and high standard error values were also reported, therefore as a solution to incorporate uncertainty into the measured values, it was assumed that wind speed in that specific time interval might is the combination of actual measured wind speed and the standard error for that time interval. Because considering the general theoretical reasoning it is known that wind speed increases with height. As a result, negative wind shear values percentage for 30-40m and 30-50m was reduced to 3-4% only. However, it was not the case for 30-60m wind shear exponent values, because even after the values adjustment, negative wind shear exponent values were more than 15%. For this reason, any further comparisons of 30-60m wind shear exponent values were not included in the analysis.

Figure 4.1 compares the annual variation of wind shear exponent values for the year 2013-2016. It can be seen that median values for all the months fall approximately close to 0.20, while the upper and lower quantile vary significantly according to the season of the year. Winter months have higher variation than the summer months.

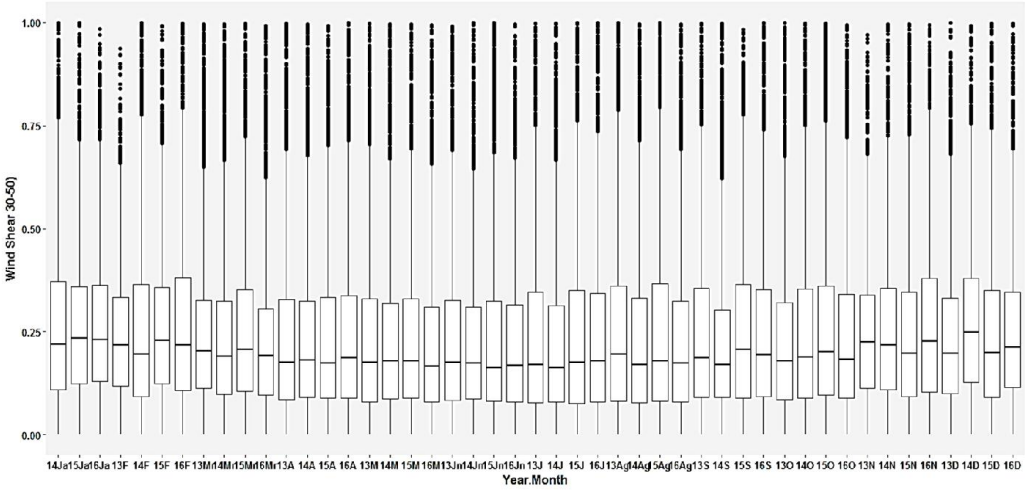

Figure 4.1 Box plot of 30-50m wind shear exponent (α) of all months of year (2013-2016)

4.1.1 Wind Shear Exponent Variation by Wind Speed

Figure 4.2 shows wind shear exponent variation with respect to change in wind speeds. It is clear that as the wind speed increases, terrain effect on the wind speed starts to decrease, which results in lower values of wind shear exponent (α). That is why as the height above the ground increase, wind speed also increases, because wind is hardly influenced by surface then. Therefore, there is an inverse relation between wind speed and wind shear exponent for any specific terrain.

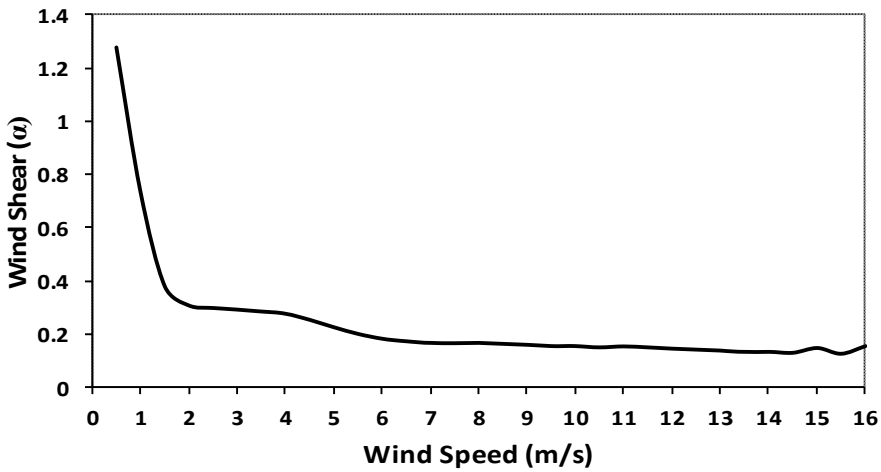

Figure 4.2 Wind shear exponent variation with respect to 10-min wind speed at 30m (2016)

4.1.2 Wind Shear Exponent Diurnal Variability

The averaged diurnal behavior of wind shear exponent can be seen in Figure 4.3 , which provides the clear evidence of variable nature of wind shear exponent. Prominent diurnal periods of the figure are the daytime (08:00-14:00hr) and the nighttime (18:00 to 07:00hr), as the wind speed increases drastically during the daytime because of the big eddies due to efficient mixing of energy and convection. In addition, during the day, sun heats up the ground, which makes the air near ground lighter and this lighter air starts to rise above the ground. As a result, surrounding cool air from the sea starts to flow towards this area. While during the night, it is opposite and calm period, as temperature goes down, so there is not much movement of the air because of low temperature difference between sea surface and land surface. Therefore, atmospheric stability is positive (unstable boundary layer) during the daytime and negative at night. Wind shear exponent is strongly influenced by temperature and wind speed variations. Therefore, during the period of reduced wind speeds at night, fairly constant wind speed at noon, abrupt increase and decrease of wind speed during early morning and late evening, temperature also varies accordingly, as a result it can be seen that late night time period and early morning shows larger spread of wind shear exponent values while it is more centered at noon due to near neutral thermal stability.

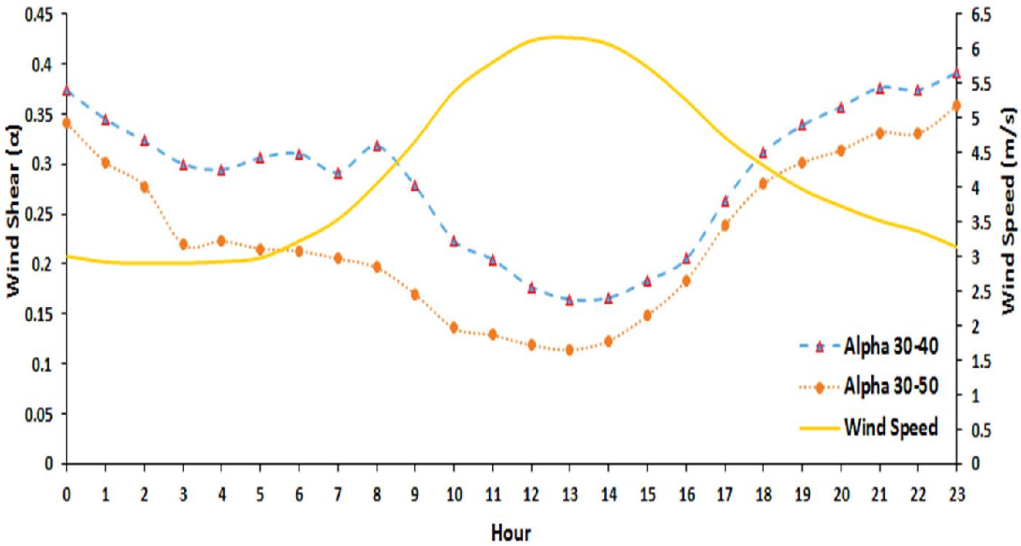

Figure 4.3 Averaged diurnal pattern of wind shear exponent (α) and wind speed 30m (2016)

4.1.3 Wind Shear Exponent Seasonal Variability

Considering seasonal trend, as illustrated in Figure 4.4, lower wind shear exponent is observed during summer period in May to July, while it reaches the peak during winter months due to cold weather. This seasonal pattern is mainly because of atmospheric stability variation with change in temperature and might be due to the effect of some other meteorological factor like humidity, grassland etc.

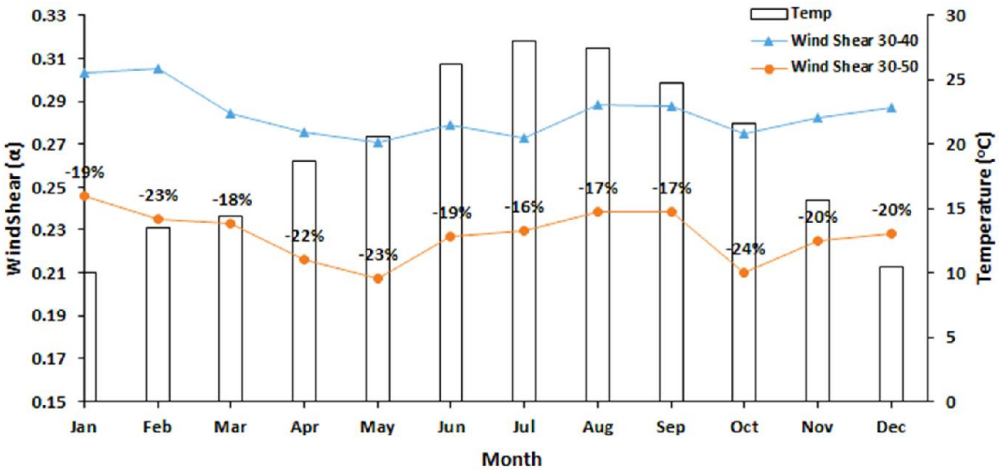

Figure 4.4 Monthly variation of wind shear exponent, wind speed and temperature (2016)

Figure 4.4 also highlights the fact that as the height from the ground increases, terrain effect starts to decrease as well. It can be seen that wind shear exponent drops 15-25% of its 30-40m wind shear exponent (α) value, when the values of 30-50m are considered.

4.1.4 Wind Shear Exponent Variability by Wind Direction

Figure 4.5 depicts the prevailing variations in wind speed and wind shear exponent with respect to wind directions at METU NCC tower site. One of the most prominent features of this graph are wind speed and wind shear exponent variations at East, South and West Directions, as shown in Figure 4.5, North & East sides of the tower are facing directly the cliff, which as a result creates turbulence and tries to reduce the wind even before it reaches near tower, therefore, as already, recommended; it is not a good idea

to install the turbine near cliff. It is evident that wind drops drastically from east to south direction which is the campus area consisting of buildings etc. So, lower wind speed and higher wind shear exponent are observed from east to south direction. Due to siting of turbine at non-flat and complex terrain, uncertainties arise in site feasibility analysis, as the wind moves over such terrain; it causes the reduction in wind speed, increase in turbulence and wind shear exponent variation. Lower wind shear exponent values are recorded from west to north, which is usually a flat barren landside.

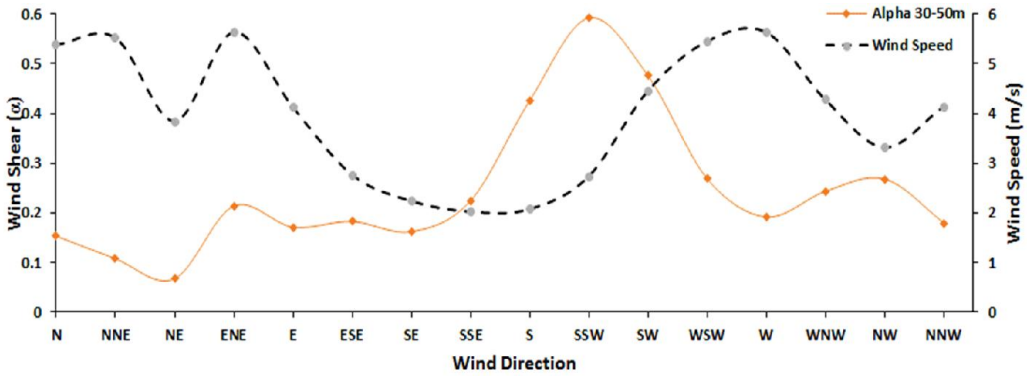

Figure 4.5 10-min wind shear exponent and wind speed variation by wind direction (2016)

4.2 Turbulence Intensity (TI)

TI is a critical parameter used in site evaluation to estimate the durability and life span of a selected wind turbine for the study site as shown in Figure 4.6.

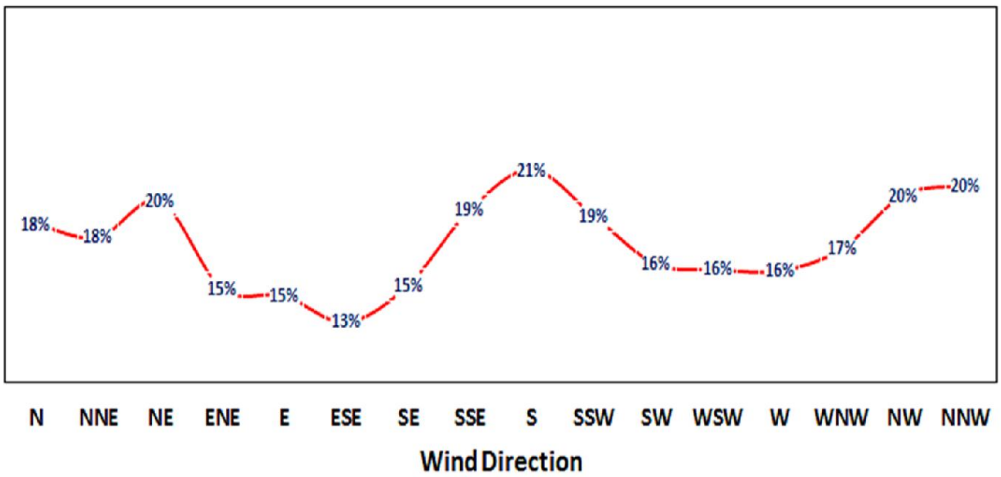

Figure 4.6 10-min turbulence intensity variations with direction (2016)

International Electrotechnical Commission (IEC) has defined turbine installation sites classes in IEC standard 61400-1 for wind turbines installation [143], based on the turbulence intensity and typical wind speed. According to the standard, Class A wind sites should have below 16% average TI at 15m/s at the hub height. Therefore, if a wind turbine is to be installed at 50m height at METU NCC, it will suffer severely from the effect of TI in terms of fatigue and loading on turbine blades, because average TI at METU NCC wind site ranges between 16-19% at 50-60m height, which is slight higher than IEC predefined classes. Figure 4.6 highlights the turbulence intensity variations as the wind direction changes. As it is evident that for many directions TI is more than IEC specified limits. For instance, the maximum turbulence reported is from south side, which is the campus buildings area and secondly as wind moves from north towards east or west, turbulence increases, as this side of the tower has grassland and small trees. Similarly, from east to south, turbulence increase 6% approximately, which is the cliff side of the tower. Therefore, a detailed analysis is required for this selected site, in order to predict the accurate values of turbulence being faced by the tower at this specific location.

4.3 Wind Shear Exponent Selection

Table 4.1 summarizes the annual average wind shear exponent (α) values calculated by different methods. Comparatively, wind shear reported by LSE method seems to predict values very close to median of the yearly wind shear exponent distribution. The prominent features of the comparison are that wind shear exponent decreases as we move above from ground, because the terrain effect will also reduce on the wind speeds. While, yearly wind shear exponent values showed contrary results, as wind shear exponent does not seem to vary too much with each year passed, which may indicate not significant variation in the terrain during these years. Wind shear exponent calculated by linear regression method showed interestingly different results from all other methods. Wind shear exponent 30-60m is not reported here in the analysis, due to numerous negative wind shear exponent, which is not usual of higher heights because wind speed should increase with height. As indicated by Figure 4.7,

logarithmic relation between wind speed at 30m and 60m shows larger spread of the data and most of the $\log V_{60}$ values lie on the negative side with large deviations, which indicates the non-linearity between both speeds. Similar comparison is shown in Figure 4.7 between wind speeds at heights of 30m and 50m, comparatively, this graph shows less deviations from the center and very less data fall under negative side of the axes.

Table 4.1 Wind shear exponent (α) values for each year calculated using different methods

Year	2013		2014		2015		2016	
α	30-40	30-50	30-40	30-50	30-40	30-50	30-40	30-50
Mean	0.265	0.228	0.286	0.228	0.288	0.229	0.283	0.226
Median	0.220	0.178	0.216	0.180	0.227	0.185	0.221	0.185
LSE	0.205	0.159	0.205	0.176	0.212	0.179	0.205	0.176
Prediction	0.387	0.403	0.481	0.380	0.466	0.371	0.484	0.386

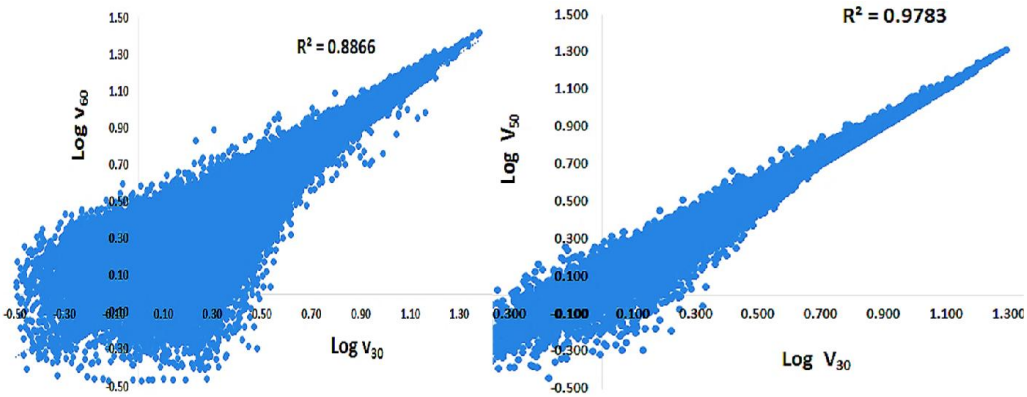

Figure 4.7 Correlation between wind speeds at different heights

For a typical site-representative wind shear exponent (α) selection, 50-meter wind speed data was extrapolated to the same height using wind shear exponent values reported in Table 4.1. 30-50 m wind shear exponent values were used for the analysis, because the extrapolation is required for higher sites and wind shear exponent decreases as we move above from the ground level, so 30-50m wind shear exponent satisfies the linear relationship between two heights wind speeds and it also

incorporates wind speed variation effects while predicting higher heights wind speeds. Table 4.2 summarizes the accuracy of each wind shear exponent value used to predict wind speed at 50 meter. To analyze the predictability power of the estimated wind shear exponent value, goodness of fit of predicted data was quantified by mean squared error (MSE), root mean squared error (RMSE) and mean absolute percentage error (MAPE) to rank each calculated wind shear exponent value.

It is evident that overall wind shear exponent (α) calculated using LSE method is much lesser than all other wind shear exponent values, as it provided the minimum RMSE value and percentage error for every year. Average annual wind shear exponent, monthly and seasonal wind shear exponent values also showed quite promising results, while one-seventh power law (wind shear exponent being equal to 0.143) seems to predict very poor results. Based on the analysis results and comparison shown in Table 4.2, the representative wind shear exponent for METU NCC tower site is 0.176 as it gives minimum percentage error in prediction, which is further used to extrapolate wind speeds at 65 m and 75 m height respectively for energy output analysis.

Table 4.2 Prediction accuracy test results of different wind shear exponent values

		Mean	**LSE**	**Monthly**	**Seasonal**	**0.143**	**0.176**
2013	MSE	0.424	0.249	0.431	0.242	1.120	0.277
	RMSE	0.651	0.499	0.656	0.492	1.058	0.526
	MAPE	17	14	17	14	24	15
2014	MSE	0.222	0.189	0.221	0.213	0.448	0.189
	RMSE	0.471	0.435	0.470	0.461	0.669	0.435
	MAPE	13	12	13	13	16	12
2015	MSE	0.241	0.209	0.240	0.231	0.464	0.208
	RMSE	0.491	0.457	0.489	0.480	0.681	0.456
	MAPE	14	13	14	14	17	12
2016	MSE	0.242	0.209	0.240	0.277	0.482	0.209
	RMSE	0.492	0.457	0.490	0.527	0.694	0.457
	MAPE	13	12	13	14	17	12

4.4 Fitted Distributions Characteristics

A preliminary question asked in the selection of a distribution is that how representative the fitted distribution is of the selected wind speed data. Following steps are being taken for selecting the best-fit distribution for the wind speed data at METU NCC.

4.4.1 Graphical Analysis

As a first step in selection, candidate distributions are compared graphically by plotting the Cullen and Frey graph, actual probability densities against the theoretical densities of each distribution and cumulative distributions.

4.4.2 Wind Shear Exponent (α) Distribution

Most frequently wind resource assessment analysis reported in literature are based on average wind shear exponent value for site evaluation without considering the random nature of wind shear exponent, therefore as discussed in section 4.1 that basic error can be incorporated in the analysis results due to the deterministic random nature of wind shear exponent, which was briefly discussed by Kirchhoff and Wagner [53] [144].

A skewness kurtosis plot of the wind shear exponent (α) values is shown by Figure 4.8. On this plot, blue circular dot shows the unbiasedly estimated skewness and kurtosis values of wind shear exponent plotted against the skewness and kurtosis values of some common distributions. Yellow scatter around the dot indicates the bootstrapped values of the data. Bootstrapping was done by drawing samples from the population dataset with replacement and this same step was repeated 5000 times.

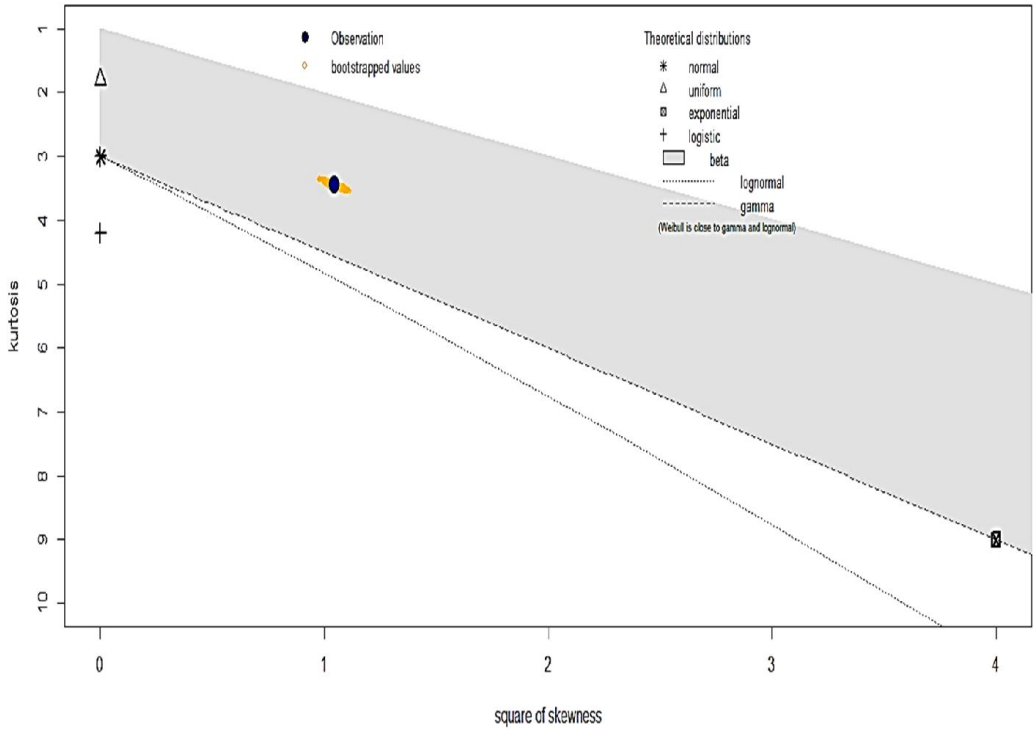

Figure 4.8 Skewness-Kurtosis plot (Cullen and Frey graph) for 30-40 wind shear exponent (α)distribution

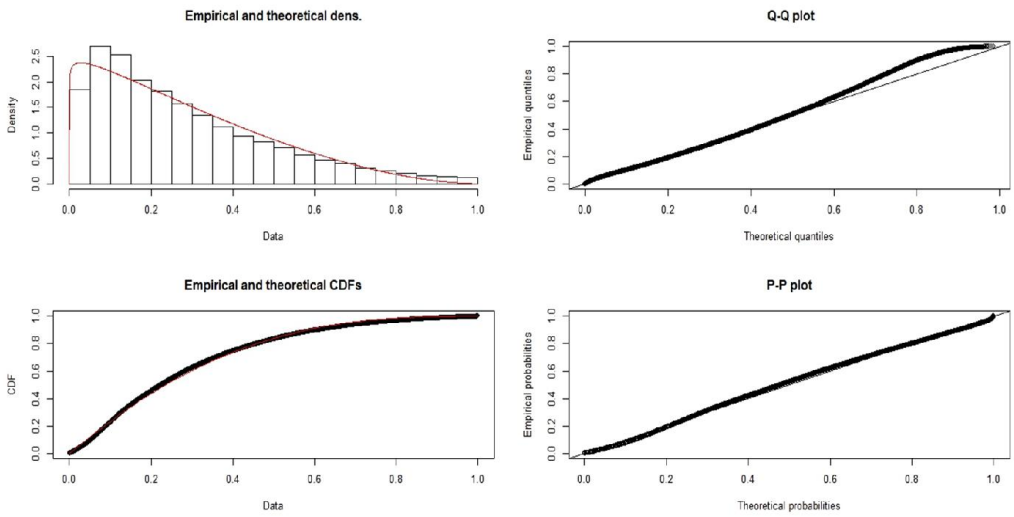

Figure 4.9 Graphical analysis of beta distribution fit using estimated parameters

Hence, the result showed that wind shear exponent distribution lies in the range of beta distribution, which is indicated as the grey shaded area in the graph. Further, beta distribution is tested for fit, by plotting PDF, CDF, Q-Q plot and P-P plots, as illustrated by Figure 4.9. This step helps in verifying or disapproving the validity of the selected distribution.

Part a of the Figure 4.9 shows the wind shear exponent probability distribution for 30-40m wind shear exponent profile as a histogram computed from 10-minute wind shear exponent values and grouped by 0.05 bin size. Red line over the histogram represents the estimated empirical beta distribution. As it appears from the histogram that large majority of wind shear exponent is distributed between 0.0-0.2, which is relatively consistent with the site representative wind shear exponent (α) 0.176 computed by LSE method. However, it is important to mention that there might be a significant difference in the wind shear exponent range if negative wind shear exponent values were considered here. Q-Q plot indicates the weakness of fit of the assumed distribution at the tails, while P-P plot shows the strong relation of assumed fit with actual data at the center. Similarly, CDF shows the good compromise between beta distribution and wind shear exponent distribution.

Goodness of fit hypothesis tests were performed to rank each of the parameter estimation method of the fitted distribution. This part of the selection gives the test statistics to statistically validates the significance level of fit for each estimation method . Table 4.3 summarizes the data for the goodness of fit test results. Visibly, MGE method performed efficiently in parameter estimation as compared to maximum likelihood method. Although, all three goodness of fit techniques showed very closeness to the actual data but based on the minimum AIC and BIC values, parameters estimated by the CVM are most suitable comparatively, therefore, parameters for wind shear exponent distribution are taken from CVM goodness of fit estimation.

(α= 1.07, β= 2.88)

Table 4.3 30-40 Wind shear exponent distribution parameter estimation statistics

		Maximum Likelihood	Maximum Goodness of Fit		
			CVM	**KS**	**AD**
Parameters	α	1.01	1.07	1.08	1.05
	β	2.44	2.88	2.83	2.72
G.O.F Test statistics	Loglikelihood	14450	14044	14146	14268
	AIC	-28896	-28084.24	-28289.14	-28533.3
	BIC	-28878	-28067	-28271	-28515
	Kolmogorov-Smirnov	0.0486	0.0264	0.0225	0.0272
	Cramer-von Mises	42.42	9.76	12.29	12.73
	Anderson-Darling	237	162	148	142

4.4.3 Wind Speed Distribution

A similar skewness-kurtosis plot of the wind speed data (2003-2016) is shown in Figure 4.10. The blue circular dot is the point where wind speed data lies according to the shape of its distribution and the yellow scatter shows the 10,000 times bootsrapped values by taking the samples from wind speed population data. From this comparison, three distributions Weibull, Lognormal and Gamma appear as strong candidates for further comparison. Fine dotted line represents lognormal and other dotted line is for gamma distribution, while weibull lies between these two distributions.

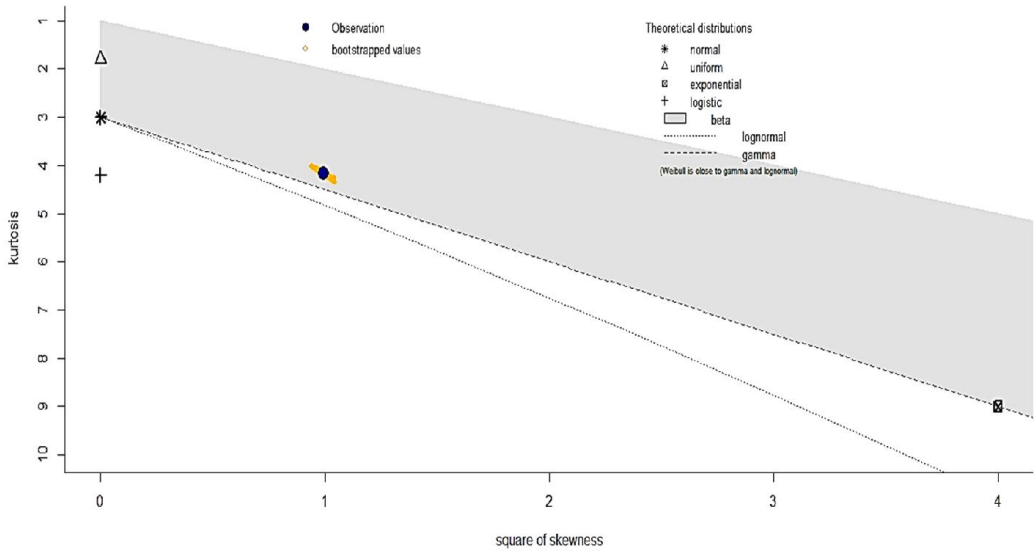

Figure 4.10 Skewness-Kurtosis plot (Cullen and Frey graph) for 30m wind speed distribution

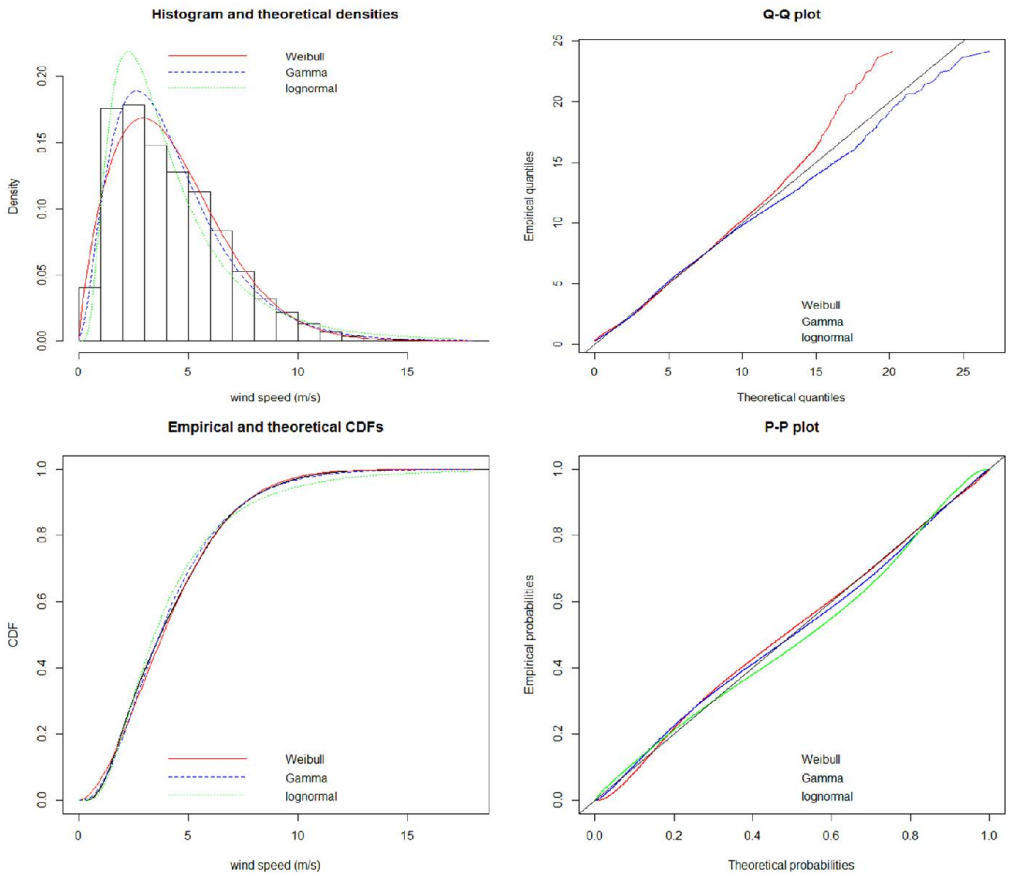

Figure 4.11 Goodness of fit plots for selected distributions fitted to wind speed data (2013-16)

Figure 4.11 illustrates four basic goodness of plot which are considered as a classical approach of testing the goodness of fit for any distribution data. PDF and CDF plots are the basic plots for preliminary analysis, as can be seen that lognormal distribution is overestimating the probability of occurrence of wind speeds ranging from 0-5 m/s, while Weibull distribution is underestimating the probabilities of low wind speeds, hence, Gamma distributions seems to better describe the wind speed distribution. Whereas, Probability-Probability plot and Quantile-Quantile plot are considered complementary and significant in graphically comparing assumed distributions. A key aspect of the Q-Q plot in the top right corner of the figure emphasizes the fact that none of the candidate distributions correctly describes the right tail of the wind speed data. However, P-P plot seems to suggest that both gamma and Weibull distributions show good fit at the center of distribution, while lognormal totally lacks the fit.

4.4.4 Goodness of Fit Tests Result

The results yielded by the goodness of fit tests provide convincing evidence that Gamma distribution could be preferred for its better description of the empirical distribution of the wind speed data at METU NCC. The test statistics shown in Table 4.4, appears to suggest that even though Weibull is considered widely as a representative distribution of the wind speed data but in case of METU NCC, it does not appear to efficiently describe the dataset. While other tests relatively fail to show significant evidence, Anderson Darling test showed promising results, as it is the most powerful test used to analyze the goodness of fit. As it appears, lognormal distribution lacks to describe wind speed distribution in all cases, there might be some chance for Weibull but as mentioned before it will not be a good representative for low wind speeds, which have high percentage at METU NCC.

Table 4.4 Goodness of fit test statistics

	Weibull	**Gamma**	**Lognormal**
Akaike's Information Criterion	890157	885717	893599
Bayesian information Criterion	890178	885734	893620
Kolmogorov-Smirnov	0.0329	0.0281	0.0522
Cramer-von Mises	56.06	50.66	158.307
Anderson-Darling	424	290	936

4.4.5 Estimated Parameters

In order to further penalize the selected Gamma distribution, estimated parameters by maximum likelihood method and maximum goodness of fit method are compared to measure the distance between empirical distribution and fitted parameters distribution. Three classical goodness of fit tests were considered for the comparison, Kolmogorov-Smirnov, Cramer-Von Mises and Anderson Darling. Based on the test statistics and results from AIC and loglikelihood, parameters estimated by maximum goodness of fit using AD fit method are found to be the most suitable ones for the Gamma distribution of wind speed data at METU NCC. ($\alpha = 2.55$, $\theta = 0.61$)

Table 4.5 Wind speed distribution parameter estimation statistics

		Maximum Likelihood	**Maximum Goodness of Fit**		
			CVM	**KS**	**AD**
Parameters	α	2.73	2.43	2.46	2.55
	θ	0.65	0.57	0.58	0.61
G.O.F Test statistics	Loglikelihood	-442857	-443685	-443491	-443142
	AIC	885717	887375	886987	886288.
	BIC	885738	887396	887007	885308
	Kolmogorov-Smirnov	0.028	0.017	0.016	0.019
	Cramer-von Mises	50.77	20.86	21.35	26.14
	Anderson-Darling	290	247	225	205

4.5 Verification of Power Curve

Different power curves obtained by two different ways of estimating the power curve of a wind turbine at METU NCC site were tested using the real time measured wind speed data. Both methods were quantified as the mean residuals to the actual manufacturer provided power curves. Manufacturer provided curve is used as the reference power curve and other power curves are relatively compared to it for the accuracy of the estimation method. Figure 4.12 represents the available wind power at METU NCC and it also highlights the amount of power which actually can be extracted from the wind considering the Betz limit 59%.

4.5.1 Power Curve 1

A standard power curve of Enercon-E40-500 kW wind turbine is derived from 10 minute averaged values of wind speeds at hub height. The results displayed in Figure 4.12 show that using the binning method defined by IEC standard resulted in overprediction of power, as compared to manufacturer power curve, at low speeds ranging between 3.5-9 m/s, while it predicted close results for speeds higher than 9 m/s. the overestimation of the power by bin method shifted the power curve to the left from the actual turbine power curve. Whereas, manufacturer provided power curve is truly represented by the power curve obtained by curve fitting method. The curve fitting scatter precisely defines each speed power output relative to the corresponding manufacturer curve.

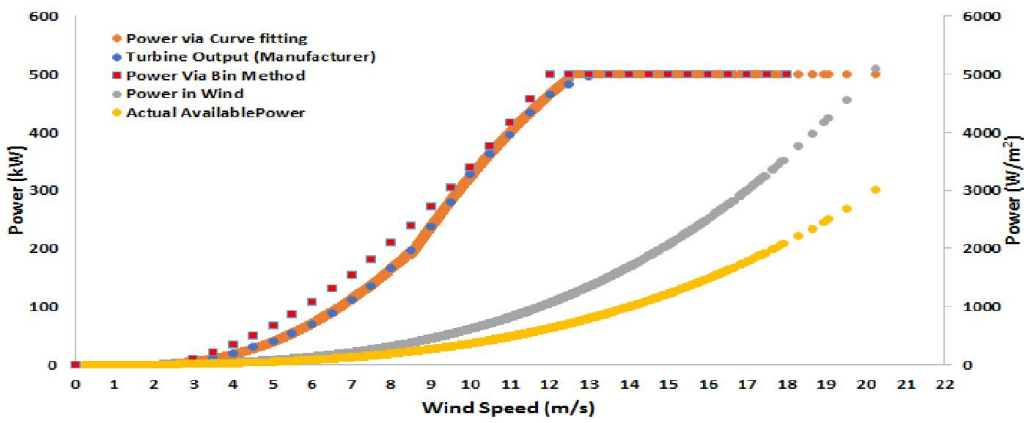

Figure 4.12 Power curve of Enercon-E40-500 kW wind turbine for 50m hub height

Similarly, coefficient of performance measured using power predicted by curve fitting method is shown in Figure 4.13. It can be seen that such approach produces Cp values similar to actual Cp of the turbine (Manufacturer provided). The jagged appearance of the curve fitting method at high wind speeds manifests the challenge of modelling the Cp values from on-site measured wind speed data.

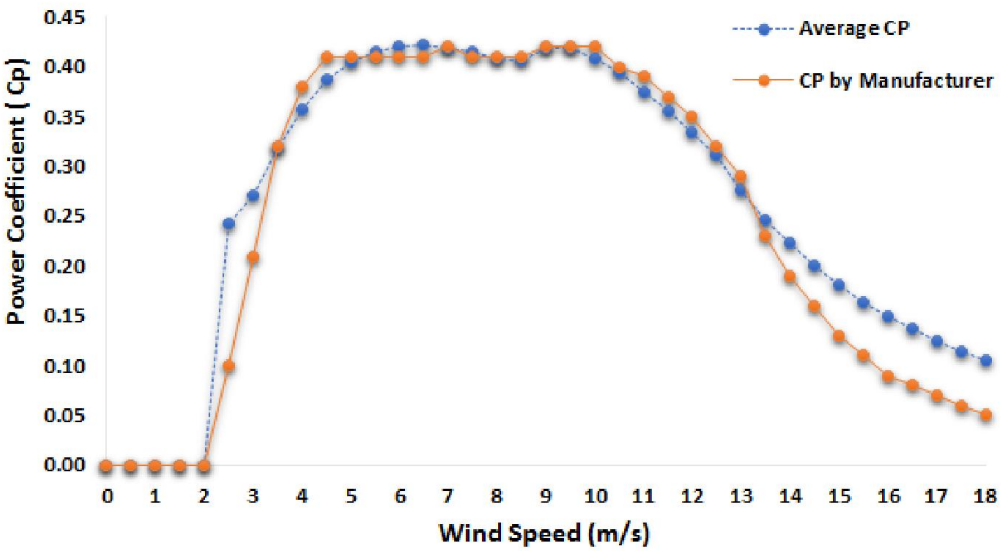

Figure 4.13 Comparison between estimated average Cp and actual Cp of wind turbine

4.5.2 Power Curve 2

The results of the two approaches using 10 min average wind speeds of METU NCC tower are shown in Figure 4.14. The resulting power curves of Lagerwey LW 52 750 kW wind turbine clearly shows that the correlation between power output and wind speed is much better for the curve fitting method than for the method of bins. Also, change in performance of IEC method of binning is unusually strange, as the power and turbine curve changes. This points to the fact that binning the data for power curve estimation may result in loss of information and also binning method fails to incorporate stochastic nature of wind. As a result, few measurements in a specific power bin increases the uncertainty of the average bin power.

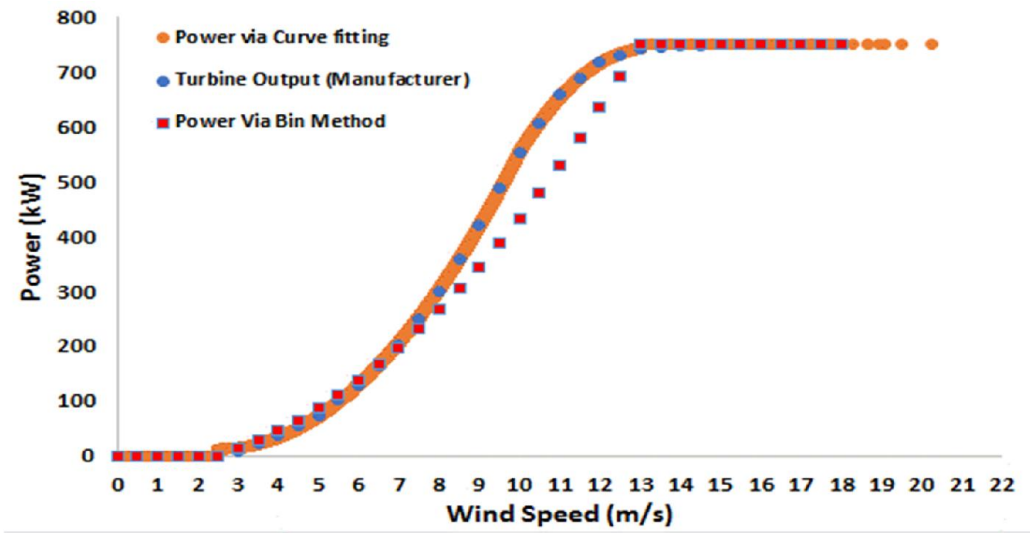

Figure 4.14 Power Curve of Lagerwey LW 52 750 kW wind turbine

4.5.3 Power Curve 3

The power curve of Enercon E-58-1MW wind turbine shown in Figure 4.15 highlights the fact that method of bins may comply well with the large capacity wind turbine power curve as the power curve by this method show in Figure 37 looks smoothed in both ends. These results are opposite to the results seen on 500kW and 750kW wind turbines power curve. Which means that method of bin seems to be significantly sensitive to parameter changes.

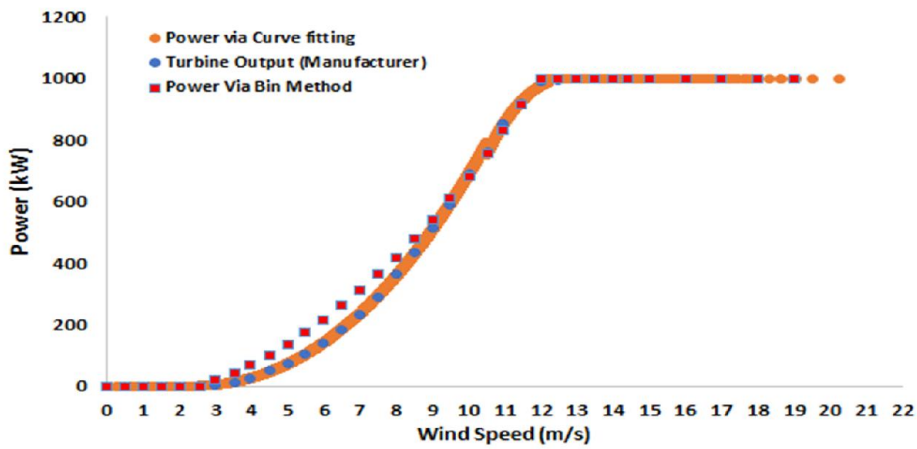

Figure 4.15 Power curve of Enercon E-58-1MW wind turbine for 50m hub height

Nevertheless, curve fitting technique seems to be much successful in both cases, power curve and Cp estimation, as shown in Figure 4.15 and Figure 4.16 respectively. These results of the developments and investigation promised a method that could be used in wind resource assessment of any site to estimate real time site-based power curve and coefficient of performance of selected wind turbine.

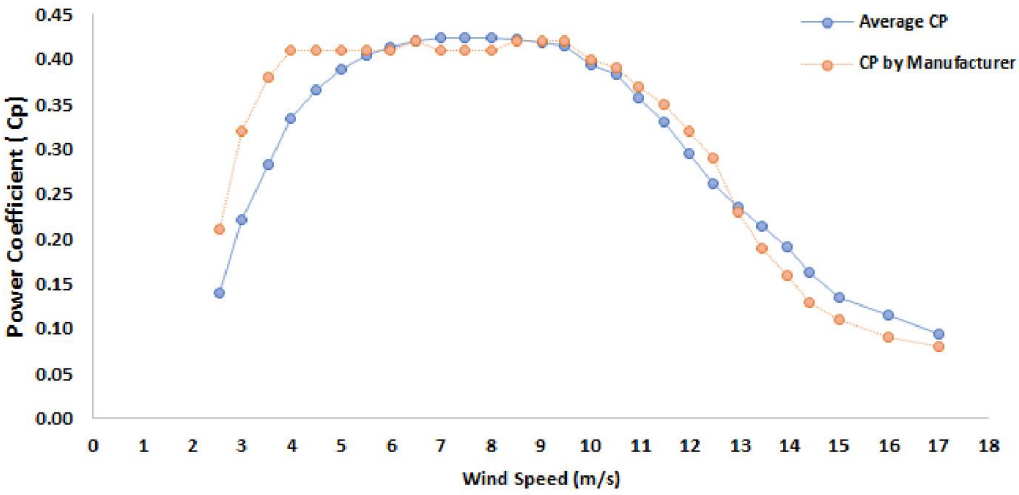

Figure 4.16 Comparison between estimated average Cp and actual Cp of wind turbine

4.6 Annual Energy Production

A hypothetical wind plant is assumed of 500kW, 750kW and 1MW installed capacity wind turbine at METU NCC mast site. The 10-min average wind speeds at 30m height and a wind shear exponent of 0.176 were used to estimate wind speeds at 65m and 75m heights. Following three scenarios were analyzed for the feasibility of installation a wind turbine at METU NCC.

In first scenario, a 500kW rated power wind turbine was tested for energy yield at 50m, 65m and 75m hub heights. Figure 39, Figure 40 and Figure 41 illustrates the considerable differences of estimated WED from month to month. As can be seen, higher WED is recorded in March, which is the peak spring time and spring gales are quite strong throughout this month ranging from 6-7 m/s on average.

It is quite interesting to note that estimated WED is minimum in February which is winter season time in North Cyprus. It is believed that since the wind speed is influenced by the significant rainy days in this month that is why energy density recorded is relatively low. However, in the remaining winter months' turbine output gradually increases from November to February, as compared to summer season. North Cyprus summer has very hot and humid days with very low sea breeze, making summer month much hotter and of high temperatures, especially temperature in July and August reaches above 40°C. Hence, the turbine output decreases drastically during these months which is almost half of that obtained in March (i.e. spring season). WED for the rest of the month's ranges between these two low and high peak months. Moreover, resulting annual mean turbine output is estimated to be 92759,106611 and 113607 kWh/month respectively.

Next, the comparison in Figure 4.17, Figure 4.18 and Figure 4.19 also indicates the percentage increase in WED as we move from lower height 50m to upper heights 65m and 75m. As the significant increase of 21-25% in output is observed during summer months for both the heights, because wind is much cooler at upper heights, which results in efficient mixing of air. While during winter season, there is no notable difference in temperate between different heights that is why wind output different is

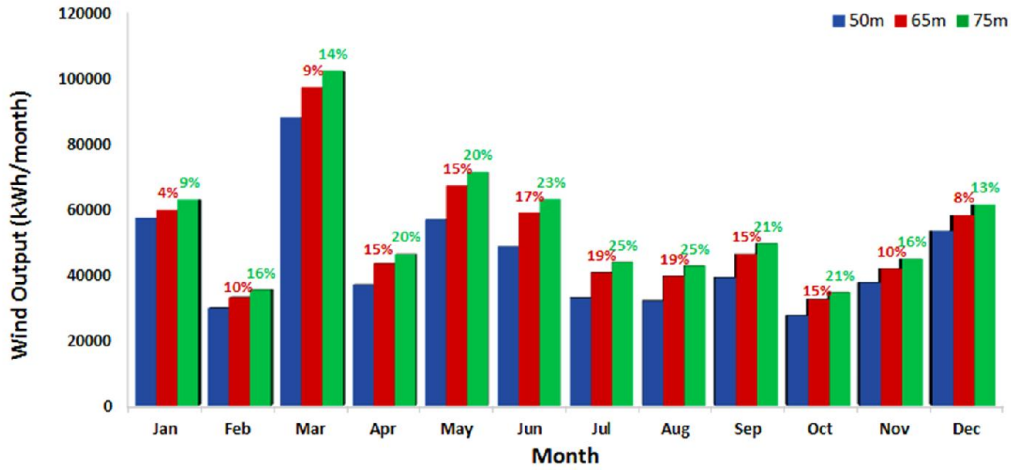

Figure 4.17 Monthly variation of wind energy density at different heights for a 500kW horizontal axis wind turbine

around 5-6%, which is not quite high during this period of the year. Yearly variation of WED at different heights is also shown by the Figure 4.20.

Case 2: 750 kW
Year 2016

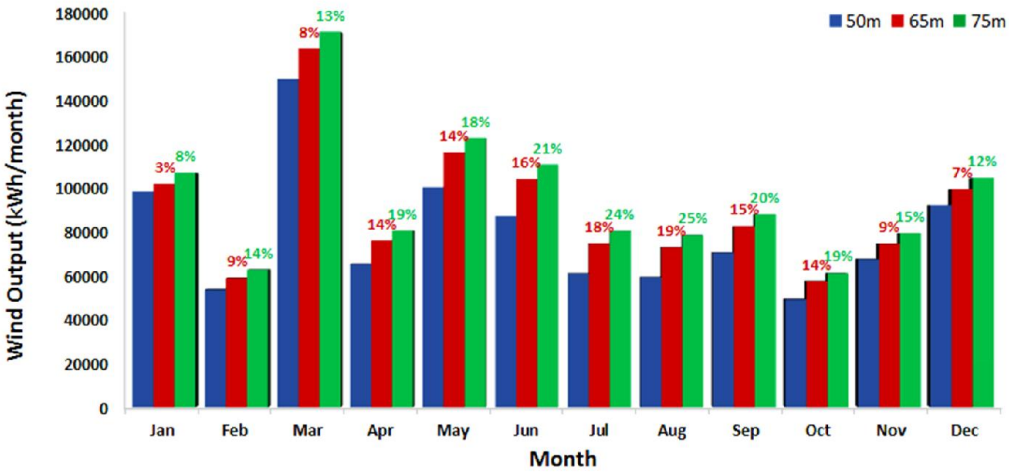

Figure 4.18 Monthly variation of wind energy density at different heights for a 750kW wind turbine

Case 3 1 MW
Year 2016

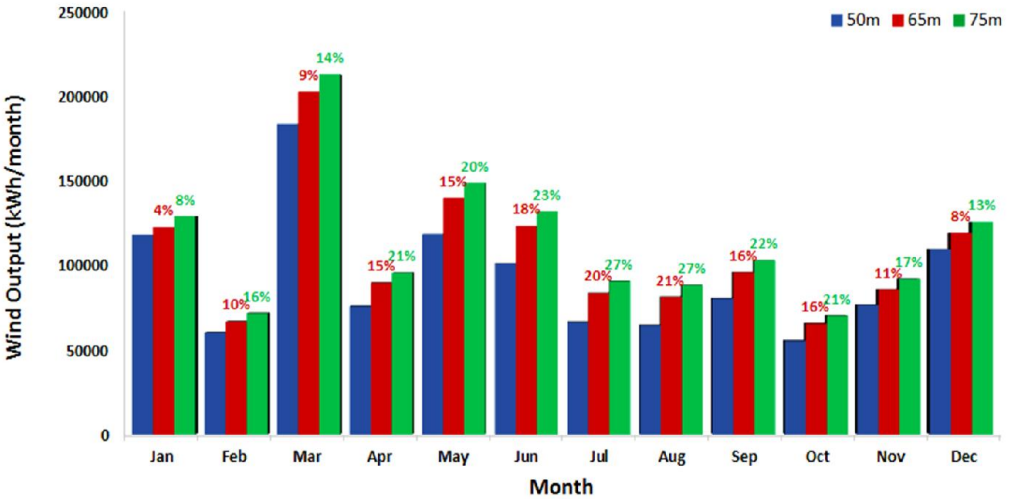

Figure 4.19 Monthly variation of wind energy density at different heights for a 1MW wind turbine

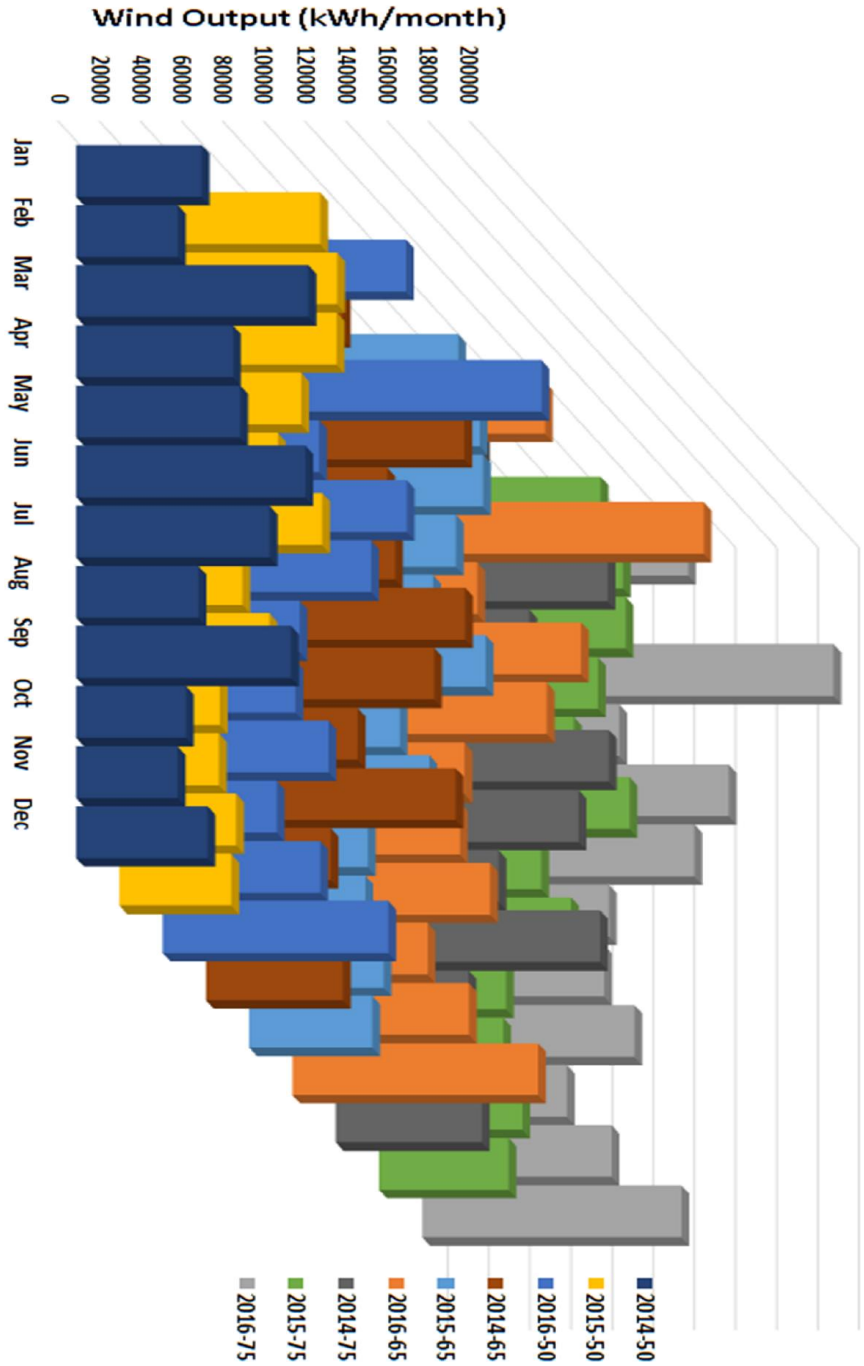

Figure 4.20 Monthly variation of wind energy density for all years at different heights for a 1MW wind turbine

4.7 Economic Analysis Result

Economic analysis was performed for a range of turbines with different heights using each year wind speed data to select an optimum height and turbine configuration. Capital cost for each configuration is taken as 1467 USD/kW [145], a discount rate of 9% [146] and operation & maintenance cost of 0.019 USD/kWh [147] is used. Resulting values of Levelized Cost of Energy (LCOE) and Net Present Value (NPV) are reported in Table 4.6, which also shows the comparison between estimated annual capacity factor of each selected turbine for each year. Capacity factor of a turbine is a key determinant factor in feasibility of any project. The configurations are ranked based on resulting annual Capacity factor, LCOE and NPV values. It is strikingly evident that amongst the different studied configurations 750kW turbine with a hub height of 75m is the most feasible to consider for installation at METU NCC, as it possesses the highest capacity factor of 18%, a minimum LCOE of 0.116 USD/kW and 0.663 million USD NPV value. As mentioned earlier, a negative value of NPV indicates the project is not economically feasible to install, for instance, for the year 2014 and 2014, installation of 1MW wind turbine at METU NCC might have unfeasible as indicated by the negative NPV values in the table.

Table 4.6 Comparison of Levelized Cost of Energy (LCOE)

		LCOE (USD/kW)			**NPV** (million USD)			**Capacity Factor**		
	Year	**50m**	**65m**	**75m**	**50m**	**65m**	**75m**	**50m**	**65m**	**75m**
1 MW	2016	0.153	0.136	0.129	0.24	0.49	0.62	13%	15%	16%
	2015	0.182	0.164	0.155	-0.07	0.12	0.21	10%	12%	13%
	2014	0.182	0.162	0.154	-0.06	0.13	0.23	10%	12%	13%
750 kW	2016	0.136	0.122	0.116	0.367	0.563	0.663	15%	17%	18%
	2015	0.142	0.127	0.121	0.301	0.482	0.581	14%	16%	17%
	2014	0.141	0.127	0.120	0.303	0.495	0.595	14%	16%	17%
500 kW	2016	0.157	0.139	0.132	0.099	0.219	0.280	12%	14%	15%
	2015	0.164	0.146	0.138	0.056	0.168	0.227	12%	13%	14%
	2014	0.164	0.145	0.137	0.056	0.174	0.235	12%	14%	14%

Chapter 5

CONCLUSION AND RECOMMENDATIONS

Wind resource assessment at a geographical site is a complex polymorphic procedure, as it involves step-by-step execution of different site assessment methodologies. This assessment study sought to focus on statistically evaluating the wind energy potential of METU NCC wind tower site. The feasibility analysis in this research were performed with the help of different statistical software's such as MS Excel, Matlab, WRPlot, R software and WAsP. The site evaluation ranged from characterization of wind speeds, examining wind shear exponent effect in a complex terrain, statistical distributions, AEP estimation and economic analysis of the feasible wind turbine. Based on the analysis results, major conclusions of this study are:

Analysis results suggest that METU NCC has fair potential for wind power generation and with an average wind speed of 5-5.5 m/s, it can be categorized as IEC Class I site. Although Class I resources are not sufficient, however seasonal and diurnal variations favor against the argument as strongest winds were observed in spring and winter months. In addition, low wind speeds were recorded in summer months but due to summer vacations, energy consumption is also less in summer and maximum power can be utilized from PV power plant on campus. Despite the fact that, measured data was lost for few months and data collection had significant quality issues for instance large standard deviations were noticed within 24-hour wind speeds, averaging 10-min wind speeds to hourly and daily values were considered inadequate in terms of describing the stochastic nature of wind. Analysis based on as minimum resolution as 10-min proved to be more efficient in providing a better understanding of wind speed fluctuations. Similarly, synthetic dataset such as TMY data for METU NCC were found to be inefficient as it entirely failed to represent the actual site resources. Seasonal wind speed variations appeared to be mainly influenced by variation in ambient temperature with some anomalous discrepancies effect due to rainy season.

Also, it is recommended to undertake pressure and temperature variation while calculating air density values.

For accurate representation of the probability distribution of wind speed at METU NCC, a comparison between different bin size methods for bin width of histogram showed that choosing a small bin size results in less fluctuations at each bin, which in wind speed case is less efficient method. Similarly, a larger bin can result in very bad resolution of the data. So, Freedman Diaconi's method was found to best define the underlying distribution of the wind speeds at METU NCC.

An extrememly important step in wind power assessment is to precisely predict the power produced at turbine hub height. Several techniques were tested to calculate the wind shear exponent for a complex terrain such as the one at METU NCC. A new method Least Square Error method (LSE) was proposed in the study for wind shear exponent calculation. Wind shear exponent values were calculated using each year measured wind speed at three heights as 30-40,30-50 and 30-60.

Analyis results showed no regular yearly pattern exist in wind shear exponent values as it does not change significantly with year. However, wind shear exponent is strongly influenced by the seasonal variation, as the highest values were found in winters and lowest in summers. Also significant diurnal variations were observed in wind shear exponent values due to heating and cooling cycle. In terms of direction, the prevailing wind directions were found to be SE (Cliff side) and SW (Campus buildings area), as high wind shear exponent values were recorded from these side which mainly influence wind speed coming from these direction. In addition, the overall monthly mean turbulence intensity values were also found to be above IEC allowable limit for wind turbines.

The overall mean wind shear exponent obtained using power law, linear regression least square error method and $1/7^{th}$ power law was 0.228,0.384, 0.176 and 0.143 respectively. Finally, To assess the accuracy of using a single wind shear exponent for the power law, estimated wind shear exponent values by each methods were tested by

calculating MSE, RMSE and MAPE. Without this information, a critical resource analysis on the extrapolated wind speeds cannot be made. Analysis results showed that, in spite of being very relevant and precise for wind speed extrapolation, $1/7^{th}$ wind shear exponent 0.143 was shown not to be suitable to predict accurate results. Based on the results, the study recommends a value of 0.176 to be the representative wind shear exponent for METU NCC site, which was further used in the analysis to extrapolate wind speeds to 65m and 75m. Estimated wind shear exponent values were also tested to check if wind shear exponent follows Beta distribution. Goodness of fit results indicated that maximum goodness of fit method's predicted Beta distribution parameters are the most suitable for wind shear exponent distribution. Hence, the presented methodology for wind shear exponent, estimated single shear value and wind shear exponent distribution parameters are hoped to be an addition to the literature because such analyses were made for the first time at METU NCC wind site.

In this study, the scrutiny of different statistical distributions for wind speed application has been statistically compared at selected location in METU NCC. A skewness and kurtosis graph was used to make graphical analysis as a preliminary approach in distribution selection. Later, goodness of fit tests were conducted to test the accuracy of the fit of candidate distributions. From the test results, it was evidently revealed that wind speed distribution is better presented by Gamma distribution than any other distribution. Further statistical diagnosis of the precise parameter estimation method for wind speed Gamma distribution is discussed and presented.

Furthermore, the power curve of a selected wind turbine was determined by curve fitting and IEC defined binning method. Curve fitting technique was shown to be a good method to accurately describe a turbine power curve. This method resulted in reduction of a scatter from the actual manufacturer provided power curve.

Lastly, measured wind speed data was analyzed for power generation from 500, 750 and 1000 kW wind turbines. The annual AEP for 500kW turbine is about 543, 621.6 and 661.6 MWh at 50 m, 65 m and 75 m hub heights respectively. The annual AEP for 750kW wind turbine is 957.3, 1085.3 and 1150.5 MWh at 50 m, 65 m and 75 m

respectively. Similarly, annual AEP calculated for 1MW wind turbine was 1113.1, 1279.3 and 1363.3 MWh at all three heights respectively.

Finally, all three turbines at three different heights were analyzed for economic benefits. Economic analysis results showed that electricity generation from 500 kW wind turbine would have capacity factors of 12%, 14% and 15% with an LCOE of 0.157, 0.139 and 0.132 USD/kW for 50m, 65m and 75m hub heights. A 750 kW wind turbine will have CF of 15%, 17% and 18% with an LCOE 0.136, 0.122 and 0.116 USD/kW respectively. In case of 1 MW turbine CF was 13%, 15% and 16% with LCEO to be 0.153, 0.136 and 0.129 USD/kW respectively.

Therefore, considering the capacity factor and LCEO values for each turbine at 50, 65 and 75-meter hub heights, the investment at 50m height seems to cost extra. However, 750kW wind turbine at 75m hub height seems to be the most attractive investment in terms of technical and economic feasibility.

As for the future work, before taking any further action, all the anemometers should be calibrated again to verify the large standard deviation and also for finding the cause of recording low wind speeds at higher heights. Although, Turbulence intensity values found in this study were for wind speeds less than 15m/s, A detailed CFD analysis are still required to analyze the turbulence effect on the tower measurement due to the surrounding complex terrain.

It is important to compare the theoretical results of this study to the output of a real wind farm. Without this information, there is always a possibility of large uncertainty in the predicted results. If such data is not available, TMY data can be reliable after its accuracy has been tested again by using the new estimated wind shear exponent. Imputation techniques can also be used by using different statistical tools and methods to impute wind speeds for higher heights by using the reliable wind data available for lower heights and then compare this data with extrapolated wind speeds by power law.

It would be quite interesting to conduct similar study for the feasibility of small scale wind turbines at household level. Because the power curve varies from turbine to turbine, so it will further determine the feasibility of wind power at METU NCC location.

Furthermore, a detailed study must be performed on the economic and environmental model because Capital cost, operation and maintenance cost for economic estimation in this study are taken to be point estimation for the analysis, also inflation rate is not considered in the analysis.

REFERENCES

[1] "Electric power consumption (kWh per capita) | Data." [Online].Available: http://data.worldbank.org/indicator/EG.USE.ELEC.KH.PC?end=2013&start=1971&view=chart. [Accessed: 22-Oct-2016].

[2] IEA, "World Energy Outlook 2015." INTERNATIONAL ENERGY AGENCY.

[3] IEA, "IEA Statistics." INTERNATIONAL ENERGY AGENCY.

[4] World Energy Council, "World Energy Resources 2016." WORLD ENERGY COUNCIL.

[5] International Environmental Agency (IEA), "World Energy Outlook Fact sheet 2013." IEA Publications.

[6] World Energy Council, "World Energy Perspectives 2016." WORLD ENERGY COUNCIL.

[7] Biricik,OC Ozerdem, "Overview of Energy System and Major Power Quality Problems in North Cyprus," presented at the International Journal on "Technical and Physical Problems of Engineering," 2011, vol. Issue 8 Volume 3, pp. 71–75.

[8] "KIB – TEK SANTRALLARI." [Online].Available: http://www.kibtek.com/Santrallar/Sant2007FalRap.htm. [Accessed: 27-Oct-2015].

[9] A. Tariq, "METHODOLOGY TO SIZE LARGE SCALE SOLAR PV INSTALLATIONS FOR INSTITUTIONS WITH UNIDIRECTIONAL METERING," MS Thesis, Middle East Technical University, Northern Cyprus Campus, Northern Cyprus, 2014.

[10] E. Erdil, M. Ilkan, and F. Egelioglu, "An experimental study on energy generation with a photovoltaic (PV)–solar thermal hybrid system," *Energy*, vol. 33, no. 8, pp. 1241–1245, Aug. 2008.

[11] Olusola O. Bamisile, Mustafa Dagbasi "Analysis of Serhatkoy Photovoltaic Power Plant and Production over the Years it Application to a Central City in Nigeria (Markurdi).," Int. J. Eng. Res., vol. V4, no. 04, Apr. 2015.

[12] "Sunny Cyprus provides power for our Campus!" [Online].Available: https://ncc.metu.edu.tr/announcement/sunny-cyprus-provides-power-our-campus. [Accessed: 24-May-2017].

[13] "Greatest renewable energy project of North Cyprus at UKÜ," Turkish Republic of Northern Cyprus, 30-Mar-2016. [Online].Available: http://mfa.gov.ct.tr/greatest-renewable-energy-project-north-cyprus-uku/. [Accessed: 24-May-2017].

[14] "RENEWABLE ENERGY RESOURCES BOARD CONVENED AT CIU," *Cyprus International University*, 21-Nov-2016. [Online]. Available: http://www.ciu.edu.tr/en/campus-life/news/renewable-energy-resources-board-convened-ciu. [Accessed: 24-May-2017].

[15] G. Partasides, "Feed-in Tariff specifications, features, amendments, and current and future challenges in Cyprus," presented at the Workshop on Renewable Energy Policies A Side Event at the Third IRENA Assembly Meeting, Abu Dhabi, 12-Jan-2013.

[16] "CDM: Mari Wind Farm Project." [Online].Available: https://cdm.unfccc.int/Projects/DB/TUEV-SUED1158659001.38. [Accessed: 03-Jun-2017].

[17] "CDM: Wind Park at the Orites Archimandritas, Cyprus." [Online].Available: https://cdm.unfccc.int/Projects/DB/TUEV-RHEIN1305648455.02. [Accessed: 03-Jun-2017].

[18] "CDM: Kambi Wind Farm Project." [Online].Available: https://cdm.unfccc.int/Projects/DB/TUEV-RHEIN1250391030.42. [Accessed: 03-Jun-2017].

[19] "CDM: Stivo wind park on Cyprus." [Online].Available: http://cdm.unfccc.int/Projects/DB/RWTUV1351601538.46. [Accessed: 03-Jun-2017].

[20] "CDM: Klavdia Wind Farm Project." [Online].Available: http://cdm.unfccc.int/Projects/DB/DNV-CUK1307522365.51. [Accessed: 03-Jun-2017].

[21] "CDM: Alexigros Wind Farm Project." [Online].Available: https://cdm.unfccc.int/Projects/DB/TUEV-SUED1158658365.34. [Accessed: 03-Jun-2017].

[22] "CDM: Agia Anna Wind Farm Project." [Online].Available: https://cdm.unfccc.int/Projects/Validation/DB/L5Z8JISEBF1V2989J2O7OEO93EP473/view.html. [Accessed: 03-Jun-2017].

[23] "EAC - Customer Service." [Online].Available: https://www.eac.com.cy/EL/CustomerService/Pages/default.aspx. [Accessed: 27-Oct-2015].

[24] M. Altunc, A. Tokgozlu, S. Tolun, Z. Aslan, Z. Unsalan, and H. Goymen, "Comparison of wind energy potential," presented at the International Conference, Environmental Problems of the Mediterranean Region, Near East University, Nicosia. N. Cyprus, 2002, pp. 80–4.

[25] D. Solyali, M. Altunç, S. Tolun, and Z. Aslan, "Wind resource assessment of Northern Cyprus," *Renew. Sustain. Energy Rev.*, vol. 55, pp. 180–187, Mar. 2016.

[26] M. Ilkan, E. Erdil, and F. Egelioglu, "Renewable energy resources as an alternative to modify the load curve in Northern Cyprus," *Energy*, vol. 30, no. 5, pp. 555–572, Apr. 2005.

[27] C. P. Jacovides, C. Theophilou, F. S. Tymvios, and S. Pashiardes, "Wind statistics for coastal stations in Cyprus," *Theor. Appl. Climatol.*, vol. 72, no. 3–4, pp. 259–263, Sep. 2002.

[28] "Mission." [Online].Available: http://ncc.metu.edu.tr/res/mission. [Accessed: 23-Oct-2016].

[29] M. R. Pathirana and A. Muhtaroglu, "Multifaceted Feasibility Analysis of PV Solar Application in Northern Cyprus," *Int. J. Renew. Energy Res. IJRER*, vol. 3, no. 4, pp. 941–950, Dec. 2013.

[30] S. M. H. Ali, “OPTIMAL PHOTOVOLTAIC SIZE ESTIMATION FOR A CAMPUS AREA CONSIDERING UNCERTAINTIES IN LOAD, POWER GENERATION AND ELECTRICITY RATES,” MS Thesis, Middle East Technical University, Northern Cyprus Campus, Northern Cyprus, 2015.

[31] M. YENEN, “MODELING ELECTRICAL ENERGY PRODUCTION IN NORTHWESTERN CYPRUS BASED ON SOLAR AND WIND MEASUREMENTS,” MS Thesis, Middle East Technical University, Northern Cyprus Campus, Northern Cyprus, 2015.

[32] W. Frost, *Engineering handbook on the atmospheric environmental guidelines for use in wind turbine generator development /*. Washington, D.C. :, 1978.

[33] M. A. Baseer, J. P. Meyer, M. M. Alam, and S. Rehman, “Wind speed and power characteristics for Jubail industrial city, Saudi Arabia,” *Renew. Sustain. Energy Rev.*, vol. 52, pp. 1193–1204, Dec. 2015.

[34] A. B. Tabrizi, J. Whale, T. Lyons, and T. Urmee, “Rooftop wind monitoring campaigns for small wind turbine applications: Effect of sampling rate and averaging period,” *Renew. Energy*, vol. 77, pp. 320–330, May 2015.

[35] Y.-H. Wan, *Wind power plant behaviors: analyses of long-term wind power data*. National Renewable Energy Laboratory, 2004.

[36] M. L. Kubik, P. J. Coker, and C. Hunt, “Using meteorological wind data to estimate turbine generation output: a sensitivity analysis,” in *World Renewable Energy Congress-Sweden; 8-13 May; 2011; Linköping; Sweden*, 2011, pp. 4074–4081.

[37] A. Honrubia, A. Vigueras-Rodríguez, and E. Gómez-Lázaro, “The Influence of Turbulence and Vertical Wind Profile in Wind Turbine Power Curve,” in *Progress in Turbulence and Wind Energy IV*, M. Oberlack, J. Peinke, A. Talamelli, L. Castillo, and M. Hölling, Eds. Springer Berlin Heidelberg, 2012, pp. 251–254.

[38] R. Wagner, I. Antoniou, S. M. Pedersen, M. S. Courtney, and H. E. Jørgensen, “The influence of the wind speed profile on wind turbine performance measurements,” *Wind Energy*, vol. 12, no. 4, pp. 348–362, May 2009.

[39] A. Honrubia, A. Vingueras-Rodriguez, E. G. Lazaro, D. Rodriguez, M. Mejias, and I. Lainez, "The influence of wind shear in wind turbine power estimation," *measurements*, vol. 2, p. 9, 2010.

[40] "Wind Speed and Power Characteristics at Different Heights for a Wind Data Collection Tower in Saudi Arabia." [Online].Available: https://www.academia.edu/23852929/Wind_Speed_and_Power_Characteristics_at_Different_Heights_for_a_Wind_Data_Collection_Tower_in_Saudi_Arabia. [Accessed: 29-Oct-2016].

[41] M. N. Schwartz and D. L. Elliott, *Wind shear characteristics at central plains tall towers*. National Renewable Energy Laboratory, 2006.

[42] M. Schwartz and D. Elliott, "Towards a Wind Energy Climatology at Advanced Turbine Hub-Heights: Preprint," National Renewable Energy Lab., Golden, CO (US), NREL/CP-500-38109, May 2005.

[43] D. Saeidi, M. Mirhosseini, A. Sedaghat, and A. Mostafaeipour, "Feasibility study of wind energy potential in two provinces of Iran: North and South Khorasan," *Renew. Sustain. Energy Rev.*, vol. 15, no. 8, pp. 3558–3569, Oct. 2011.

[44] I. A. Pérez, M. A. García, M. L. Sánchez, and B. de Torre, "Analysis and parameterisation of wind profiles in the low atmosphere," *Sol. Energy*, vol. 78, no. 6, pp. 809–821, Jun. 2005.

[45] C. L. Archer and M. Z. Jacobson, "Spatial and temporal distributions of U.S. winds and wind power at 80 m derived from measurements," *J. Geophys. Res. Atmospheres*, vol. 108, no. D9, p. 4289, May 2003.

[46] D.L. Sisterson,B.B Hicks,R.L. Coutler, M.L. Wesley, "Difficulties in using power laws for wind energy assessment.," Sol. Energy, 1983.

[47] D. Weisser and T. j. Foxon, "Implications of seasonal and diurnal variations of wind velocity for power output estimation of a turbine: a case study of Grenada," *Int. J. Energy Res.*, vol. 27, no. 13, pp. 1165–1179, Oct. 2003.

[48] I. Y. F. Lun and J. C. Lam, "A study of Weibull parameters using long-term wind observations," *Renew. Energy*, vol. 20, no. 2, pp. 145–153, Jun. 2000.

[49] S. Pashardes and C. Christofides, “Statistical analysis of wind speed and direction in Cyprus,” *Sol. Energy*, vol. 55, no. 5, pp. 405–414, Nov. 1995.

[50] A. S. S. Dorvlo, “Estimating wind speed distribution,” *Energy Convers. Manag.*, vol. 43, no. 17, pp. 2311–2318, Nov. 2002.

[51] R. N. Farrugia, “The wind shear exponent in a Mediterranean island climate,” *Renew. Energy*, vol. 28, no. 4, pp. 647–653, Apr. 2003.

[52] A. Garcia, J. L. Torres, E. Prieto, and A. de Francisco, “Fitting wind speed distributions: a case study,” *Sol. Energy*, vol. 62, no. 2, pp. 139–144, Feb. 1998.

[53] R. H. Kirchhoff and F. C. Kaminsky, “Wind shear measurements and synoptic weather categories for siting large wind turbines,” *J. Wind Eng. Ind. Aerodyn.*, vol. 15, no. 1, pp. 287–297, Dec. 1983.

[54] J. C. Doran, “Inherent uncertainties in meteorological parameters for wind turbine design,” 1982.

[55] S. Rehman and N. M. Al-Abbadi, “Wind shear coefficients and their effect on energy production,” *Energy Convers. Manag.*, vol. 46, no. 15–16, pp. 2578–2591, Sep. 2005.

[56] M. L. Ray, A. L. Rogers, and J. G. Mcgowan, *1 Analysis of wind shear models and trends in different terrains*. .

[57] W. D. Lubitz, “Power Law Extrapolation of Wind Measurements for Predicting Wind Energy Production,” *Wind Eng.*, vol. 33, no. 3, pp. 259–271, May 2009.

[58] R. Soler-Bientz, S. Watson, and D. Infield, “Evaluation of the Wind Shear at a Site in the North-West of the Yucatan Peninsula, Mexico,” *Wind Eng.*, vol. 33, no. 1, pp. 93–107, Jan. 2009.

[59] E. Fırtın, Ö. Güler, and S. A. Akdağ, “Investigation of wind shear coefficients and their effect on electrical energy generation,” *Appl. Energy*, vol. 88, no. 11, pp. 4097–4105, Nov. 2011.

[60] “Wind resource analysis program (WRAP) 2002,” Minnesota Department of Commerce, St. Paul, Minnesota, USA, 2002.

[61] S. Rehman and N. M. Al-Abbadi, “Wind shear coefficient, turbulence intensity and wind power potential assessment for Dhulom, Saudi Arabia,” *Renew. Energy*, vol. 33, no. 12, pp. 2653–2660, Dec. 2008.

[62] I. Fyrippis, P. J. Axaopoulos, and G. Panayiotou, “Wind energy potential assessment in Naxos Island, Greece,” *Appl. Energy*, vol. 87, no. 2, pp. 577–586, Feb. 2010.

[63] T. L. Tiang and D. Ishak, “Technical review of wind energy potential as small-scale power generation sources in Penang Island Malaysia,” *Renew. Sustain. Energy Rev.*, vol. 16, no. 5, pp. 3034–3042, Jun. 2012.

[64] M. R. Islam, R. Saidur, and N. A. Rahim, “Assessment of wind energy potentiality at Kudat and Labuan, Malaysia using Weibull distribution function,” *Energy*, vol. 36, no. 2, pp. 985–992, Feb. 2011.

[65] A. Keyhani, M. Ghasemi-Varnamkhasti, M. Khanali, and R. Abbaszadeh, “An assessment of wind energy potential as a power generation source in the capital of Iran, Tehran,” *Energy*, vol. 35, no. 1, pp. 188–201, Jan. 2010.

[66] Sherlock RH., “Analysing winds for frequency and duration on atmospheric pollution,” *Meteorol Monogr Am Meteorol*, vol. 1, no. 4, pp. 42–49, 1951.

[67] M. Blanchard and G. Desrochers, “Generation of autocorrelated wind speeds for wind energy conversion system studies,” *Sol. Energy*, vol. 33, no. 6, pp. 571–579, Jan. 1984.

[68] K. C. Chou and R. B. Corotis, “Simulation of hourly wind speed and array wind power,” *Sol. Energy*, vol. 26, pp. 199–212, Jan. 1981.

[69] R. B. Corotis, A. B. Sigl, and J. Klein, “Probability models of wind velocity magnitude and persistence,” *Sol. Energy*, vol. 20, no. 6, pp. 483–493, Jan. 1978.

[70] K. Conradsen, L. B. Nielsen, and L. P. Prahm, “Review of Weibull Statistics for Estimation of Wind Speed Distributions,” *J. Clim. Appl. Meteorol.*, vol. 23, no. 8, pp. 1173–1183, Aug. 1984.

[71] W. E. Bardsley, “Note on the Use of the Inverse Gaussian Distribution for Wind Energy Applications,” *J. Appl. Meteorol.*, vol. 19, no. 9, pp. 1126–1130, Sep. 1979.

[72] R. E. Luna and H. W. Church, “Estimation of long-term concentrations using a ‘universal’ wind speed distribution,” *J. Appl. Meteorol.*, vol. 13, no. 8, pp. 910–916, 1974.

[73] J. P. Hennessey, “Some Aspects of Wind Power Statistics,” *J. Appl. Meteorol.*, vol. 16, no. 2, pp. 119–128, Feb. 1977.

[74] C. G. Justus, W. R. Hargraves, and A. Yalcin, “Nationwide Assessment of Potential Output from Wind-Powered Generators,” *J. Appl. Meteorol.*, vol. 15, no. 7, pp. 673–678, Jul. 1976.

[75] D. A. Stewart and O. M. Essenwanger, “Frequency distribution of wind speed near the surface,” *J. Appl. Meteorol.*, vol. 17, no. 11, pp. 1633–1642, 1978.

[76] J. Carlin and J. Haslett, “The probability distribution of wind power from a dispersed array of wind turbine generators,” *J. Appl. Meteorol.*, vol. 21, no. 3, pp. 303–313, 1982.

[77] A. K. Azad, M. G. Rasul, M. M. Alam, S. M. A. Uddin, and S. K. Mondal, “Analysis of Wind Energy Conversion System Using Weibull Distribution,” *Procedia Eng.*, vol. 90, pp. 725–732, 2014.

[78] A. N. Celik, “A statistical analysis of wind power density based on the Weibull and Rayleigh models at the southern region of Turkey,” *Renew. Energy*, vol. 29, no. 4, pp. 593–604, Apr. 2004.

[79] S. A. E K Akpinar, “Statistical analysis of wind energy potential on the basis of the Weibull and Rayleigh distributions for Agin-Elazig, Turkey,” *Proc. Inst. Mech. Eng. Part -J. Power Energy - PROC INST MECH ENG -J POWER*, vol. 218, no. 8, pp. 557–565, 2004.

[80] P. Ramírez and J. A. Carta, “Influence of the data sampling interval in the estimation of the parameters of the Weibull wind speed probability density distribution: a case study,” *Energy Convers. Manag.*, vol. 46, no. 15–16, pp. 2419–2438, Sep. 2005.

[81] X. Li, Ed., *Green Energy*, vol. 1. London: Springer London, 2011.

[82] A. Mostafaeipour, A. Sedaghat, A. A. Dehghan-Niri, and V. Kalantar, "Wind energy feasibility study for city of Shahrbabak in Iran," *Renew. Sustain. Energy Rev.*, vol. 15, no. 6, pp. 2545–2556, Aug. 2011.

[83] Z. O. Olaofe and K. A. Folly, "Statistical Analysis of Wind Resources at Darling for Energy Production," *Int. J. Renew. Energy Res. IJRER*, vol. 2, no. 2, pp. 250–261, May 2012.

[84] J. Aidan and J. C. Ododo, "Wind Speed Distributions and Power Densities of Some Cities in Northern Nigeria," *J. Eng. Appl. Sci.*, vol. 5, no. 6, pp. 420–426, Jun. 2010.

[85] K. ULGEN, A. GENC, A. HEPBASLI, and G. OTURANC, "Assessment of Wind Characteristics for Energy Generation," *Energy Sources*, vol. 26, no. 13, pp. 1227–1237, Nov. 2004.

[86] M. Brower, Ed., *Wind resource assessment: a practical guide to developing a wind project*. Hoboken, N.J: Wiley, 2012.

[87] B. H. Bailey, S. L. McDonald, D. W. Bernadett, M. J. Markus, and K. V. Elsholz, "Wind Resource Assessment Handbook: Fundamentals for Conducting a Successful Monitoring Program," National Renewable Energy Lab., Golden, CO (US); AWS Scientific, Inc., Albany, NY (US), NREL/SR--440-22223; ON: DE97000250, Apr. 1997.

[88] "REDAR – METU NCC RENEWABLE ENERGY RESEARCH | REDAR – Northern Cyprus," *REDAR – METU NCC RENEWABLE ENERGY RESEARCH*. .

[89] "thiesclima.com - Products." [Online].Available: https://www.thiesclima.com/en/Products/Wind-First-Class/. [Accessed: 12-Apr-2017].

[90] "Wind vanes for wind resource assessment."[Online]. Available: https://www.kintech-engineering.com/htm/en/products/section/27/wind-vanes. [Accessed: 12-Apr-2017].

[91] L. Quéval, C. Joulain, and C. Casillas, “Measuring the Power Curve of a Small-Scale Wind Turbine: A Practical Example,” *Proc. 1st Int. E-Conf. Energ.*

[92] “IEC 61400-12-1:2017 | IEC Webstore.” [Online].Available: https://webstore.iec.ch/publication/26603. [Accessed: 13-Apr-2017].

[93] *Modern Applied Statistics with S | W.N. Venables | Springer*. .

[94] “IEC 61400-12-1:2005 | IEC Webstore | rural electrification, wind power.” [Online].Available: https://webstore.iec.ch/publication/5429. [Accessed: 16-Apr-2017].

[95] D. Freedman and P. Diaconis, “On the histogram as a density estimator:L2 theory,” *Z. Für Wahrscheinlichkeitstheorie Verwandte Geb.*, vol. 57, no. 4, pp. 453–476, Dec. 1981.

[96] “EXCEL Univariate: Histogram.” [Online].Available: http://cameron.econ.ucdavis.edu/excel/ex11histogram.html. [Accessed: 16-Apr-2017].

[97] S. A. Kalogirou, “Generation of typical meteorological year (TMY-2) for Nicosia, Cyprus,” *Renew. Energy*, vol. 28, no. 15, pp. 2317–2334, Dec. 2003.

[98] A. L. S. Chan, T. T. Chow, S. K. F. Fong, and J. Z. Lin, “Generation of a typical meteorological year for Hong Kong,” *Energy Convers. Manag.*, vol. 47, no. 1, pp. 87–96, Jan. 2006.

[99] “Meteonorm: Features.” [Online].Available: http://meteonorm.com/en/features. [Accessed: 27-Oct-2015].

[100] M. L. Kubik, D. J. Brayshaw, P. J. Coker, and J. F. Barlow, “Exploring the role of reanalysis data in simulating regional wind generation variability over Northern Ireland,” *Renew. Energy*, vol. 57, pp. 558–561, Sep. 2013.

[101] M. L. Kubik, P. J. Coker, J. F. Barlow, and C. Hunt, “A study into the accuracy of using meteorological wind data to estimate turbine generation output,” *Renew. Energy*, vol. 51, pp. 153–158, Mar. 2013.

[102] V. Kotroni, K. Lagouvardos, and S. Lykoudis, “High-resolution model-based wind atlas for Greece,” *Renew. Sustain. Energy Rev.*, vol. 30, pp. 479–489, Feb. 2014.

[103] J. Smith, “California Polytechnic State University Wind Resource Assessment,” *Masters Theses Proj. Rep.*, Sep. 2011.

[104] D. Elliott, B. Chadraa, and L. Natsagdorj, “Mongolia Wind Resource Assessment Project,” National Renewable Energy Lab., Golden, CO (US), NREL/CP--500-25148; WF7C0201; ON: DE00001316, Sep. 1998.

[105] J. F. Manwell, J. G. McGowan, and A. L. Rogers, *Wind energy explained: theory, design and application*, 2nd ed. Chichester, U.K: Wiley, 2009.

[106] A. G. Davenport, “Rationale for determining design wind velocities,” *ASCE J. Struct. Div.*, vol. 86, no. 5, pp. 39–68, Oct. 1960.

[107] C. G. Justus and A. Mikhail, “Height variation of wind speed and wind distributions statistics,” *Geophys. Res. Lett.*, vol. 3, no. 5, pp. 261–264, May 1976.

[108] S. Emeis and M. Turk, “Comparison of Logarithmic Wind Profiles and Power Law Wind Profiles and their Applicability for Offshore Wind Profiles,” in *Wind Energy*, P. D. J. Peinke, P. D.-I. P. Schaumann, and D. S. Barth, Eds. Springer Berlin Heidelberg, 2007, pp. 61–64.

[109] S. Emeis, “How well does a power law fit to a diabatic boundary-layer wind profile.”

[110] “WebMET - The Meteorological Resource Center.” [Online].Available: http://www.webmet.com/met_monitoring/625.HTML. [Accessed: 18-Apr-2017].

[111] F. C. Kaminsky, “Four probability densities /log-normal, gamma, Weibull, and Rayleigh/ and their application to modelling average hourly wind speed,” presented at the International Solar Energy Society, Annual Meeting, 1977, pp. 19–6.

[112] W. Weibull, “A statistical distribution function of wide applicability,” *J. Appl. Mech.*, vol. 18, pp. 293–297, 1951.

[113] S. Persaud, D. Flynn, and B. Fox, “Potential for wind generation on the Guyana coastlands,” *Renew. Energy*, vol. 18, no. 2, pp. 175–189, Oct. 1999.

[114] A. M. Law and W. D. Kelton, *Simulation modeling and analysis*, 2nd ed. New york: McGraw-Hill, 1991.

[115] R. Kollu, S. R. Rayapudi, S. V. L. Narasimham, and K. M. Pakkurthi, “Mixture probability distribution functions to model wind speed distributions,” *Int. J. Energy Environ. Eng.*, vol. 3, no. 1, p. 27, Dec. 2012.

[116] N. Masseran, A. M. Razali, K. Ibrahim, A. Zaharim, and K. Sopian, “The probability distribution model of wind speed over east Malaysia,” *Res. J. Appl. Sci. Eng. Technol.*, vol. 6, no. 10, pp. 1774–1779, 2013.

[117] N. L. Johnson, S. Kotz, and N. Balakrishnan, *Continuous univariate distributions*, 2nd ed. New York: Wiley, 1994.

[118] D. R. Wingo, “Computing Maximum-Likelihood Parameter Estimates of the Generalized Gamma Distribution by Numerical Root Isolation,” *IEEE Trans. Reliab.*, vol. R-36, no. 5, pp. 586–590, Dec. 1987.

[119] E. L. Crow and K. Shimizu, Eds., *Lognormal distributions: theory and applications*. New York: M. Dekker, 1988.

[120] K. V. Bury, *Statistical distributions in engineering*. Cambridge ; New York: Cambridge University Press, 1999.

[121] M. V. Jambunathan, “Some Properties of Beta and Gamma Distributions,” *Ann. Math. Stat.*, vol. 25, no. 2, pp. 401–405, Jun. 1954.

[122] C. S. Forbes, Ed., *Statistical distributions /: Catherine Forbes ... [et al.]*, 4th ed. Hoboken, N.J: Wiley, 2011.

[123] *Probabilistic Techniques in Exposure Assessment - A | Alison C. Cullen | Springer*. .

[124] J. Wolfowitz, “The Minimum Distance Method,” *Ann. Math. Stat.*, vol. 28, no. 1, pp. 75–88, Mar. 1957.

[125] J. Wolfowitz, “Estimation by the Minimum Distance Method in Nonparametric Stochastic Difference Equations,” *Ann. Math. Stat.*, vol. 25, no. 2, pp. 203–217, 1954.

[126] M. Kac, J. Kiefer, and J. Wolfowitz, "On Tests of Normality and Other Tests of Goodness of Fit Based on Distance Methods," *Ann. Math. Stat.*, vol. 26, no. 2, pp. 189–211, Jun. 1955.

[127] F. James, Ed., *Statistical methods in experimental physics*, 2nd ed. Hackensack, NJ: World Scientific, 2006.

[128] H. Cramér, "On the composition of elementary errors," *Scand. Actuar. J.*, vol. 1928, no. 1, pp. 13–74, Jan. 1928.

[129] R. Mises, *Wahrscheinlichkeit Statistik und Wahrheit: Einführung in die Neue Wahrscheinlichkeitslehre und ihre Anwendung*. 1936.

[130] T. W. Anderson, "On the Distribution of the Two-Sample Cramer-von Mises Criterion," *Ann. Math. Stat.*, vol. 33, no. 3, pp. 1148–1159, Sep. 1962.

[131] A. Kolmogorov, "Sulla Determinazione Empirica di una Legge di Distribuzione," *G. DellIstituto Ital. Degli Attuari*, vol. 4, pp. 83–91, 1933.

[132] N. Smirnov, "Table for Estimating the Goodness of Fit of Empirical Distributions," *Ann. Math. Stat.*, vol. 19, no. 2, pp. 279–281, Jun. 1948.

[133] S. Mathew, *Wind energy: fundamentals, resource analysis and economics*. Berlin; New York: Springer, 2006.

[134] "Wind turbine power curves." [Online].Available: http://www.wind-power-program.com/turbine_characteristics.htm. [Accessed: 04-Jun-2017].

[135] V. Sohoni, S. C. Gupta, and R. K. Nema, "A Critical Review on Wind Turbine Power Curve Modelling Techniques and Their Applications in Wind Based Energy Systems," *J. Energy*, vol. 2016, p. e8519785, Jul. 2016.

[136] A. Kusiak, H. Zheng, and Z. Song, "Models for monitoring wind farm power," *Renew. Energy*, vol. 34, no. 3, pp. 583–590, Mar. 2009.

[137] S. Shokrzadeh, M. J. Jozani, and E. Bibeau, "Wind Turbine Power Curve Modeling Using Advanced Parametric and Nonparametric Methods," *IEEE Trans. Sustain. Energy*, vol. 5, no. 4, pp. 1262–1269, Oct. 2014.

[138] "Wind Turbine Data Analysis," WindAnalysis.m, 14-Oct-2013. [Online].Available: https://www.mathworks.com/matlabcentral/mlc-

downloads/downloads/submissions/43908/versions/1/previews/html/WindAnalysis.html#6. [Accessed: 21-Apr-2017].

[139] C. Carrillo, A. F. Obando Montaño, J. Cidrás, and E. Díaz-Dorado, "Review of power curve modelling for wind turbines," *Renew. Sustain. Energy Rev.*, vol. 21, pp. 572–581, May 2013.

[140] S. M. H. Ali, M. J. S. Zuberi, M. A. Tariq, D. Baker, and A. Mohiuddin, "A study to incorporate renewable energy technologies into the power portfolio of Karachi, Pakistan," *Renew. Sustain. Energy Rev.*, vol. 47, pp. 14–22, Jul. 2015.

[141] A. Betz, *Introduction to the theory of flow machines*. Oxford; New York: Pergamon Press, 1966.

[142] O. Yissa Dawde, *Wind Resource Data Analysis : The case of MYDERHU project site, Tigray regional state, Ethiopia*. 2013.

[143] I. E. Commission, "IEC 61400-1: Wind turbines part 1: Design requirements," *Int. Electrotech. Comm.*, 2005.

[144] R. Wagner, *Accounting for the speed shear in wind turbine power performance measurement*. Risø National Laboratory for Sustainable Energy, 2010.

[145] T. Fichter, F. Trieb, M. Moser, and J. Kern, "Optimized Integration of Renewable Energies into Existing Power Plant Portfolios," *Energy Procedia*, vol. 49, pp. 1858–1868, Jan. 2014.

[146] S.M.SAJED SADATI, "ASSESSMENT OF RENEWABLE ENERGY BASED MICRO-GRIDS FOR SMALL COMMUNITIES," MIDDLE EAST TECHNICAL UNIVERSITY NORTHERN CYPRUS CAMPUS, 2016.

[147] "IRENA | Publications | Reports and papers | Renewable Energy Cost Analysis - Wind Power." [Online].Available: http://www.irena.org/menu/index.aspx?mnu=Subcat&PriMenuID=36&CatID=141&SubcatID=230. [Accessed: 01-May-2017].

APPENDIX A

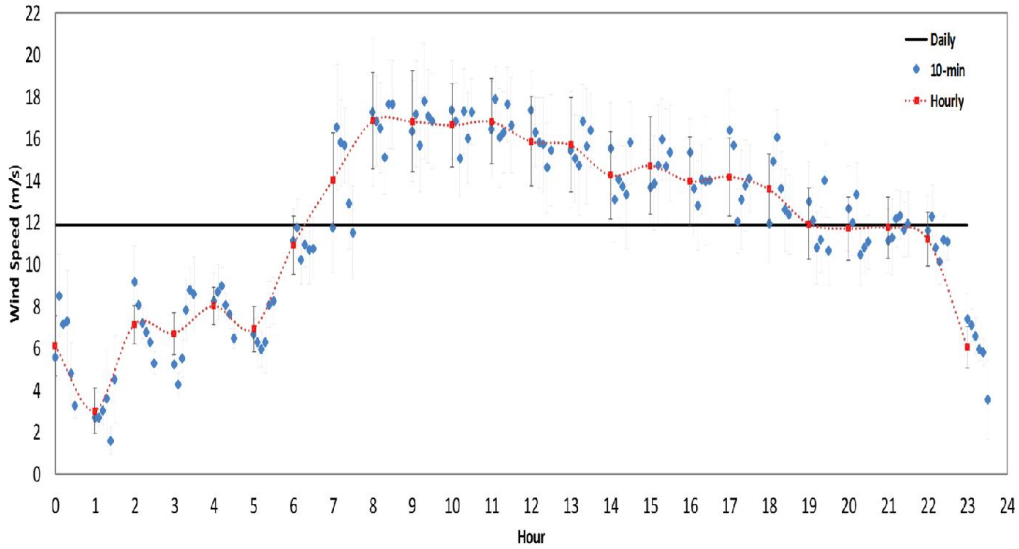

Figure A.1 Diurnal variation of 50m wind speed on a typical day (19 Jan 2016)

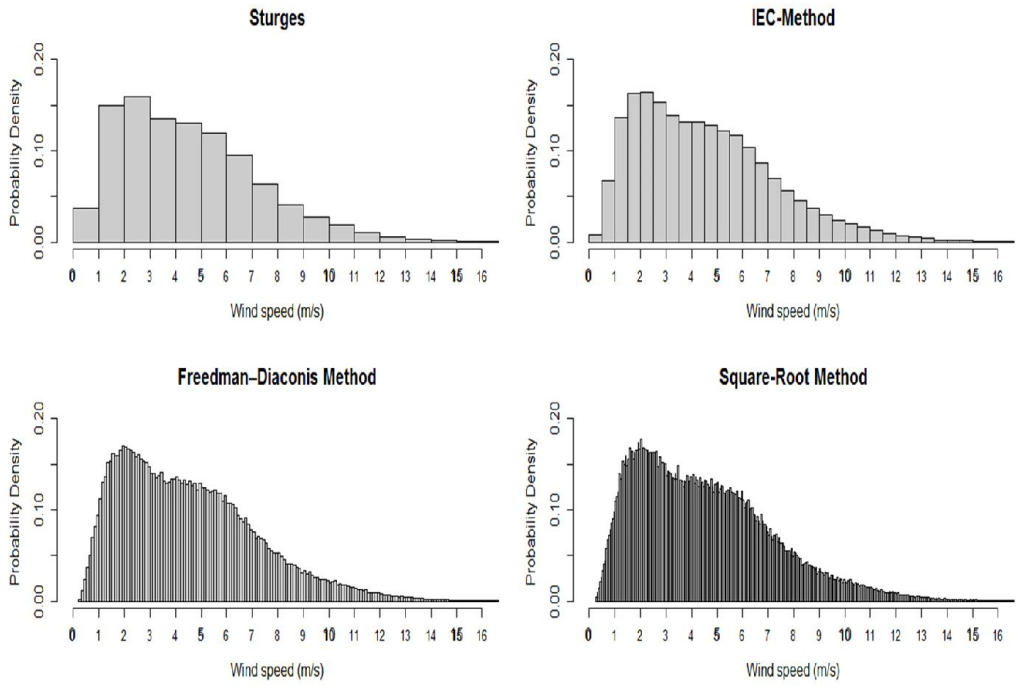

Figure A.2 Histogram of 50-meter wind speed data of all years (2013-2016)

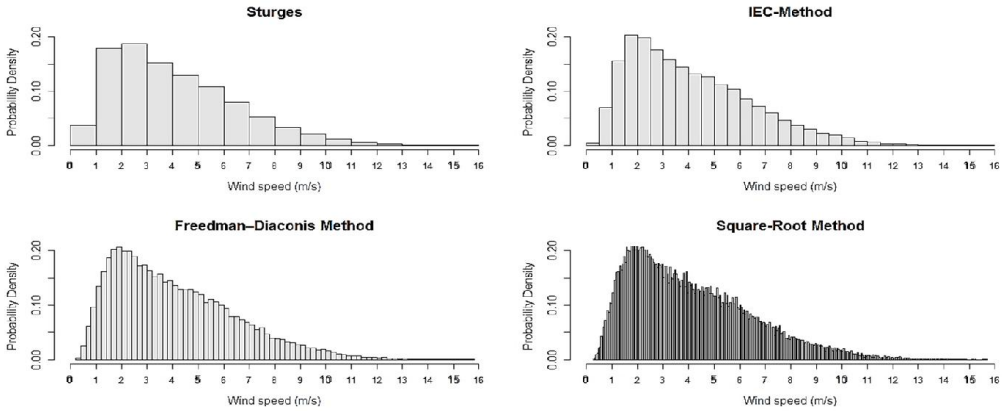

Figure A.3 Histogram of 30-meter wind speed data (2014)

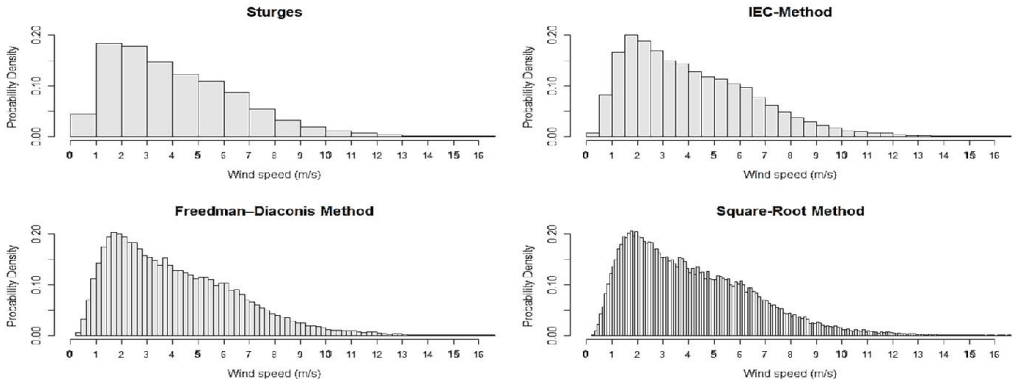

Figure A.4 Histogram of 30-meter wind speed data (2015)

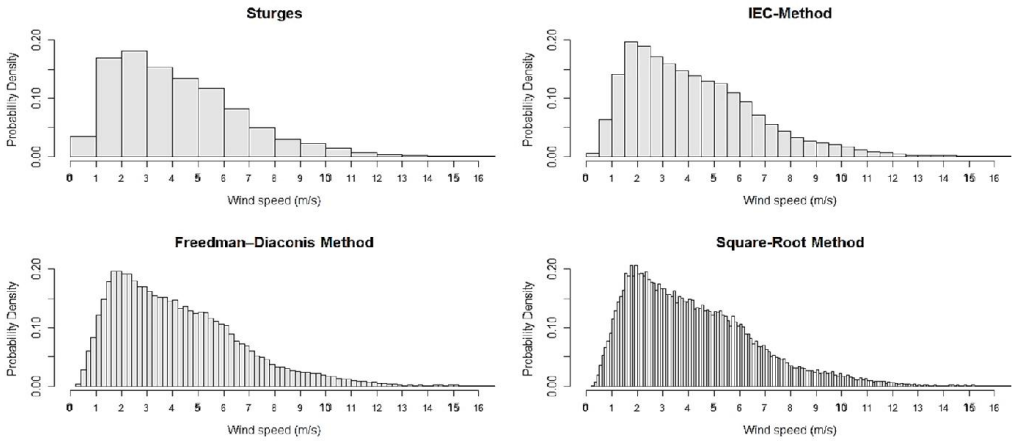

Figure A.5 Histogram of 30-meter wind speed data (2016)

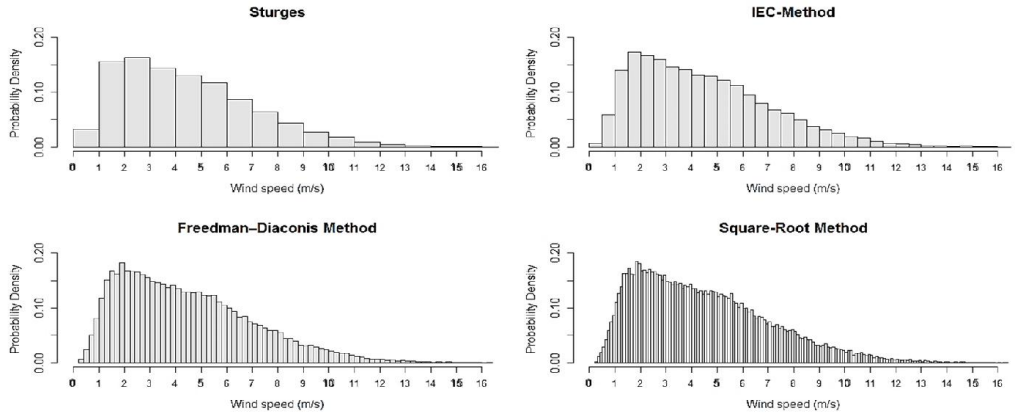

Figure A.6 Histogram of 50-meter wind speed data (2014)

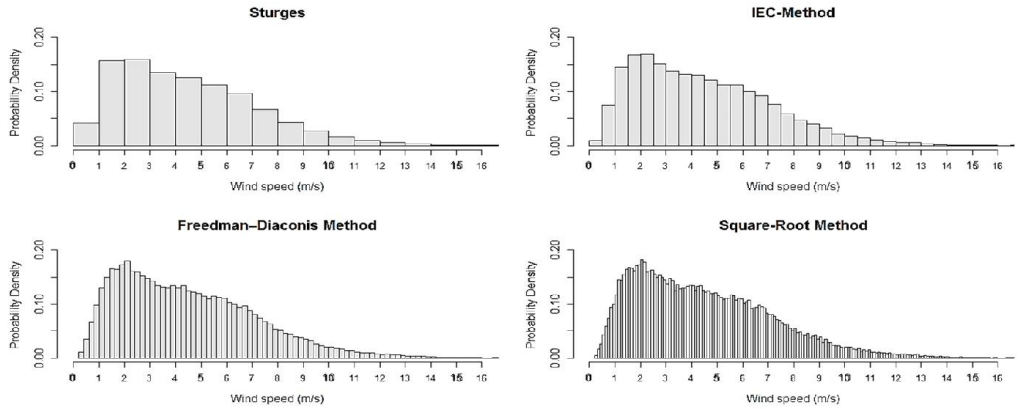

Figure A.7 Histogram of 50-meter wind speed data (2015)

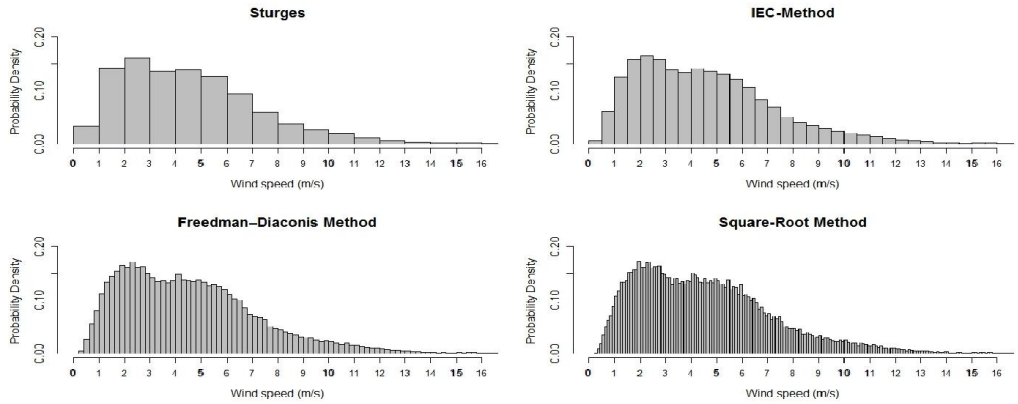

Figure A.8 Histogram of 50-meter wind speed data (2016)

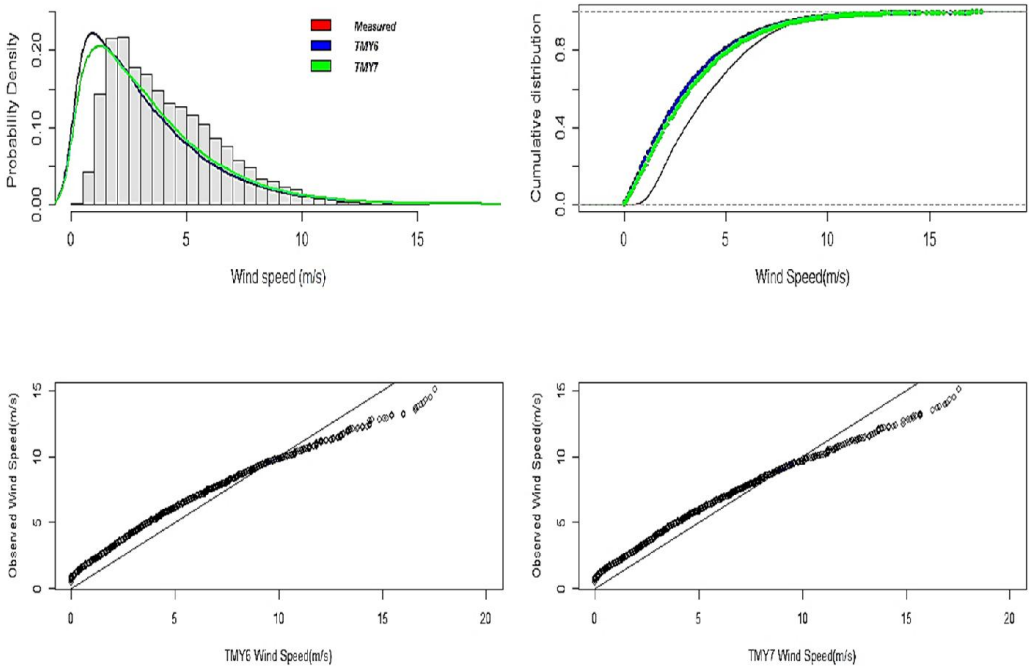

Figure A.9 PDF & CDF comparison of measured wind speeds 30m (2013-2016) & TMY generated wind speeds

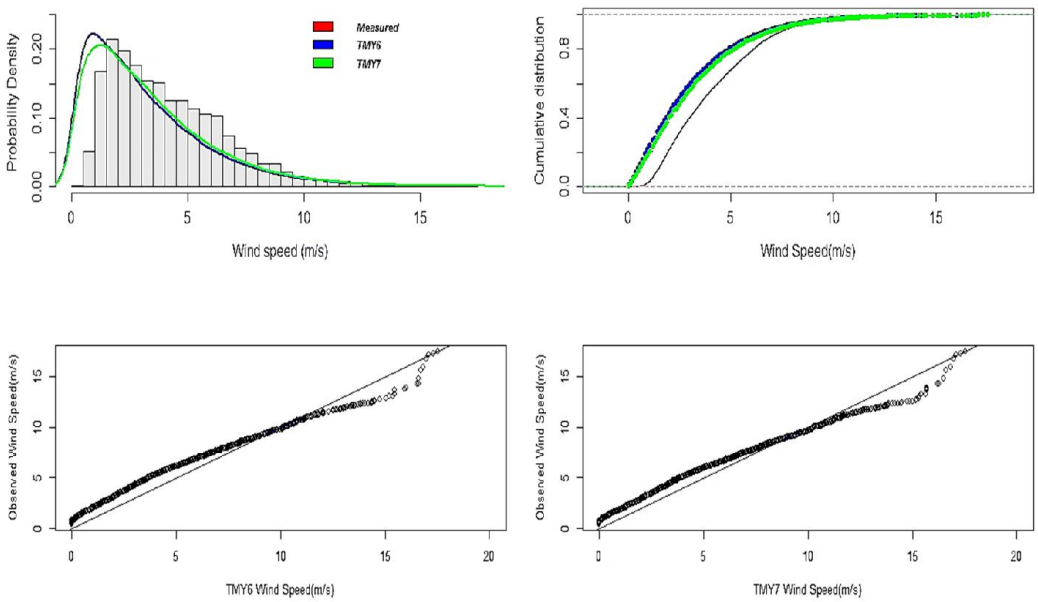

Figure A.10 PDF & CDF comparison of measured wind speeds 30m (2015) & TMY generated wind speeds

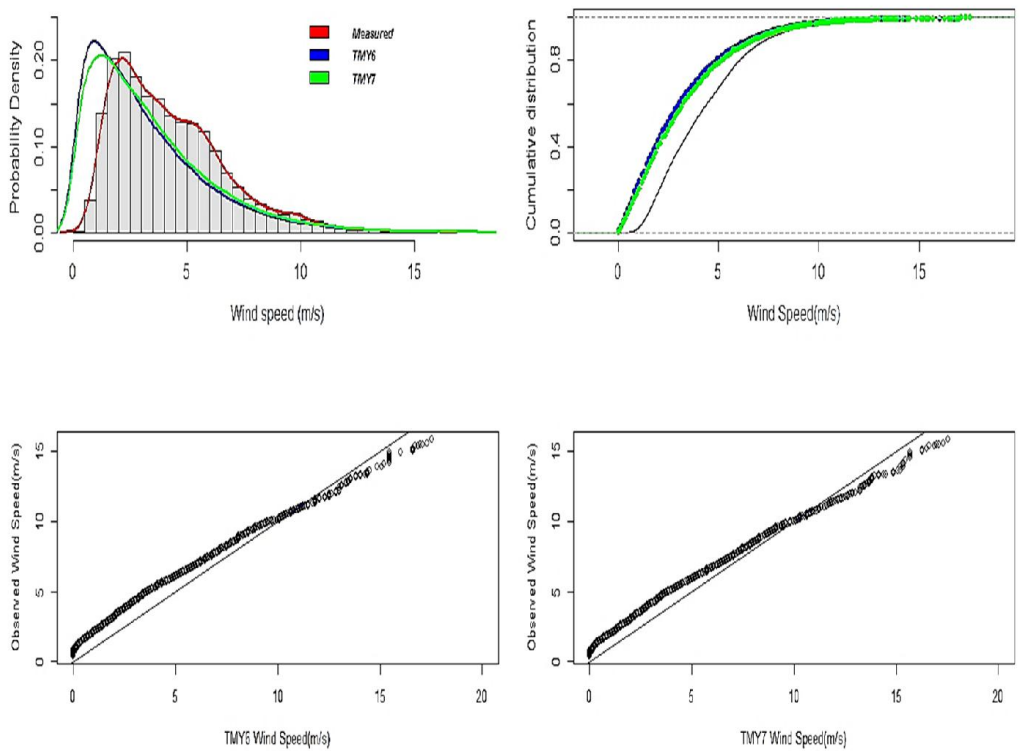

Figure A.11 PDF & CDF comparison of measured wind speeds 30m (2016) & TMY generated wind speeds

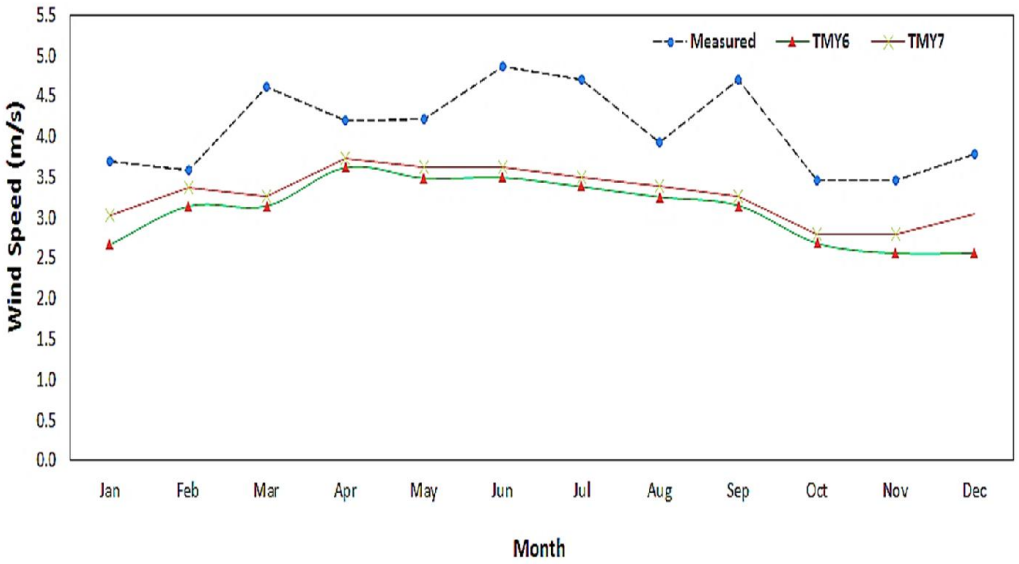

Figure A.12 Average monthly 30m wind speeds (2014) and TMY wind speeds

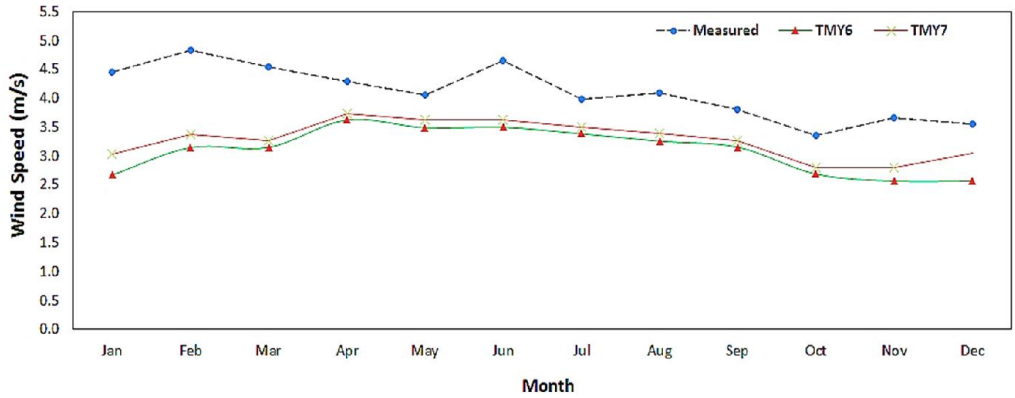

Figure A.13 Average monthly 30m wind speeds (2015) and TMY wind speeds

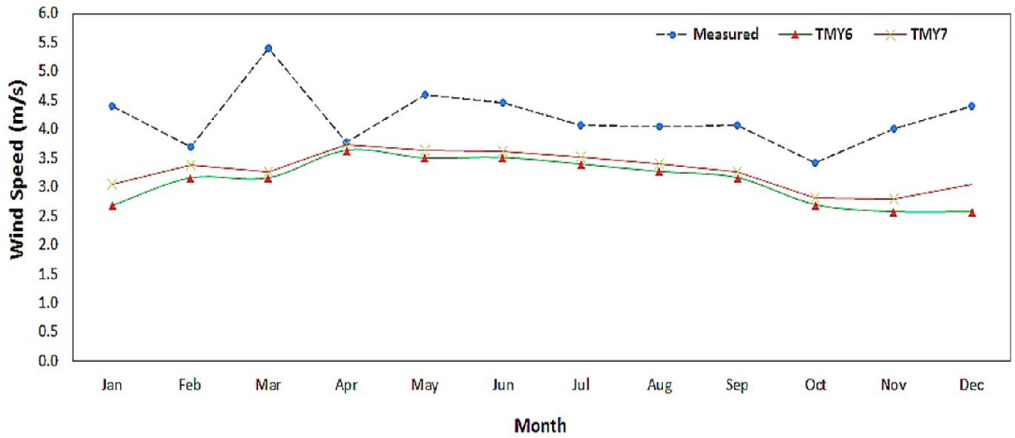

Figure A.14 Average monthly 30m wind speeds (2016) and TMY wind speeds

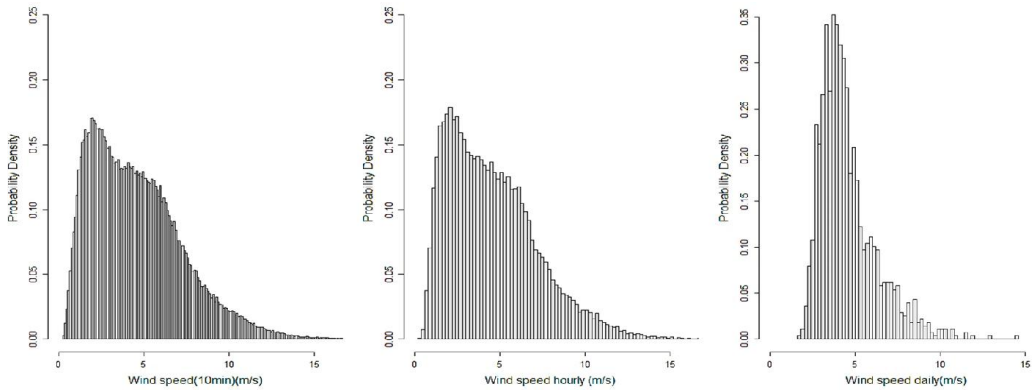

Figure A.15 Histogram of 50-meter wind speed with different resolutions (2013-2016)

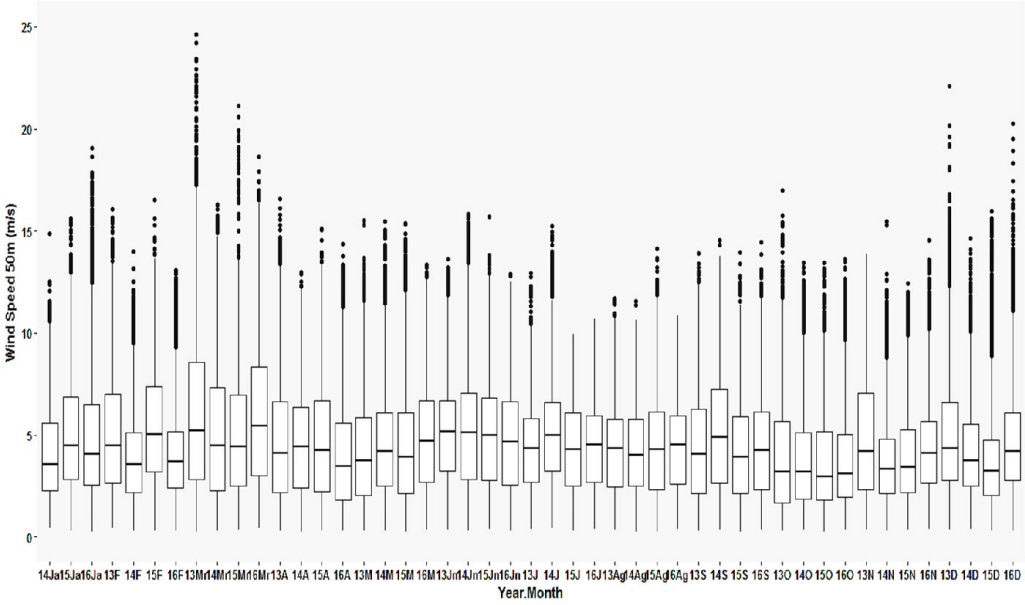

Figure A.16 Box plot of 10 min wind speed (30 meter) data of all years (2013-2016)

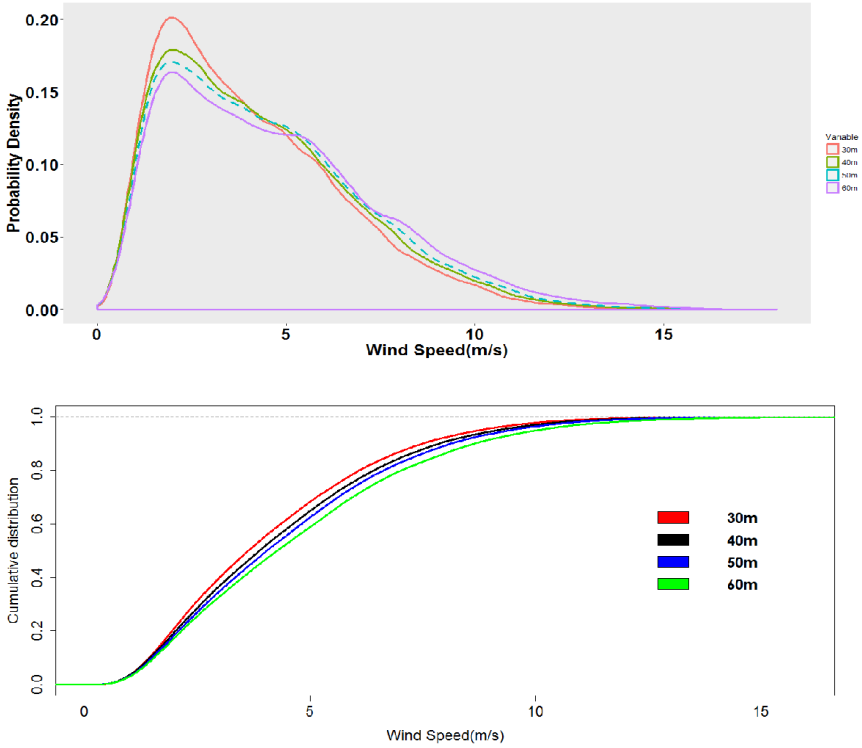

Figure A.17 Probability Density and Cumulative Distribution Function of 2014 wind speeds

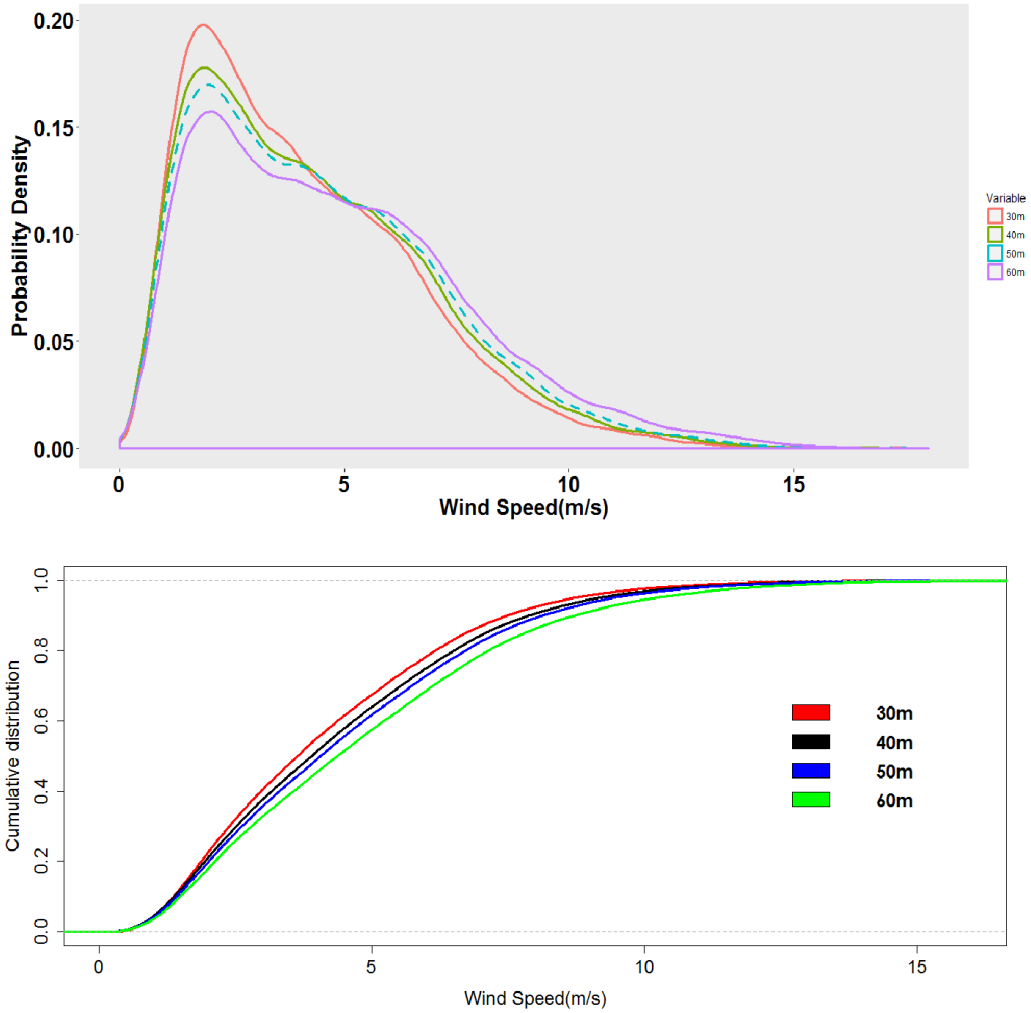

Figure A.18 Probability Density and Cumulative Distribution Function of 2015 wind speeds

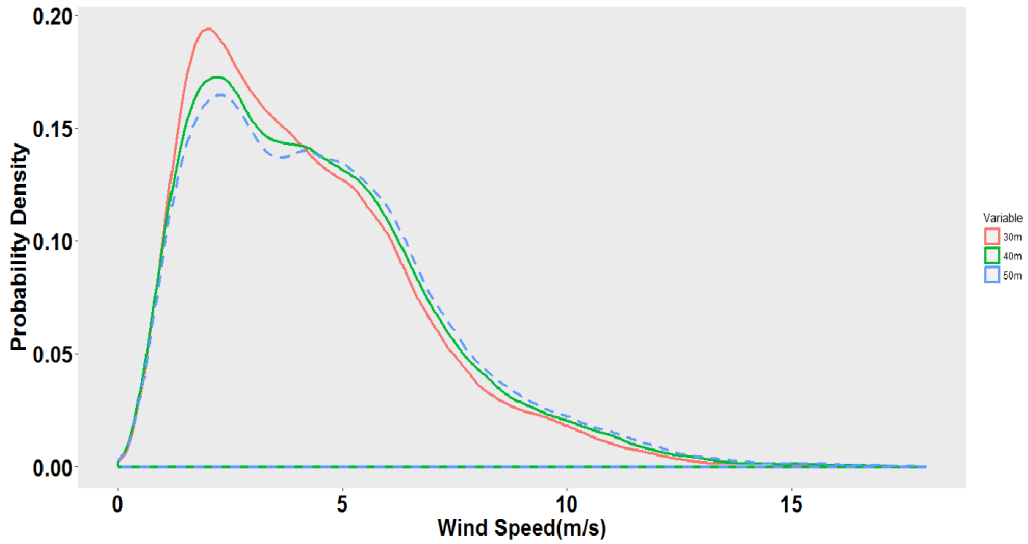

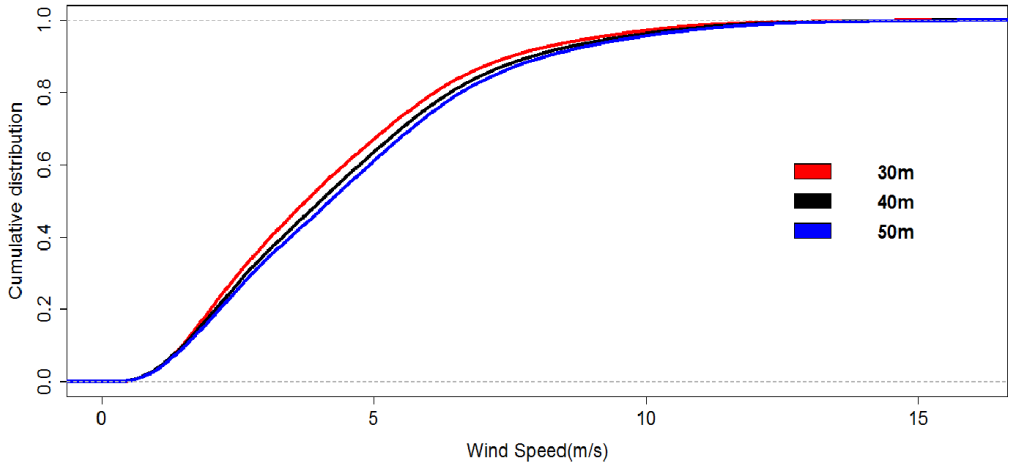

Figure A.19 Probability Density and Cumulative Distribution Function of 2016 wind speeds

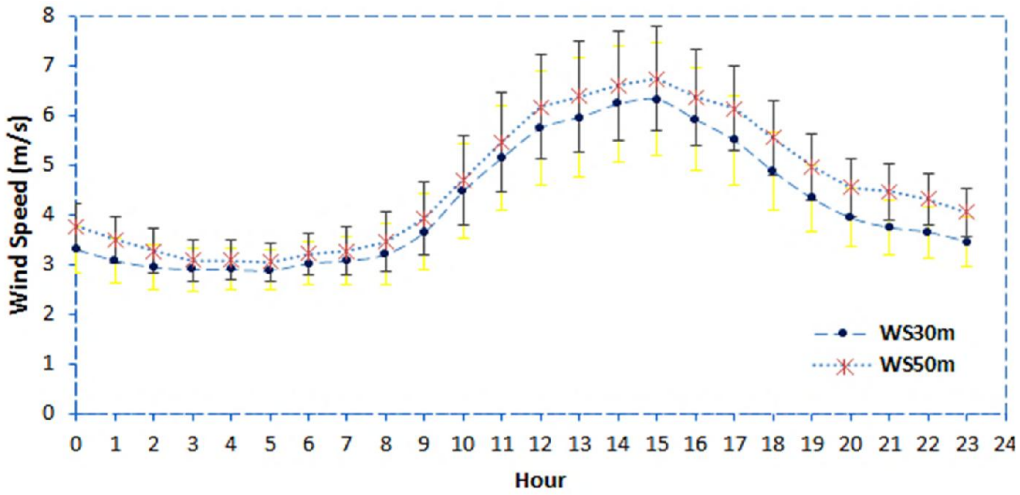

Figure A.20 Averaged diurnal variation of wind speed at 30m & 50m height (2014)

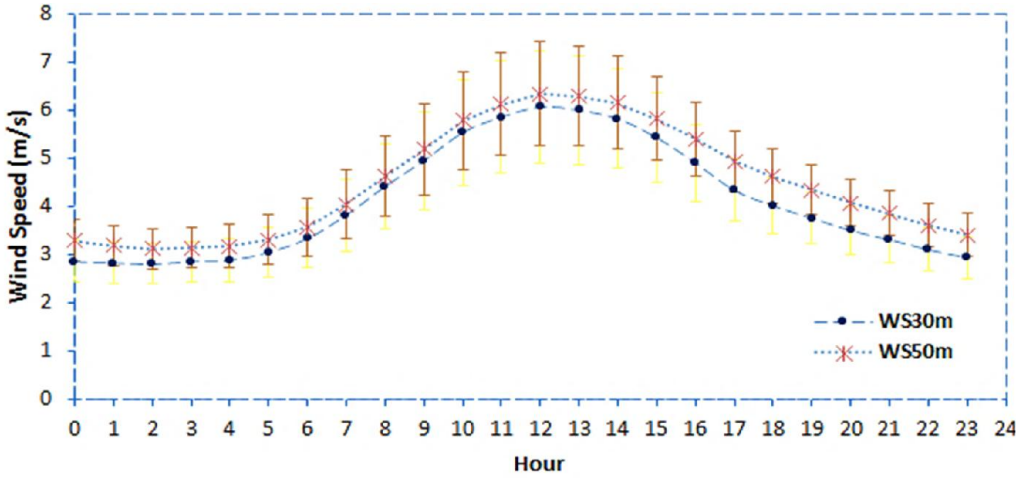

Figure A.21 Averaged diurnal variation of wind speed at 30m & 50m height (2015)

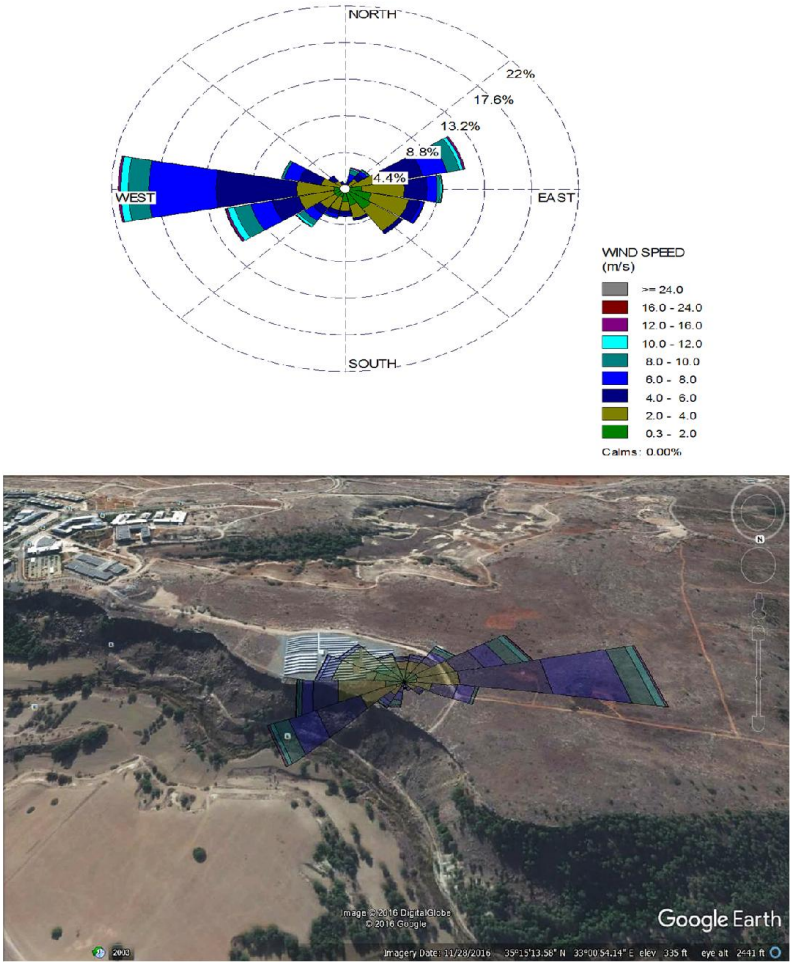

Figure A.22 Wind Rose of wind speed direction at 48meter height for year 2015

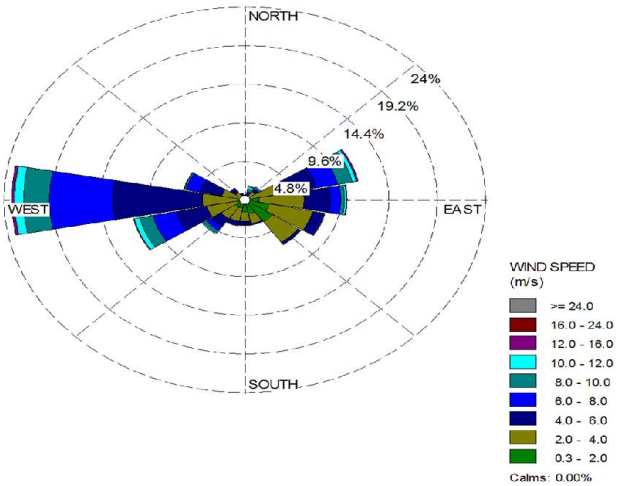

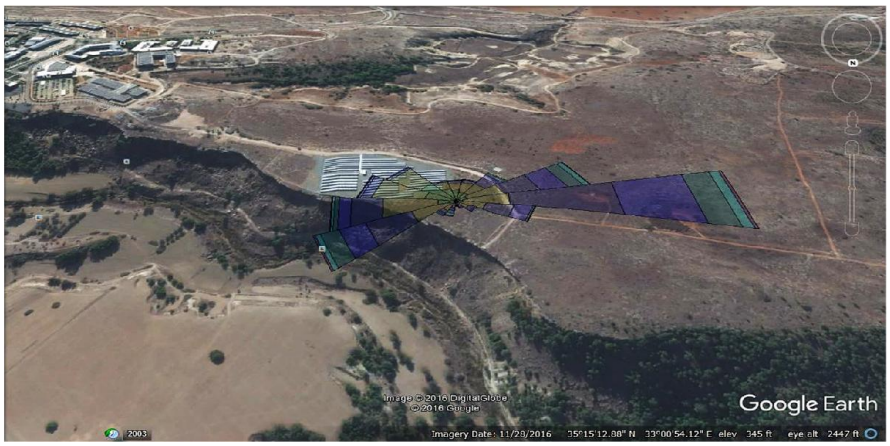

Figure A.23 Wind Rose of wind speed direction at 48meter height for year 2014

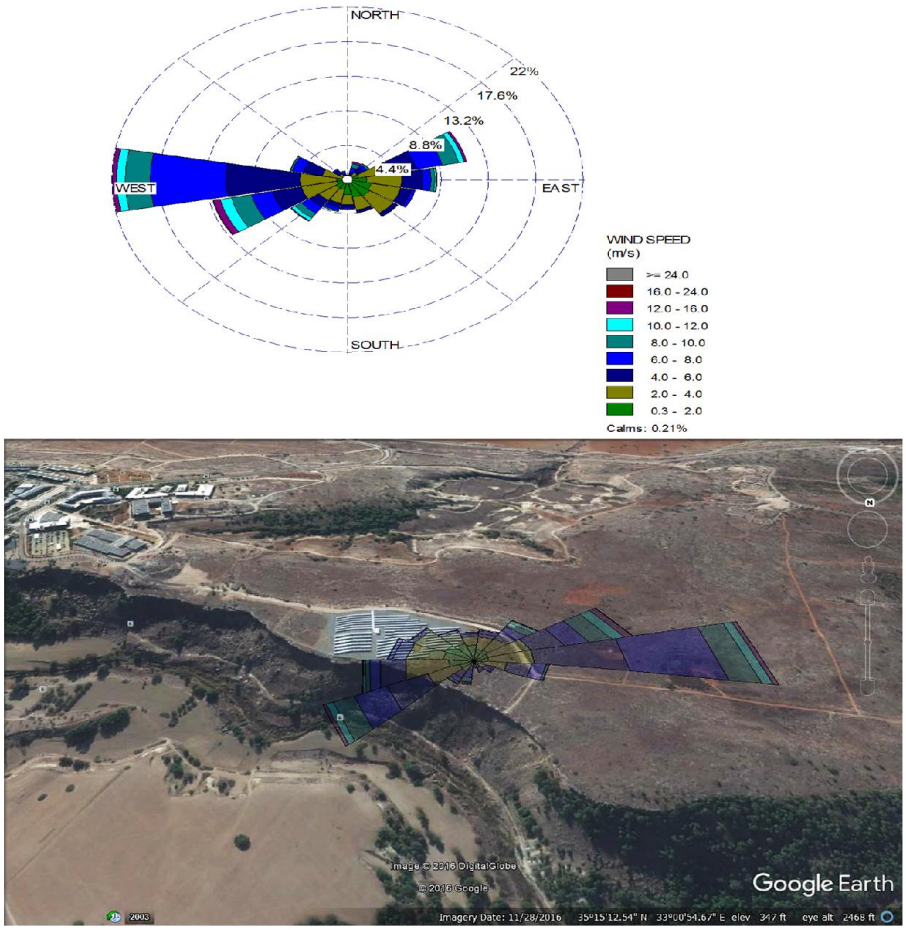

Figure A.24 Wind Rose of wind speed direction at 58meter height for year 2015

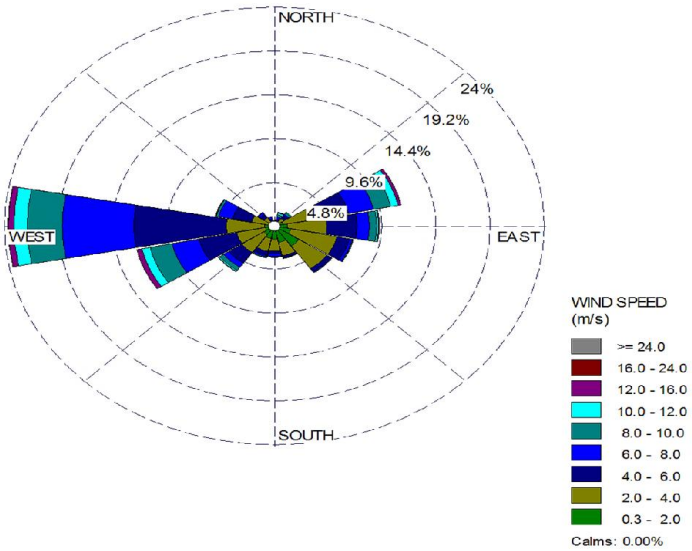

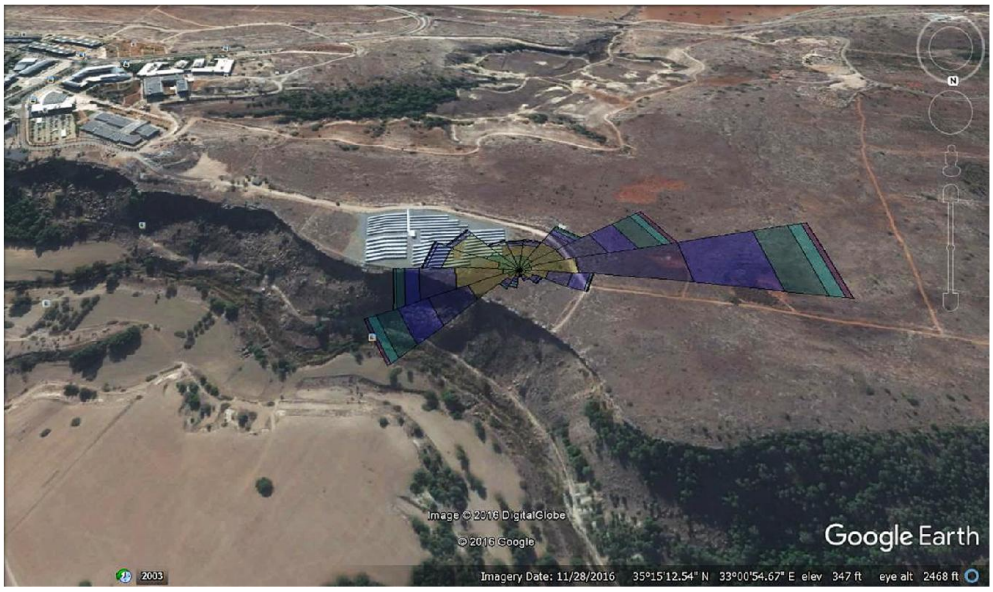

Figure A.25 Wind Rose of wind speed direction at 58meter height for year 2014

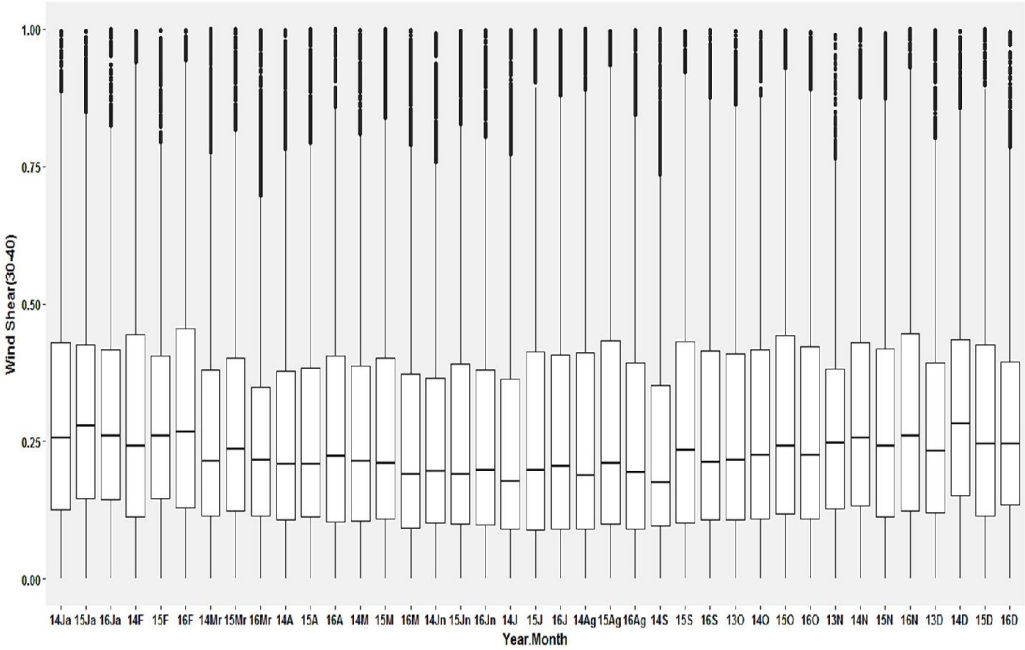

Figure A.26 Box plot of 30-50m wind shear exponent (α) values of all years (2013-2016)

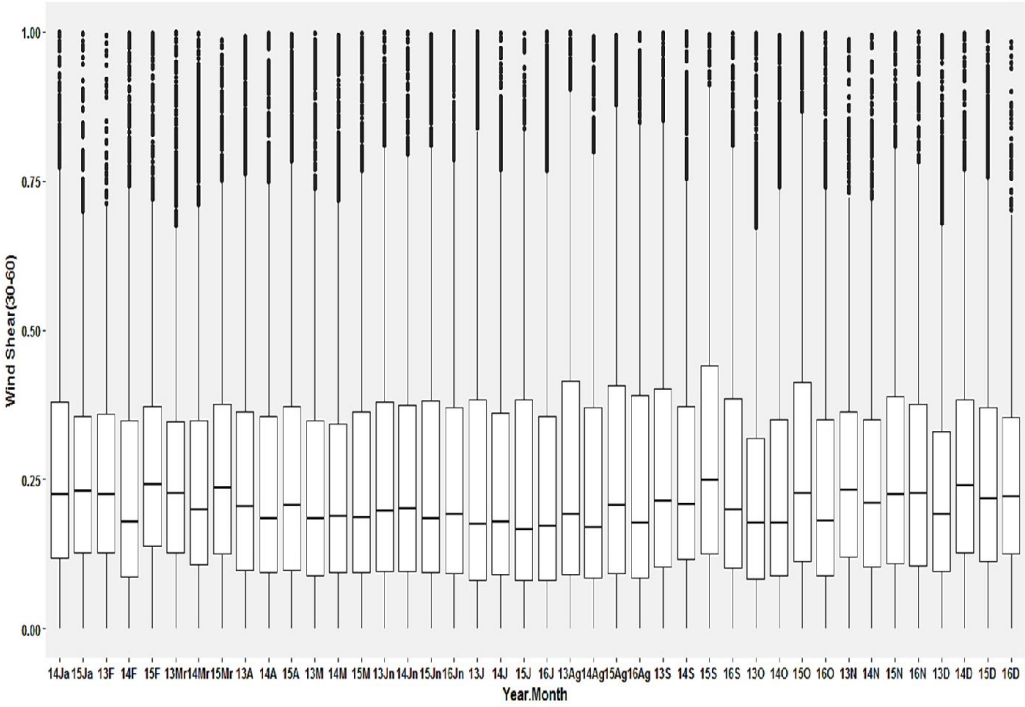

Figure A.27 Box plot of 30-50m wind shear exponent (α) values of all years (2013-2016)

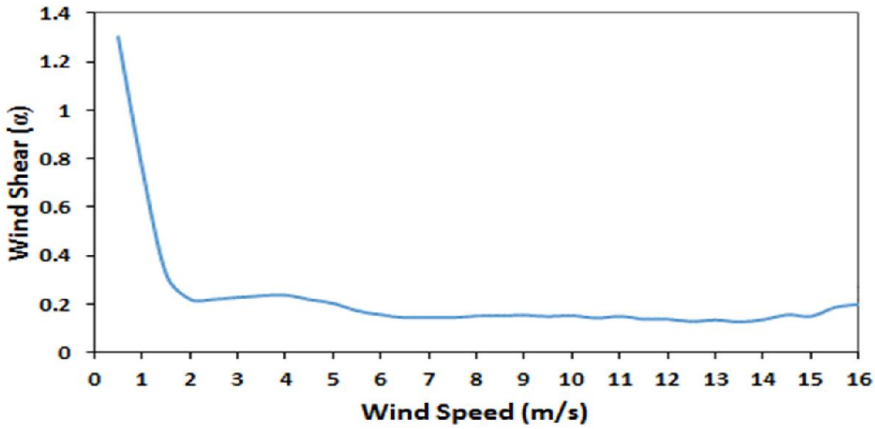

Figure A.28 Wind shear exponent variation with respect to 10-min wind speed at 30m (2013)

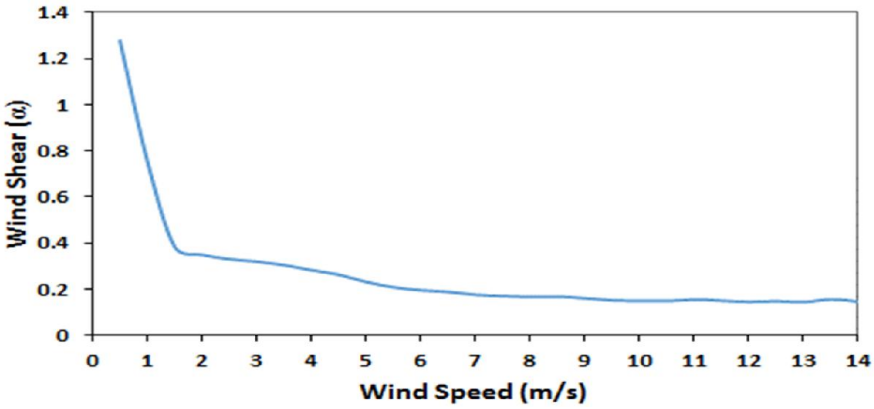

Figure A.29 Wind shear exponent variation with respect to 10-min wind speed at 30m (2014)

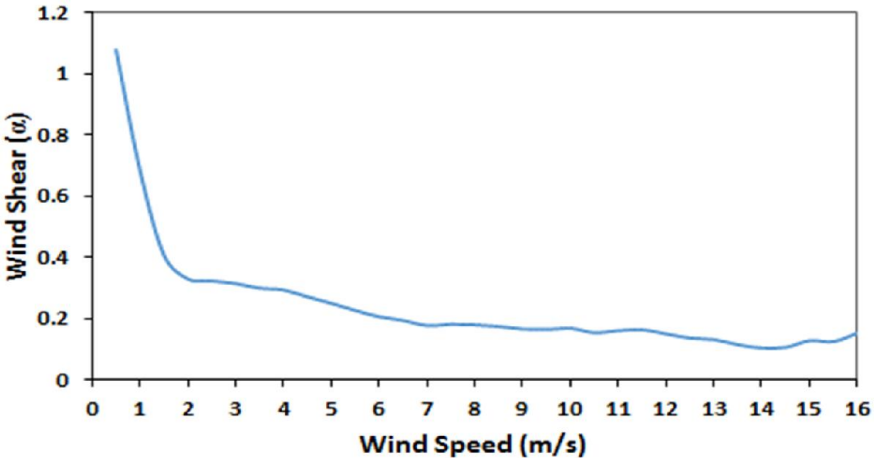

Figure A.30 Wind shear exponent variation with respect to 10-min wind speed at 30m (2015)

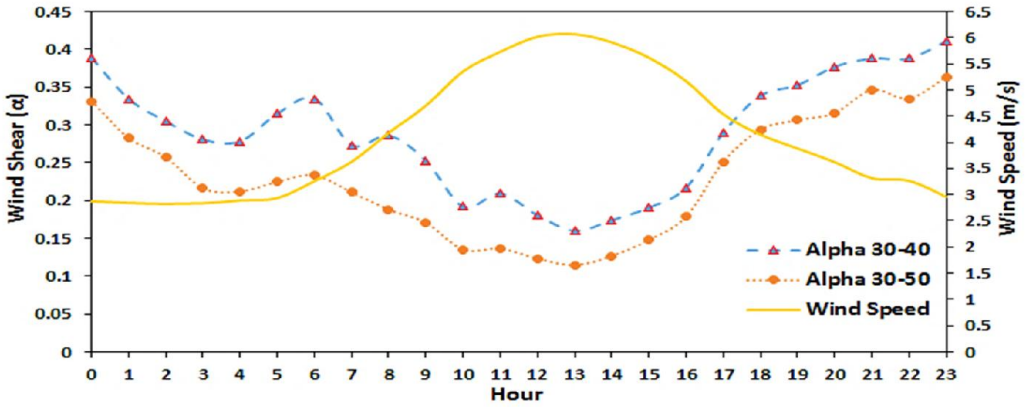

Figure A.31 Averaged diurnal pattern of wind shear exponent (α) and wind speed 30m (2014)

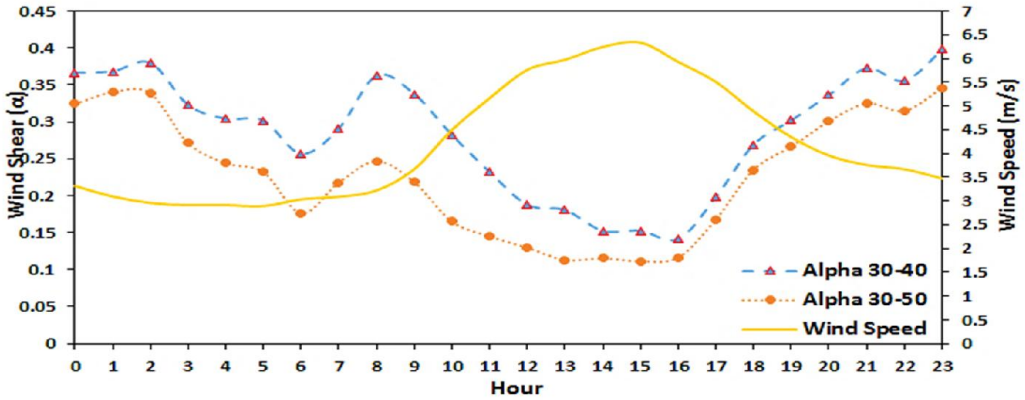

Figure A.32 Averaged diurnal pattern of wind shear exponent (α) and wind speed 30m (2015)

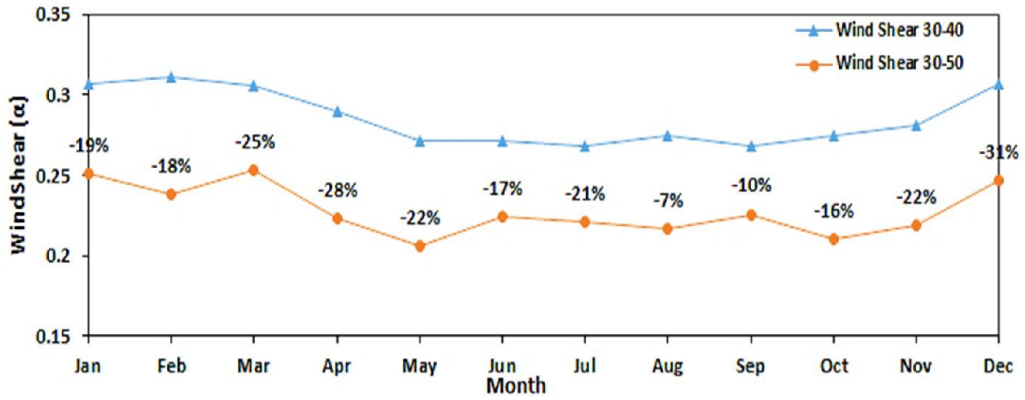

Figure A.33 Monthly variation of wind shear exponent and 30m wind speed (2014)

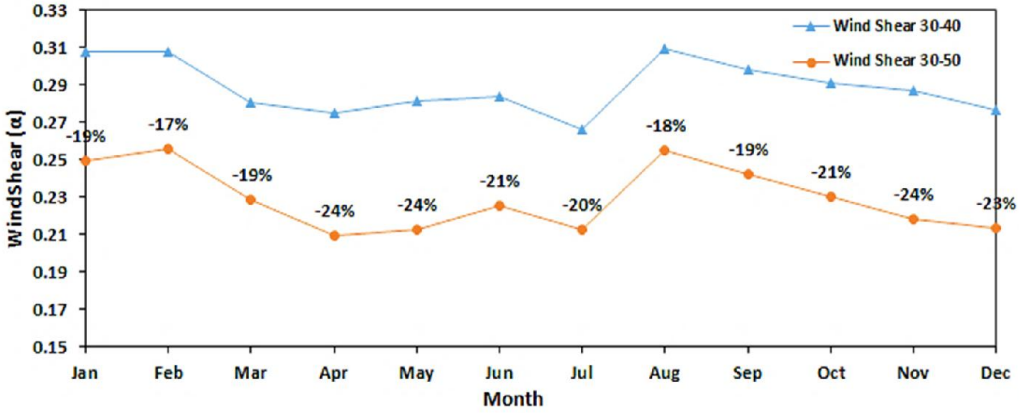

Figure A.34 Monthly variation of wind shear exponent and 30m wind speed (2015)

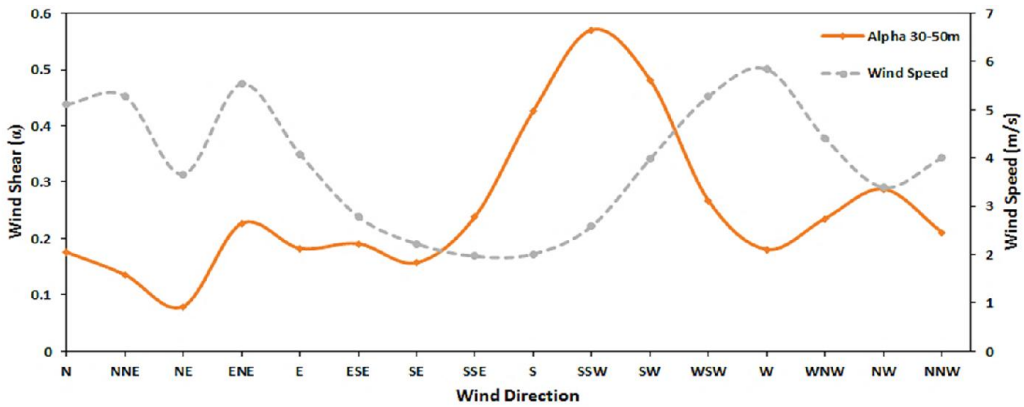

Figure A.35 Monthly variation of wind shear exponent and 30m wind speed (2014)

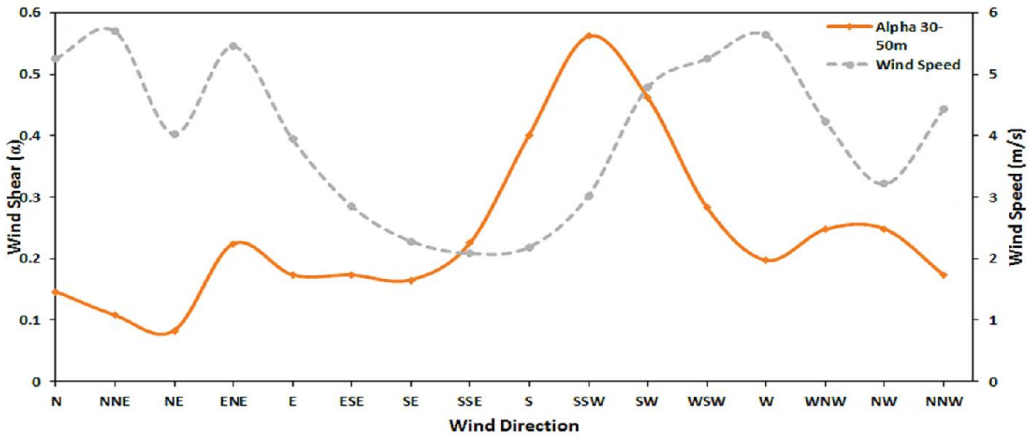

Figure A.36 Monthly variation of wind shear exponent and 30m wind speed (2015)

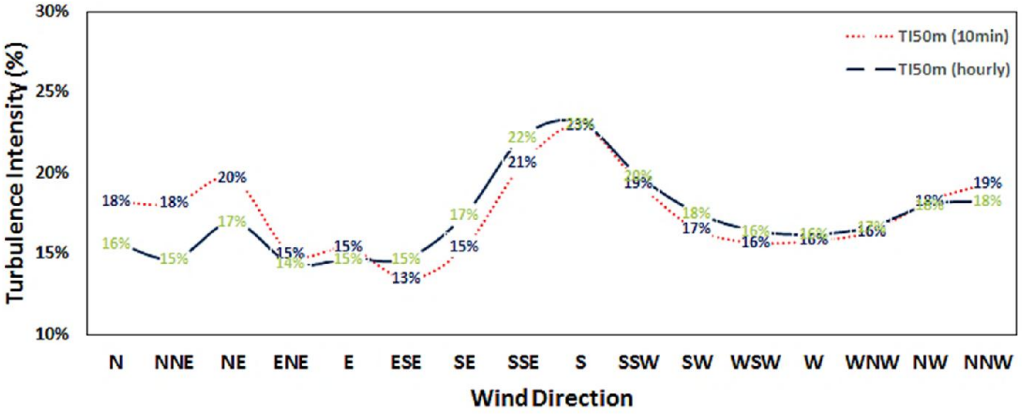

Figure A.37 10-min and hourly turbulence intensity variations with direction at 50m (2014)

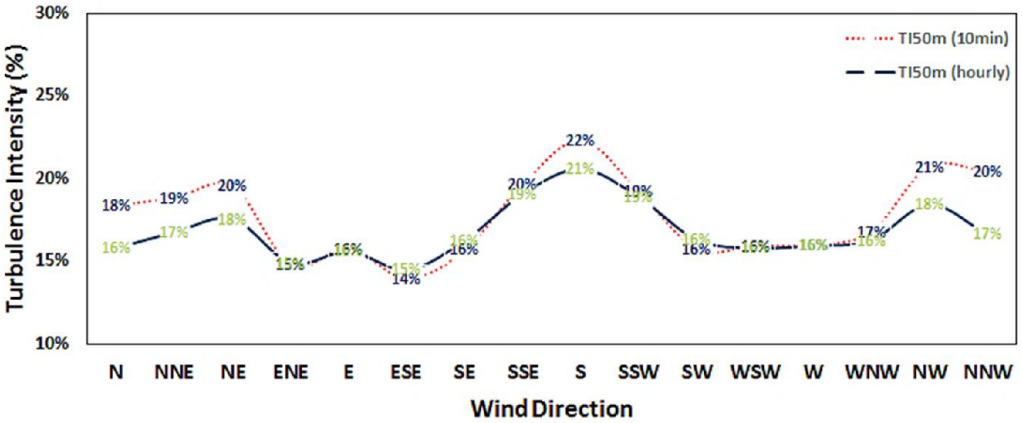

Figure A.38 10-min and hourly turbulence intensity variations with direction at 50m (2015)

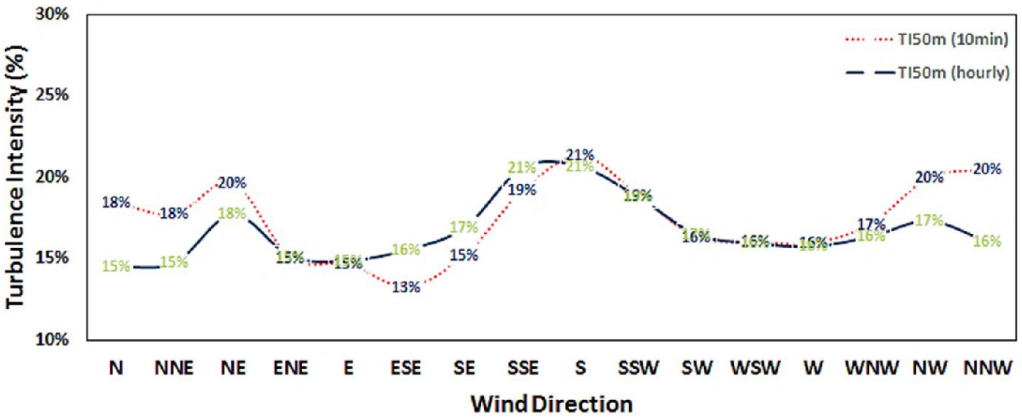

Figure A.39 10-min and hourly turbulence intensity variations with direction at 50m (2016)

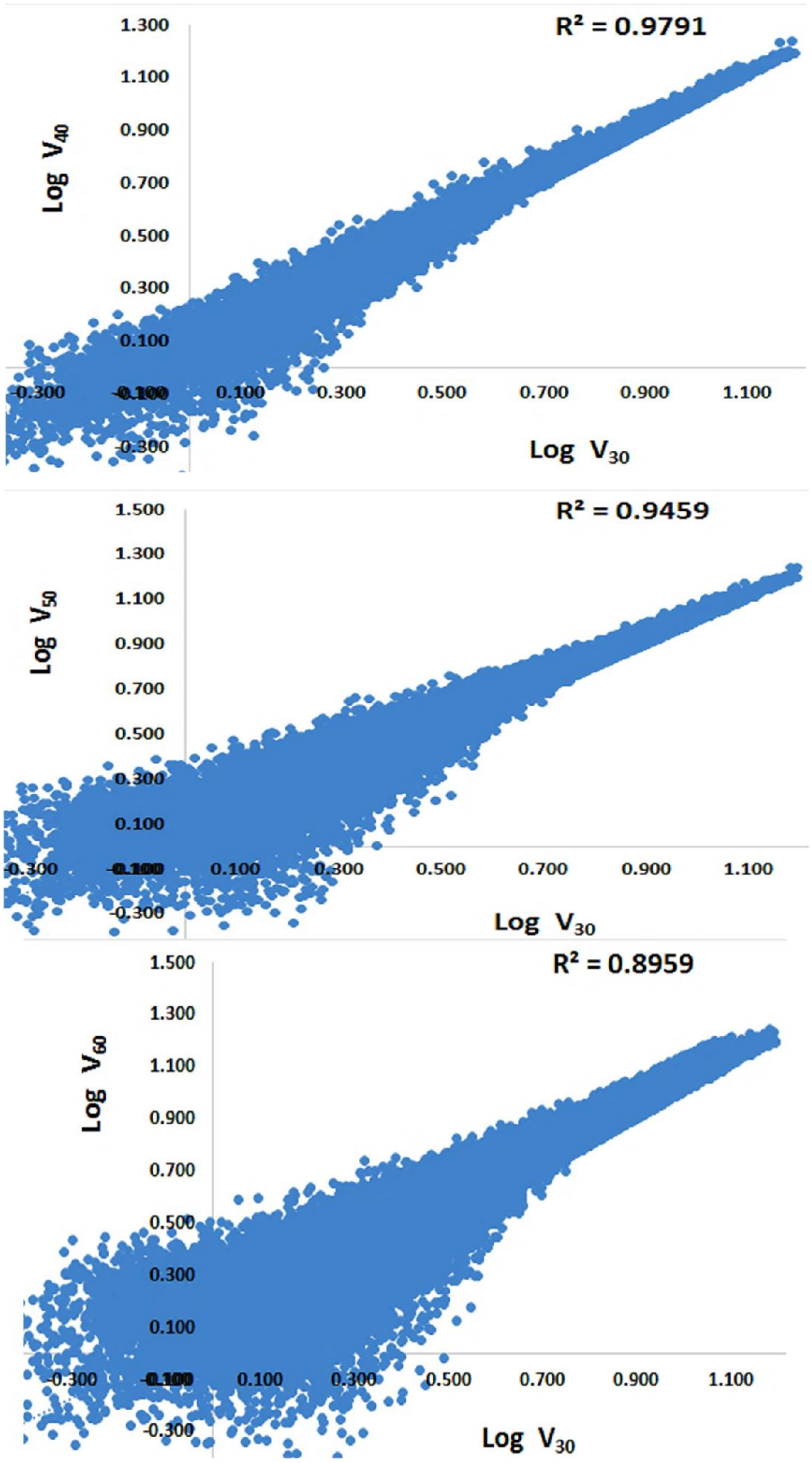

Figure A.40 Correlation between wind speed at different heights (2014)

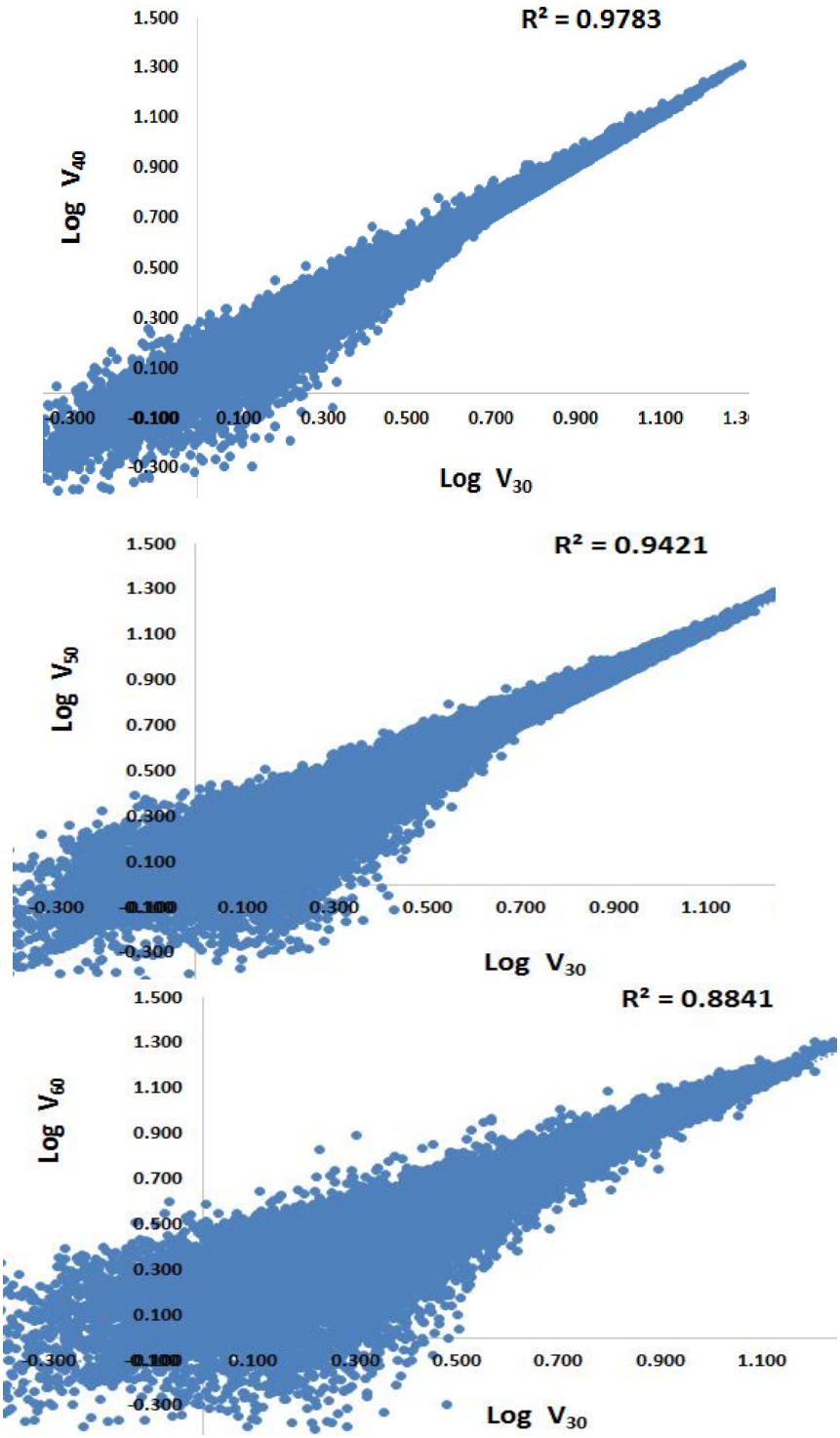

Figure A.41 Correlation between wind speed at different heights (2015)

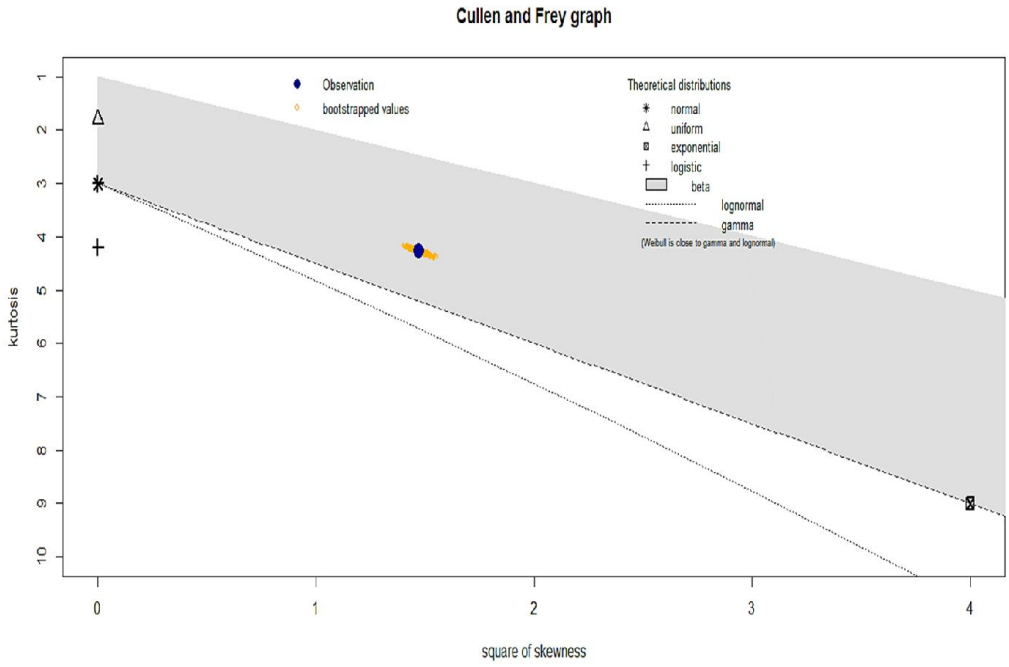

Figure A.42 Skewness-Kurtosis plot (Cullen and Frey graph) for 30-50 wind shear exponent (α) distribution

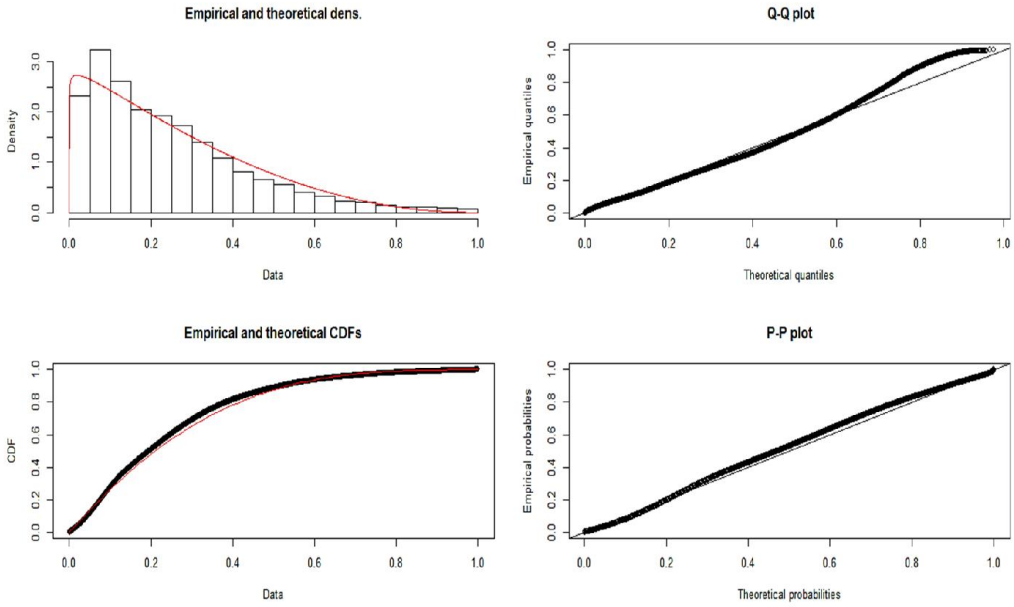

Figure A.43 Graphical analysis of beta distribution fit using estimated parameters by MLE method

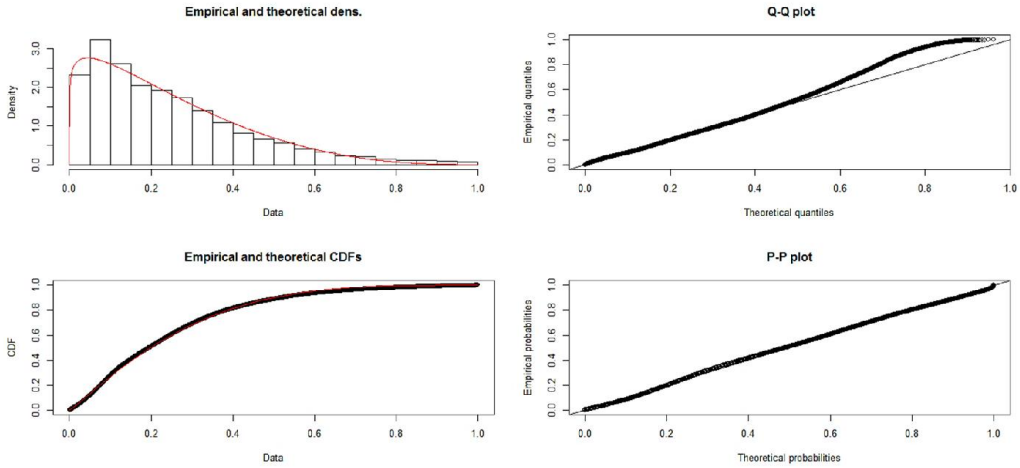

Figure A.44 Graphical analysis of beta distribution fit using estimated parameters by CVM method

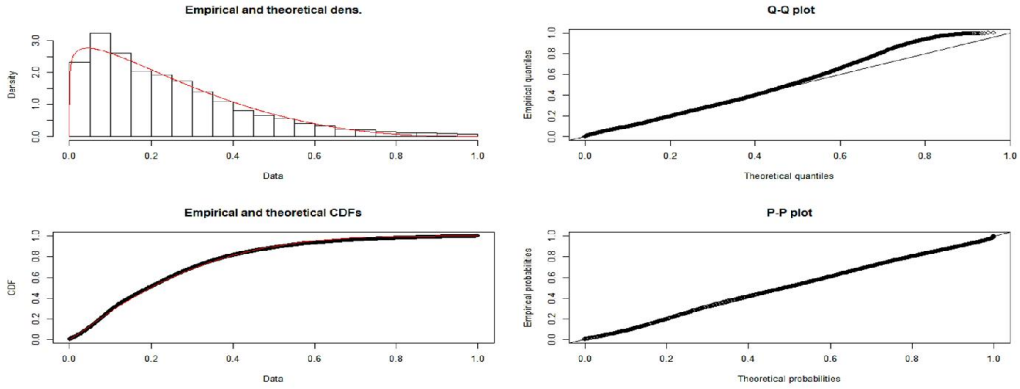

Figure A.45 Graphical analysis of beta distribution fit using estimated parameters by KS method

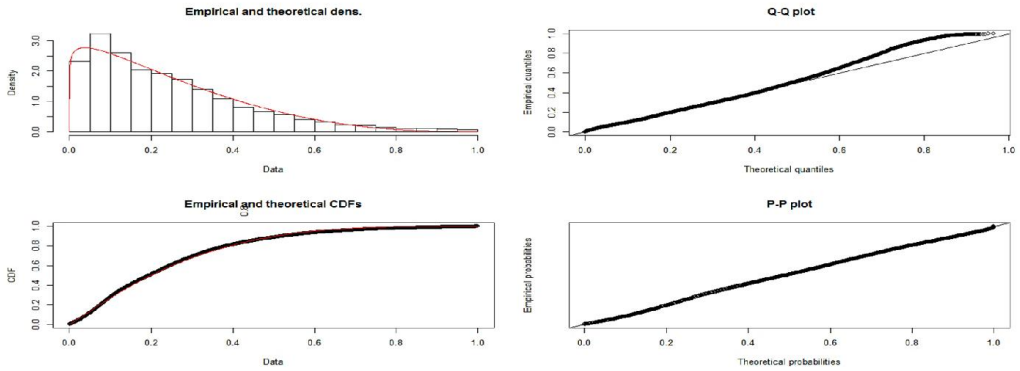

Figure A.46 Graphical analysis of beta distribution fit using estimated parameters by AD method

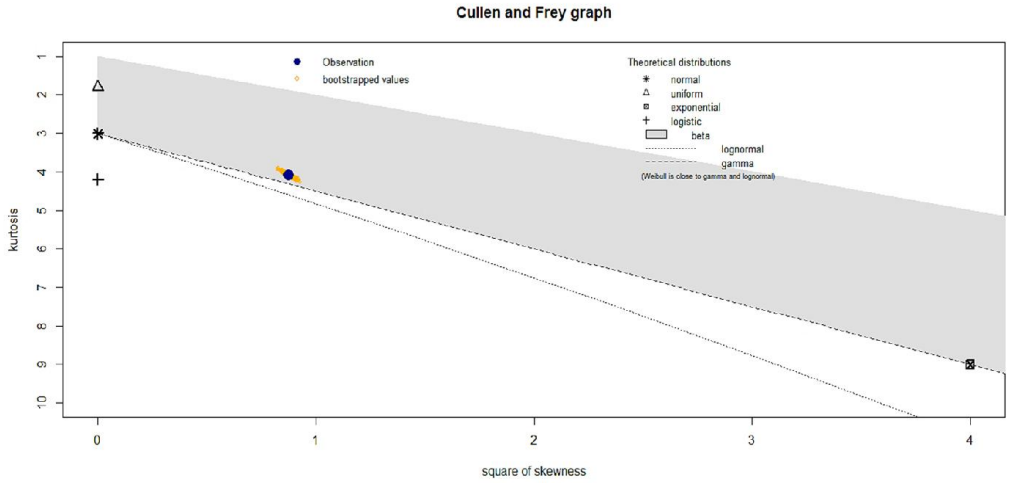

Figure A.47 Skewness-Kurtosis plot (Cullen and Frey graph) for 50m wind speed distribution

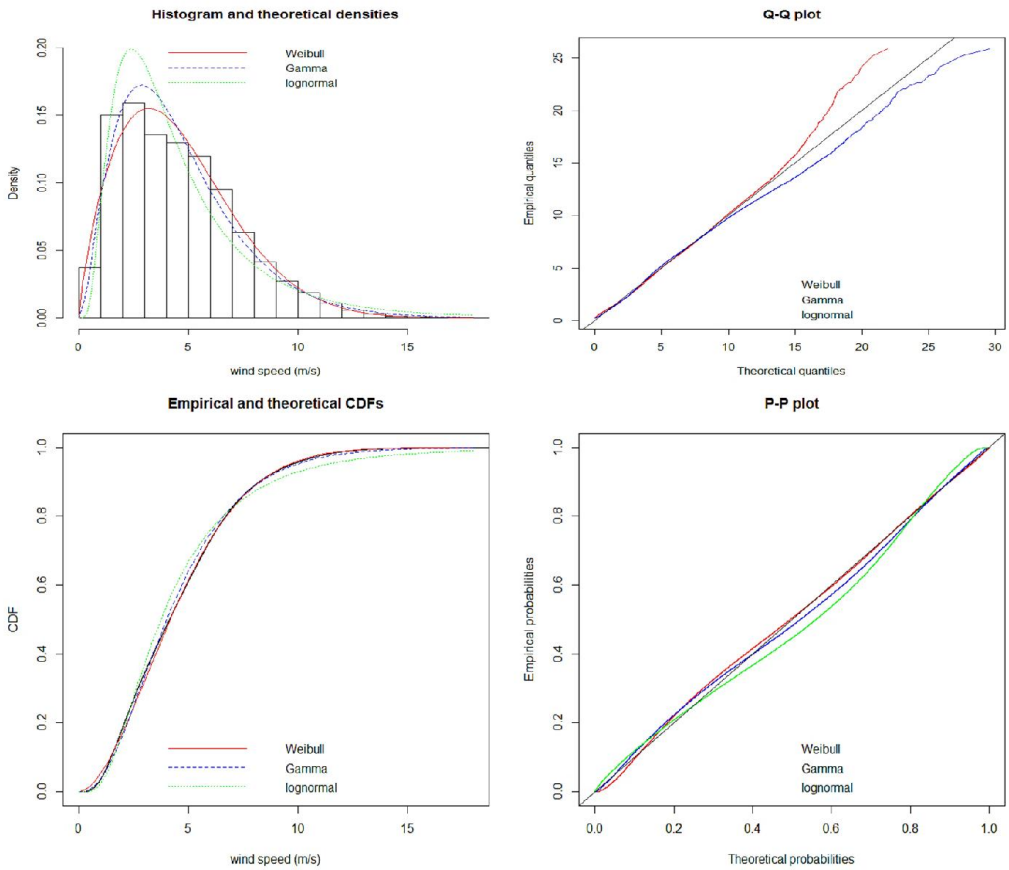

Figure A.48 Goodness of fit plots for selected distributions fitted to 50m wind speed data (2013-16)

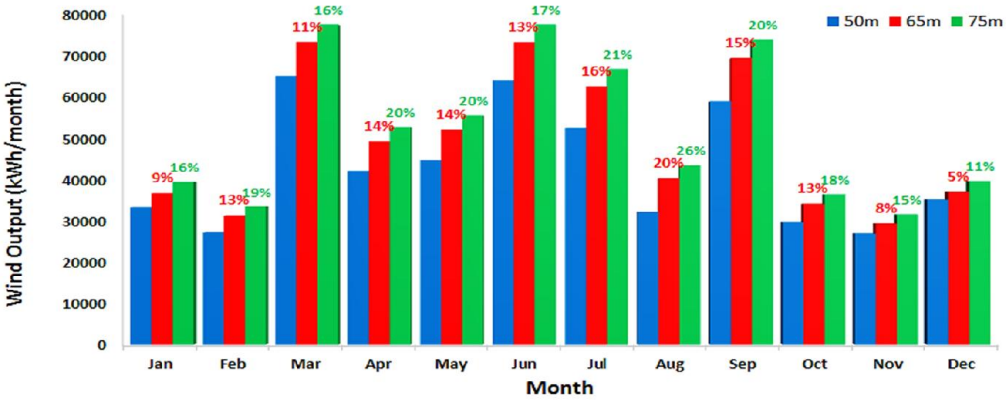

Figure A.49 Monthly variation of wind energy density at different heights for a 500kW (2014)

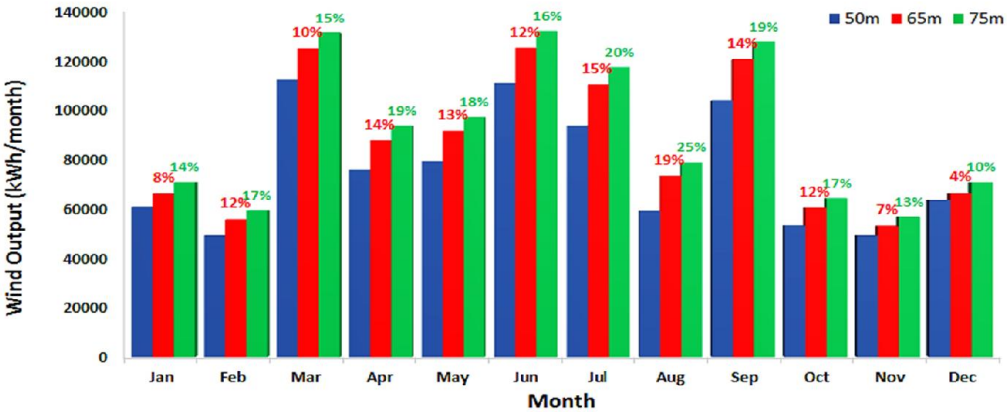

Figure A.50 Monthly variation of wind energy density at different heights for a 750kW wind turbine (2014)

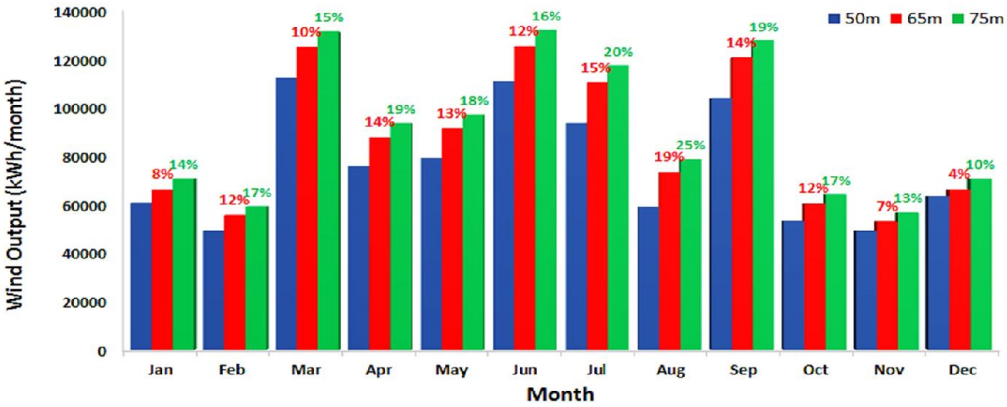

Figure A.51 Monthly variation of wind energy density at different heights for a 1MW wind turbine (2014)

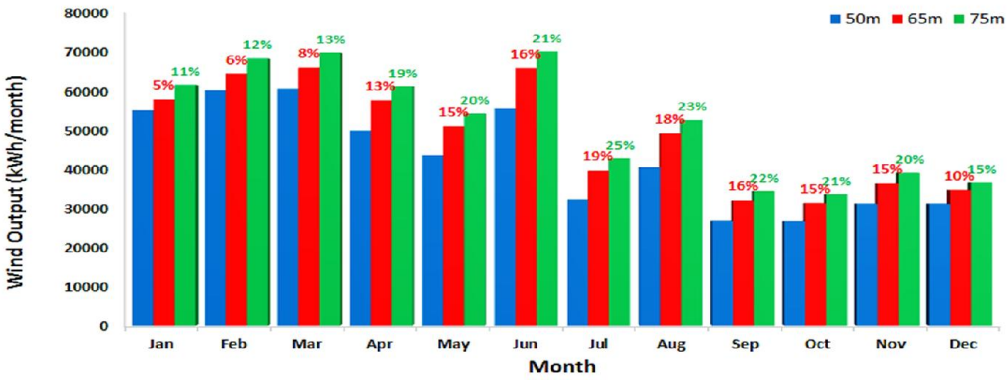

Figure A.52 Monthly variation of wind energy density at different heights for a 500kW (2015)

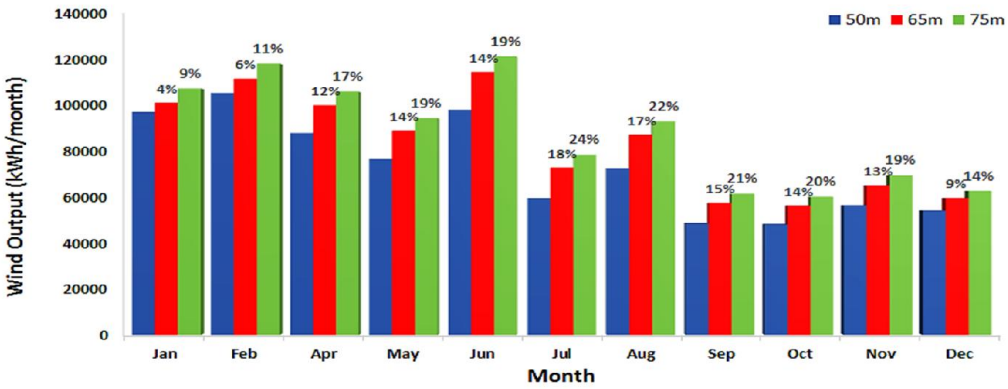

Figure A.53 Monthly variation of wind energy density at different heights for a 750kW wind turbine (2015)

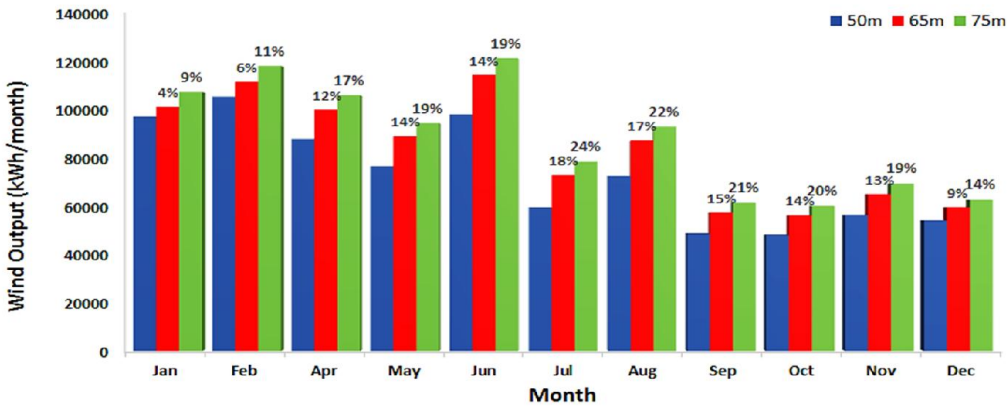

Figure A.54 Monthly variation of wind energy density at different heights for a 1MW wind turbine (2015)

APPENDIX B

Table B.1 Goodness of fit test statistics for 50m wind speed distribution

	Weibull	Gamma	Lognormal
Akaike's Information Criterion	925044	923096	935580
Bayesian Information Criterion	925064	923116	935600
Kolmogorov-Smirnov	0.026	0.029	0.062
Cramer-von Mises	30.131	55.553	234.142
Anderson-Darling	306.441	245.546	1352.661

Table B.2 Wind turbines specifications

	Units	Enercon E-40	Lagerwey LW 52	Enercon E-58
Rated Power	kW	500	750	1000
Cut-in Speed	m/s	2.5	2.5	2.5
Rated Speed	m/s	12	13	12
Cut-out speed	m/s	25	25	34
Rotor Diameter	m	40	51	58
Rotor Swept Area	m^2	1,275	2083	2697